

Hydraulic functioning of bioswales under polder conditions

A field-survey in Rotterdam



Nàdia Mobron
11 July 2019

Hydraulic functioning of bioswales under polder conditions

A field-survey in Rotterdam

Master of Science Thesis

For the degree of Master of Science in Civil Engineering at
Delft University of Technology

Author: Nàdia Anna Catharina Mobron

Student number: 4302613

Date: 18 August 2019

Location: Rotterdam, The Netherlands

Technical University of Delft (TU Delft)

Ingenieursbureau Rotterdam (IBR)

Thesis committee:

Dr. ir. F. H. M. van de Ven, TU Delft/Deltares

Dr. Ir. M. ten Veldhuis, TU Delft

Dr. Ir. A. Askarinejad, TU Delft

Ir. J. Nelissen, IBR

Ir. G. van der Hout, IBR

Preface

This research could only be realised thanks to the aid and active involvement of many people. To start, the budget for this research was provided by Water Sensitive Rotterdam (WSR) in order to contribute to a more climate resilient city. Special thanks goes to Joost Nelissen, for securing this budget and assisting in managing both the project and budget. I would like to thank Ella van der Hout as well, for assisting in the research set-up, interpretation of field-data and checking the general writing. Thanks goes to my TU Delft graduation committee members as well, Frans van de Ven, Marie-Claire ten Veldhuis and Amin Askarinejad, for helping me through the tougher questions, giving constructive feedback and looking for solutions together.

As a by-product from this field-survey, a discharge measuring device was designed and tested in both the laboratory and field, which can be used to measure the discharge from both submerged as free-flowing drains ending in manholes. This monitoring set-up was constructed by Willem van Bommel from the VLG (Veldmeet- en Laboratoriumgroep), who made the whole monitoring set-up possible, and assisted in the field-survey and results interpretation as well. The placement of the piezometers, location determination (GPS), installation of the discharge measuring device and the laboratory experiments were done by the VLG as well. Special thanks to the Sophie Mannuputy, who performed the saturated hydraulic conductivity tests and kept an eye on all the soil-related laboratory work. Lastly, without the field-team constantly switching the batteries of the discharge measuring device, little results would have been available. The GKB group facilitated the filling of the bioswales, as well as the outflow of the discharge measuring device and the perimeter security.

At last Michelle ter Haar and Lars Geitebeek should be named, for their constant support, constructive feedback and ability to make every working day a little bit more fun.

Summary

Bioswales contribute to climate resilience, as they positively impact the urban water infrastructure by improving the water balance and water quality. However, current bioretention design ignores the facts that different designs in different soils and climatic locations produce different performance results. In order to construct a design which performs well in the conditions of Rotterdam, the municipality of Rotterdam decided to research their current bioswales. The effect of polder conditions on the hydraulic performance, as well as the effect of different storm-types and initial conditions will be researched.

To this end, 5 bioswales located in Rotterdam, The Netherlands are monitored on their hydraulic behaviour. The discharge of the drain, groundwater levels in and at the edge of the bioswale and the water level in the bioswale are monitored for 4 of the bioswales. One bioswale only has groundwater and surface water measurements. For 3 of the 5 bioswales, 4 storm simulations are performed by artificially filling the bioswales. The Heavy dry storm (1) is a short, high intensity storm in dry conditions, the Heavy wet storm (2) a short, high intensity storm in wet conditions, the Two-Peak storm (3) is a storm with two consecutive peaks and the Medium storm (4) is a medium intensity storm of longer duration. As metrics used in literature to describe the hydraulic behaviour don't always reflect the behaviour well, some less-known and completely new metrics are introduced as well. The metrics describing the hydraulic swale performance are compared with the LID goals and sewer guidelines. Soil samples are taken from the swales as well, and tested in the laboratory to determine the sand, silt and loam fractions. In addition, Hydrus 2D/3D is used to estimate soil-hydraulic parameter from this soil-textural data. These parameters are also calibrated against the discharge data retrieved in the field. The storm simulation showed that the resulting peak reduction was very high for all bioswales, and still met the LID goal even for the medium storm. The peak delay showed more varying results, and met the goal for 11% for the larger storms and not at all for the Medium storm. The volume reduction goal was never met, though the reduction for large storms was higher than could have been expected (25%). The emptying time goal was not met for the larger storms either, but the medium storm easily stayed within the limit. When considering the laboratory results from the soil samples, all bioswales have very similar soil compositions. Only the top-soil of one bioswale differs, this bioswale is also much more prone to clogging. When determining the soil hydraulic parameters using the soil-texture data, the saturated hydraulic conductivities of the top-layers are extremely overestimated when comparing with the estimations from the field data and the Hydrus 2D/3D calibrated values.

The polder conditions resulted in a low volume reduction and faster and stronger reacting drain. However, the peak reduction and peak delay were still quite good due to the low permeability of the top-soil. For smaller storms, even the goal for volume reduction could be met. It was found that the structural porosity governed the infiltration, but large plants can increase the permeability to much. In addition, the textural porosity should start high enough to allow for vegetation development. Deterring the K_s proofed very difficult, and could only be done well with full-scale tests. Lastly, it is strongly advised to construct the drain completely under the groundwater table, to protect them against clogging from iron in the groundwater.

Table of content

Preface.....	III
Summary.....	IV
1 Introduction.....	1
2 Literature study: Current knowledge of the hydraulic functioning of bioswales.....	2
2.1 Purpose and design of a bioswale.....	2
2.1.1 Sustainable drainage systems.....	2
2.1.2 Bioswale design and functioning.....	2
2.2 Effluent performance metrics.....	4
2.2.1 Peak reduction, peak delay and volume reduction.....	4
2.2.2 Dutch standards and Low impact development.....	5
2.3 Emptying time and hydraulic permeability.....	5
2.3.1 Saturated hydraulic conductivity.....	5
2.3.2 Effect of seasonal variations.....	7
2.3.3 Effect of initial moisture content.....	7
2.3.4 Effect of storm size and distribution.....	8
2.3.5 Effect of media and depth.....	8
2.4 Peak flow rate ratio and peak discharge time span ratio.....	9
2.4.1 Effect of initial moisture content.....	9
2.4.2 Effect storm size and distribution.....	10
2.4.3 Effect of media and depth.....	10
2.5 Volume reduction.....	11
2.5.1 Effect of initial moisture content.....	11
2.5.2 Effect storm size and distribution.....	11
2.5.3 Effect of media and depth.....	11
2.6 Clogging soil.....	12
2.6.1 High initial failure rate.....	12
2.6.2 Equilibrium in the top-soil.....	12
2.7 Conclusions from literature review.....	13
3 Case study description.....	14
3.1 Conditions in Rotterdam.....	14
3.2 Rotterdam bioswale concept design.....	14
3.3 Bioswales selection.....	16
3.4 Description bioswales.....	16
3.4.1 Location selected bioswales.....	16
3.4.2 Inner-gardens description.....	17
3.4.3 Selected bioswale description.....	18
4 Method and materials.....	25
4.1 Storm simulations.....	25
4.1.1 Storm 1: Short large intensity storm in dry conditions.....	26
4.1.2 Storm 2: Short large intensity storm in wet conditions.....	26
4.1.3 Storm 3: Two successive storms.....	26
4.1.4 Storm 4. Medium long duration storm.....	26
4.2 Measuring equipment.....	27
4.2.1 Discharge measurements.....	27
4.2.2 Groundwater and surface water level measurements.....	28

4.3 Soil-parameters determination.....	31
4.3.1 Laboratory experiments.....	31
4.3.2 Soil-parameter determination	32
4.4 Hydrus 2D/3D calibration.....	33
4.4.1 Formula used in the model.....	33
4.4.2 Input data of the model.....	33
4.5 Adaptations metrics.....	35
4.5.1 Altering existing metrics.....	35
4.5.2 New metrics.....	35
5 Results.....	37
5.1 Field observations.....	37
5.1.1 Iron-rich seepage.....	37
5.1.2 Vegetational health.....	38
5.2 Monitoring results.....	39
5.2.1 Storm 1: Discharge.....	39
5.2.2 Storm 1: Groundwater.....	41
5.2.3 Storm 2: Discharge.....	42
5.2.4 Storm 2: Groundwater.....	44
5.2.5 Storm 3: Discharge.....	44
5.2.6 Storm 3: Groundwater.....	46
5.2.7 Storm 4: Discharge.....	47
5.2.8 Storm 4: Groundwater.....	49
5.2.9 Bioswale 7: Discharge.....	50
5.2.10 Bioswale 7: Groundwater.....	51
5.2.11 Summary findings bioswale monitoring.....	52
5.3 Field estimated saturated hydraulic conductivity.....	53
5.4 Soil-hydraulic parameters.....	53
5.4.1 Soil texture top-layer	53
5.4.2 Soil-texture sandbed	54
5.4.3 Soil (hydraulic) properties	55
5.5 Hydrus 2D/3D results.....	55
5.5.1 Neural network prediction results.....	55
5.5.2 Results from modelling.....	56
5.5.3 Calibrating soil-hydraulic properties in Hydrus 2D/3D.....	58
6 Discussion.....	59
6.1 Hydraulic functioning of bioswales: Effect of factors.....	59
6.2 Clogging.....	60
6.3 Structural and textural porosity.....	61
6.4 Measuring approach and set-up.....	62
7 Conclusion.....	63
8 Recommendations.....	64
8.1 Rotterdam bioswale.....	64
8.2 Further research.....	66
References.....	67

Appendices.....	71
Appendix 1: Height profile and pictures of dry swales.....	71
Appendix 2: Discharge measuring device.....	76
Appendix 3: Placement piezometers in the bioswales.....	81
Appendix 4: Tables result field-survey.....	87
Appendix 5: Graphs result field-survey.....	81
Appendix 6: Graphs storm simulations interrupted by rainfall.....	91
Appendix 6: Hydrus 2D/3D calibration results against field data.....	101

1 Introduction

Bioretention swales (in Dutch called “wadi’s”) have been introduced in the Netherlands around 1998 (Boogaard 2015). Bioswales can contribute to climate resilience, as they positively impact the urban water infrastructure by improving the water balance and water quality. However, current bioretention design is highly empirical, and it ignores the facts that different designs in different soils and climatic locations produce different performance results (Davis et al. 2012). In order to construct a design which performs well in the conditions of Rotterdam, the municipality of Rotterdam decided to research their current bioswales. These conditions include shallow groundwater levels with possible seepage, and low permeability native soils like clay and peat. These conditions are typical for Dutch polders. A such, recommendations from this research can also be of use to other Dutch cities with polder areas.

To be able to advise on the design for bioswales in polder conditions, 5 bioswales in the city of Rotterdam are monitored on their hydraulic performance. Besides considering the effect of polder conditions on the hydraulic performance, the effect of different storm-types and initial conditions will be researched as well. This will give a better understanding of the effect of storm intensity and distribution on the hydraulic performance, and will show which storms challenge the hydraulic performance of the bioswales most. To quantify the hydraulic behaviour of the bioswales, the following will be researched:

- The emptying times of the bioswales
- The peak reduction, peak delay and volume reduction among other metrics
- Comparing the hydraulic metrics with the LID goals and guidelines
- The effect of the initial moisture content, storm shape and size
- Range and magnitude of the effect on the groundwater table
- Whether the drain is limiting the infiltration or the bioswale top-soil (or both)
- The state of the vegetation inside the bioswale
- The (hydraulic) soil properties as (1) determined in the field, (2) from soil textural data using Hydrus and (3) from calibration with the discharge data using Hydrus

The report will start with a literature study, to give insight in the knowledge already present concerning the hydraulic behaviour of bioswales. This also includes common metrics used to describe their hydraulic behaviour and the goals set for bioretention facilities. Afterward, the case study area and the current standard design concept of Rotterdam will be discussed. Following, the measuring methodology and materials used are explained. This includes the composition of the 4 simulated storms, the discharge measuring method, placement of the piezometers in the field and soil sampling with laboratory testing. The results are divided in 3 parts, starting with (1) the field observations, followed by (2) the hydraulic performance results of the bioswales per storm simulation, and closed by (3) the laboratory soil-experiments and modelling results. In the discussion, noticeable behaviour of the swales will be interpreted and the error-sources will be reviewed. The conclusion will give a short overview of the insights which could be gained from the results, the recommendations convert this knowledge to practical recommendations for bioswales in Dutch polders.

2 Literature study: Current knowledge of the hydraulic functioning of bioswales

This chapter will start by introducing the problems of current (and future) urban water management and how bioswales could aid in solving these problems, followed by a more detailed explanation of their hydraulic functioning. After this, the metrics which are commonly used to describe the hydraulic behaviour of bioswales are introduced, as well of a number of goals they can be tested against. The effects found in literature of seasonal variations, the initial moisture content, storm size and distribution, and soil media and depth on these metrics is reported in detail. This chapter ends with a section on clogging of the top-soil and a short summary of the conclusions which could be drawn from the literature study.

2.1 Purpose and design of a bioswale

Climate change is expected to increase the storm intensity as well as the number of intense storms, while urbanisation significantly alters watershed hydrology, reducing the vegetative interception of rainfall, infiltration, and groundwater recharge resulting in an increase of the hydrograph peak and the associated runoff volume (Li et al. 2009; Driscoll et al. 1990; FHA 1996). Stormwater runoff often contains high levels of contaminants from road and building materials, vehicle components and traffic activity or dog faeces (Folkesson et al. 2009; Parker et al. 2010). Adverse impacts include downstream flooding, channel scour, fragility to droughts and flooding and sediment and pollutant transport (Barber et al. 2003; Li et al. 2009). For the current urban water infrastructure to cope with the increase in water volume and pollutants, a change in policy is needed.

2.1.1 Sustainable drainage systems

In order to effectively mitigate these impacts, sustainable drainage systems (SuDS), such as detention ponds, swales, and infiltration galleries can be used (Ellis et al. 1986; Schueler 1987; Urbanas and Stahre 1993). Unlike conventional sewer systems, they decrease and delay the peak load as well as reduce the total discharged volume. By doing so, the urban water system moves back to “predevelopment hydrology” (Energy Independence and Security Act (EISA) 2007) reducing the adverse impacts to the urban water system (Walsh et al. 2005). The specific sustainable drainage system which is considered in this report is a bioretention swale. Bioretention is increasingly used as a runoff management practice in urbanized areas. They act as a flow restrictor, leading to water storage, followed by infiltration and evapotranspiration.

2.1.2 Bioswale design and functioning

A standard bioswale is a depression covered by vegetation (usually grass), where the first soil layer enables vegetational growth and the second soil layer provides storage and sufficient infiltration capacity (Harrington 1989; Duchene et al. 1994). A drain is usually applied in the second layer or in a drainage chest below, which drains a part of the infiltrated water from the bioswale. Whether a drainage chest is used or not depends on the design purpose and groundwater level. If groundwater control is needed, a drainage chest might be needed for relatively deep groundwater conditions so that the drain can be placed at groundwater level (free-flowing drain). When the drain needs to be placed below the groundwater level (submerged drain) to protect against iron oxidising from the groundwater, a drainage chest might be needed as well.

The drainage can start immediately following the infiltration, or when the storage in the soil is exceeded depending on the placement of the drain (Urbonas and Stahre 1993). The bioswale functions as follows. During rainfall, the depression is filled with run-off from the surrounding area. This water infiltrates slowly through the first soil layer, which has the lowest permeability and should govern the infiltration. Then it enters the second soil layer, which is highly permeable and allows the water to be stored and infiltrate into the native soil or be discharged by the drain. The common design is illustrated in Figure 1 and Figure 2, giving respectively a cross-section over the width of the bioswale and the length of the swale.

There is not a simple performance value that can be ascribed to bioretention, the hydrologic performance will vary from site to site, and within a site for different rainfall events. Second, these facilities have some finite capacity to store/manage runoff for most small rainfall events. Larger events are managed less well, with some type of discharge via underdrain, overflow, or both (Heasom et al. 2006; Hunt et al. 2006, 2008; Li et al. 2009).

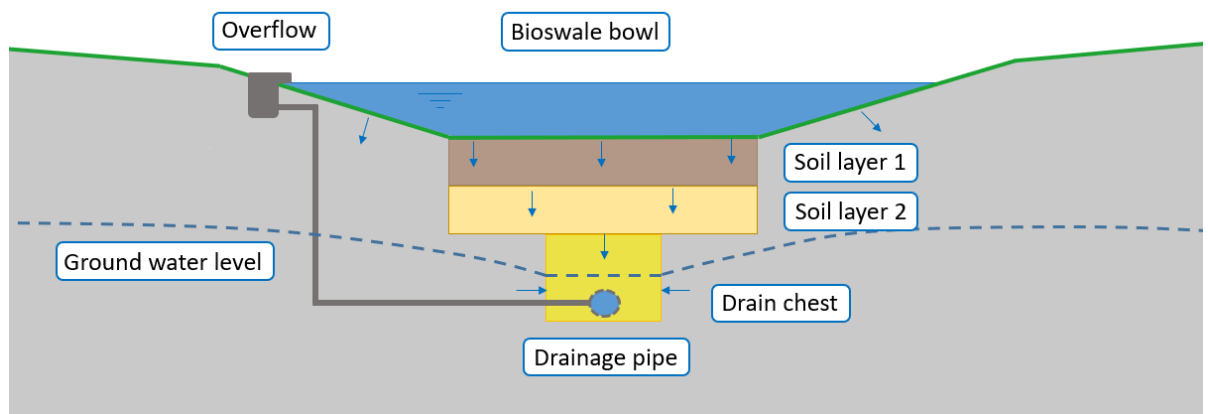


Figure 1: Schematisation bioswale with submerged drain, cross-section width

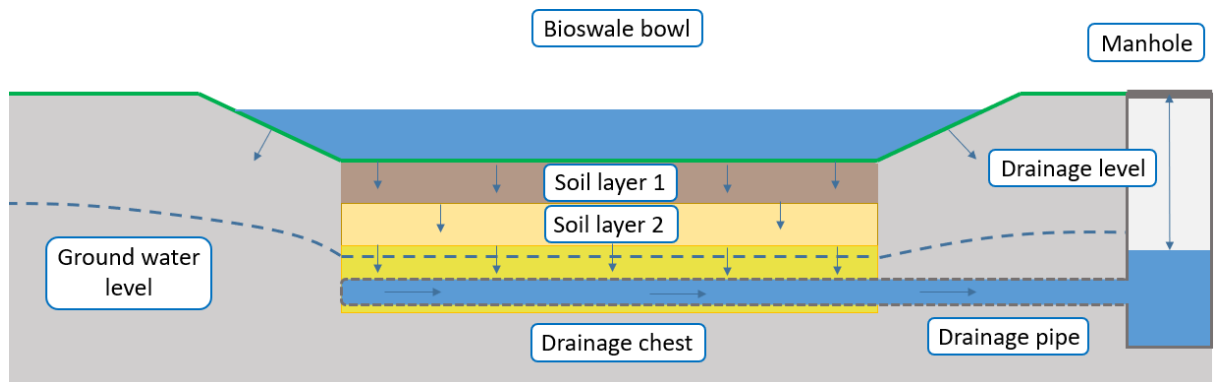


Figure 2: Schematisation bioswale with submerged drain, cross-section length

2.2 Effluent performance metrics

To quantify the hydraulic performance of bioswales, so it can be compared with guidelines and other bioswales, several metrics are used. These metrics describe the time it takes for the swale bowl to empty after a storm event, the reduction in water volume, the reduction in peak flow and the increase in peak delay. Lastly, the guidelines and goals set for these metrics are discussed.

2.2.1 Peak reduction, peak delay and volume reduction

Davis (2008) proposed three metrics for describing the restoration of hydrologic conditions by bioretention facilities: (1) the peak flow rate ratio of effluent to influent R_{peak} , (2) the peak discharge time span ratio of effluent to influent R_{delay} , and (3) the effluent/influent volume ratio f_v . These metrics were based on McCuen (2003) recommendations to maintain the predevelopment hydrology of a drainage area. These are three hydrologic metrics to evaluate the efficacy of smart growth strategies, specifically, (1) stream channel preservation; (2) travel time maintenance; and (3) hydrologic storage compensation.

$$R_{peak} = \frac{q_{peak-out}}{q_{peak-in}} \quad R_{delay} = \frac{t_{q-peak-out}}{t_{q-peak-in}} \quad f_{v-24h} = \frac{V_{out}}{V_{in}}$$

Where $q_{peak-out}$ and $q_{peak-in}$ represent the peak flow rates of the effluent and influent, $t_{q-peak-out}$ and $t_{q-peak-in}$ represent the time elapsed between the beginning of inflow and the peak effluent and the beginning of inflow and the peak influent, and V_{out} and V_{in} are the outflowing water volume from the drain and the inflowing volume from the rainfall event within 24 hours.

Davis (2008) experienced distortion of this term resulting from outflow after 24 hours, from storms with a long duration (giving unjustly very high volume reductions). These metrics are all illustrated in the graph of Figure 3 below.

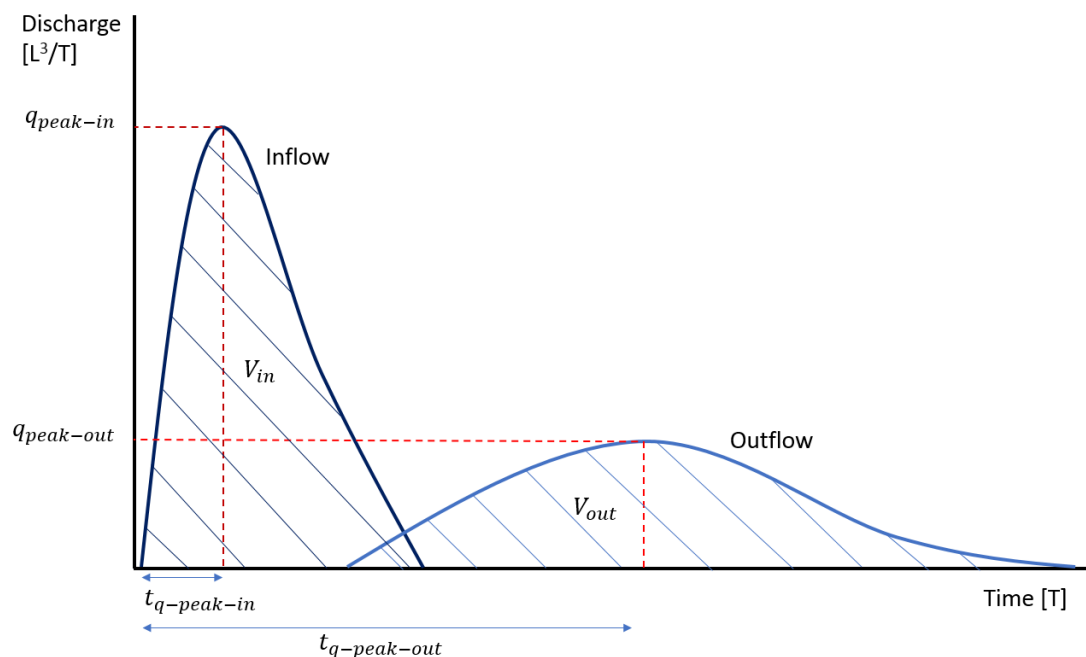


Figure 3: Representation of metrics in a hydrograph

2.2.2 Dutch standards and Low impact development (LID)

Since the bioswale as stormwater control measure is still relatively new, standards for hydraulic performance keep developing and current standards vary per region.

The targeted emptying time is usually 24 hours or shorter (only Belgium uses 24-48 hours), as the swale should be empty again for the next storm as with a conventional sewer system (Boogaard et al. 2006). Standards used in Davis (2008), Li et al. (2009) and Khan et al. (2012) relate to the discharge to the metrics originated from the Low Impact Development (LID) approach. Low impact development is an environmental philosophy that includes a focus on controlling urban rainfall and storm water runoff at the source. The goal is to manage site design and construction so that the hydrology and water quality of a developed site approximate that of the initial undeveloped land. Hence, SuDS are the tools to realize the LID goals. The LID goals were established by employing hydrologic parameters expected for undeveloped lands. These targets corresponded to a effluent/influent volume ratio of not more than 0.33 (over 24 hours), a peak flow rate ratio of 0.33 or more and a peak discharge time span ratio of at least 6 (Davis 2008).

2.3 Emptying time and hydraulic permeability

The emptying time depends on the infiltration capacity of the soil in the bioswale, as well as the water level in the bowl. To realize sufficient peak reduction and delay, the permeability of the top soil-layer cannot be too high. This limits the bowl-depth, since the bioswale should be empty again in time for the next storm (Davis et al. 2009). A number of design requirements limit the emptying time as well. The reasons for a short emptying time include (1) ensuring vegetation health, (2) concerns over the compaction of sediments, and (3) health and safety considerations, including waterborne diseases and insect nuisance. The vegetative health of one bioretention cell near Atlanta (0.6 m deep) and one near Villanova (0.9 m deep) have been researched. Though this was reasonably good, the growth of less desirable weed species was apparent over time (Hunt et al. 2012). The emptying time of these bioswales was however not reported. Another safety issue is that deeper volumes may require fencing or other drowning risk-reducing infrastructure (Hunt et al. 2012).

2.3.1 Saturated hydraulic conductivity (K_s)

As the depth is a design decision, which is simple to execute, the parameter which will be considered further is the permeability (represented with the saturated hydraulic conductivity). Though its importance is widely recognised, it proves difficult to manage in practice. International guideline recommendations for the hydraulic conductivity (K_s) of the soil vary considerably, ranging from 3 m/d in the USA/New Zealand, to 0.12 m/d and 0.48 m/d in Australia (Kluge et al. 2016). The data of a number of studies using flood-fighting (Boogaard et al. 2017; Boogaard 2015) and infiltrometer tests (Ahmed 2015) to determine the saturated hydraulic conductivity of bioswales have been collected and are given in Figure 4 and 5 below. The resulting mean gives a permeability of 1.15 m/d, far above the 0.3 to 0.5 m/d which is recommended by Rioned (Boogaard et al. 2006). Little information could be retrieved about the circumstances and design of the tested bioswales. However, it was mentioned by Boogaard et al. (2017) that the geohydraulic circumstances in Dalfsen were favorable for infiltration, with high permeability and a deep groundwater table. This can be directly found in the data, which shows that the bioswales in Dalfsen are at the high end of the spectrum.

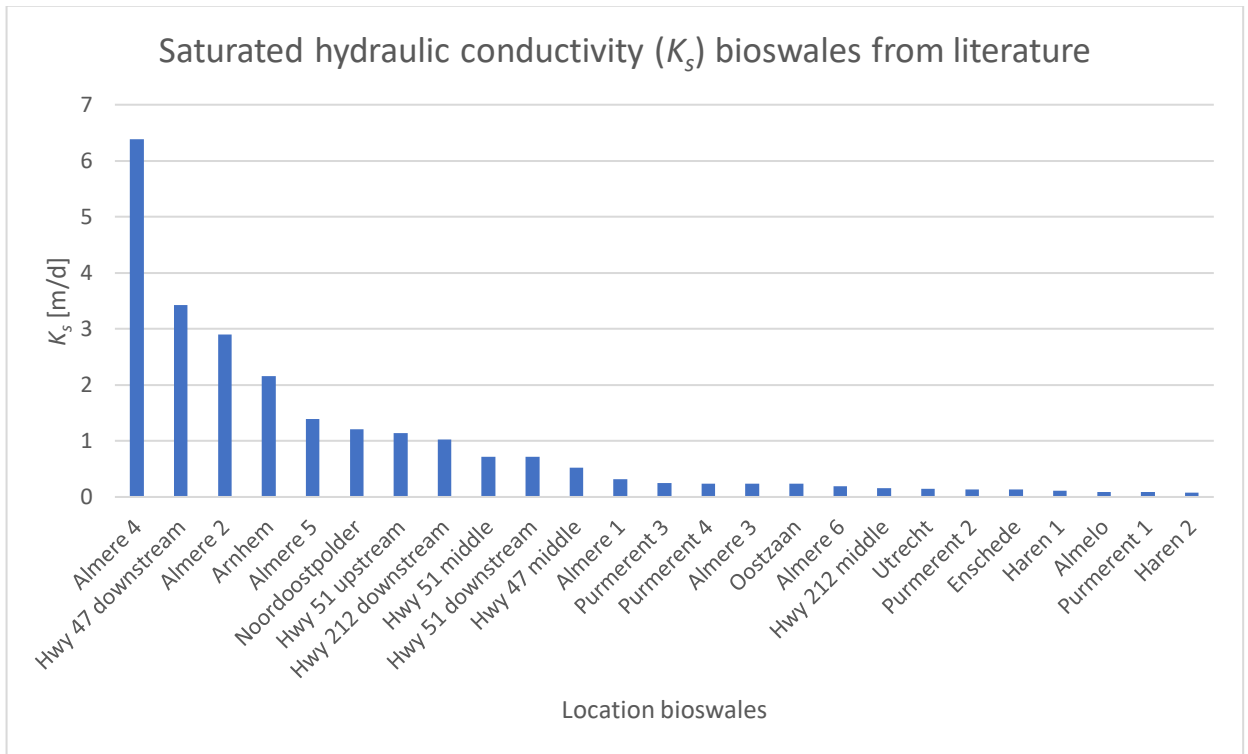


Figure 4: K_s from literature (Boogaard et al. 2017; Boogaard 2015; Ahmed 2015)

Kluge et al. (2016) found an average of 1.21 m/d for sandy loam/silty loam systems, the highest value being 6.48 m/d and the lowest 0.057 m/d. These values from German cities seem to fit the gathered data of Figure 5 reasonably well, which has a mean K_s of 0.96 m/d.

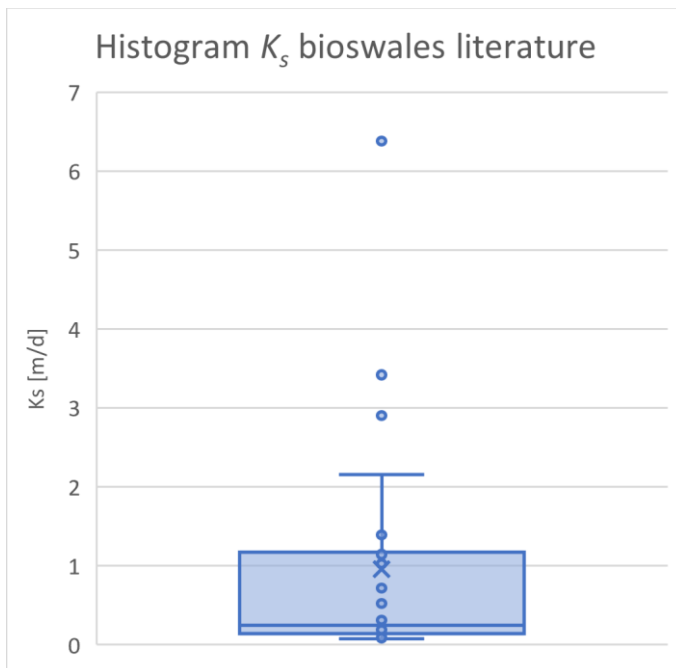


Figure 5: Histogram of K_s from studies (Boogaard et al. 2017; Boogaard 2015; Ahmed 2015)

2.3.2 Effect of seasonal variations

The seasonal variation commonly observed in the infiltration from SuDS was researched in order to determine the cause of this variation (Emerson and Traver 2008). Two SuDS were monitored, one above the surface and one below, which both show considerable seasonal variation in their infiltration data. Commonly this seasonal variation in storm-water infiltration facilities is speculated to be the result of changes in evaporation and biological processes including plant transpiration, mechanical root activity, and burrowing insects. As these mechanisms did not play a part in the infiltration facility beneath the surface, a different cause is examined. The writers propose that the before named processes are insignificant when compared to the expected temperature dependency of hydraulic conductivity. By definition, hydraulic conductivity is not exclusively a soil property. It depends on both the soil-pore structure and the properties of the permeating fluid. This is shown by the following equation (Bouwer 1978; Hillel 1998).

$$K = k \times \frac{\rho g}{\mu}$$

With:

K = hydraulic conductivity (cm/s)

k = intrinsic permeability of the soil (cm²)

ρ = density of the fluid (g/cm³)

g = gravitational acceleration (cm/s²)

μ = dynamic viscosity of the fluid (g/cm*s)

Dynamic viscosity varies by approximately 163% over a temperature range of 0 – 38°C, essentially doubling over typical temperature ranges experienced in the Northeast of the United States. Therefore, the hydraulic conductivity should be expected to vary proportionally with the temperature-induced viscosity changes of liquid water. Seasonal changes in evaporation, transpiration, and biological soil activity likely play some small role in the observed seasonal variation of infiltration BMPs as well. However, studies focusing on the temperature dependency of the hydraulic conductivity of near-surface soils have shown that evaporation and transpiration variations are often insignificant compared to the rate of infiltration (Jaynes 1990; Constantz et al. 1994; Ronan et al. 1998).

As such, it is most likely that the biological activities play the second-largest part. Ahmed, Gulliver, and Nieber (2015) did not observe any significant changes in the saturated hydraulic conductivity of fall and spring, thought this is likely caused by the high coefficient of variation (1.92-14.38) and the near constant temperature value of the applied water in the MPD infiltrometer.

2.3.3 Effect initial moisture content

In Dalfsen, 4 bioswales were tested in dry and wet conditions using full-scale tests, filling them 4 times in a row (Boogaard et al. 2017). The results show that the emptying time increases significantly after each filling, thought strongest at the second filling. The decrease in infiltration capacity after the last filling lays between the 51% and 19%, with an average of 37%. Boogaard and Klomp (2018) researched 3 of these bioswales again after a particularly dry summer in 2018. The infiltration capacities at the first filling were a factor 2 higher than the original infiltration capacities in 2017. However, after multiple fillings the infiltration capacities decreased to the same values as in 2017. This suggest that drier initial conditions increases the infiltration capacity of bioswales, including extreme droughts.

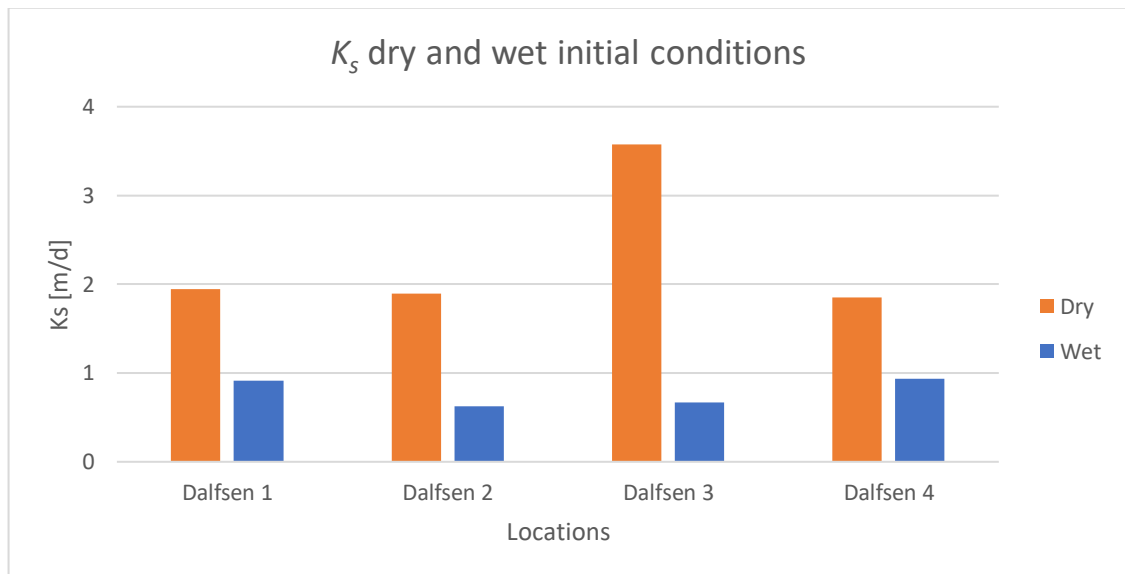


Figure 6: K_s of 1st and 4th filling of bioswales in Dalfsen (Boogaard et al. 2017)

2.3.4 Effect of storm size and distribution

No research on the effect of storm size or distribution on the emptying time could be found. However, it is logical that larger storms result in a larger runoff volume, which means more water in the bioswale and thus a longer emptying time. As such, a large storm event is usually taken as worst-case scenario for bioswales. However, it is also automatically assumed that this should be a short, high intensity storm as is commonly used for the conventional sewer system. Yet, when considering the emptying time of a bioswale, the same storm size occurring over a longer time span will likely result in worse results (longer emptying time). This due to one of the driving forces of the infiltration, namely the height of the water level in the bioswale bowl, being lower than for a short high intensity storm. The same can be said when the storm volume is divided over two storm event, occurring after each other when there is still water in the bioswale. This leaves the question what storm challenges the bioswale the most and could be considered as its design storm.

2.3.5 Effect of media and depth

Rawls et al. (1983) constructed a database which relates soil textural class to the Green-Ampt infiltration parameters. Though it proves very difficult to predict the infiltration capacity well with only soil texture data, it does show that there is a relation between the soil texture and infiltration capacity of the media. As such, for the construction of bioswales a soil-mixture for the top layer of vegetable mold (1/3th) and drainage sand (2/3th) is recommended (Boogaard et al. 2006). This should ensure an infiltration capacity of the top soil greater than 0.5 m/d, when the layer has a thickness of 0.3 – 0.5 m (Boogaard et al. 2006). It is assumed that the infiltration capacity will likely decrease over time to about 0.3 m/d (see chapter 2.6 Clogging top-soil), which is still sufficient to empty in 24 hours (water depth of 30 cm).

However, it is not undisputed that soil-texture is determining for the infiltration. Ahmed et al. (2015) researched the saturated hydraulic conductivity (K_s) of grasses roadside drainage ditches with different textural classes. For each soil texture class, the geometric mean saturated hydraulic conductivity value was either higher than the typical saturated hydraulic conductivity value or at the higher end within the typical range.

In addition, though the spatial variation of the saturated hydraulic conductivity at each site is wide, the variation of mean saturated hydraulic conductivity within soil texture is narrow. This indicates that soil texture is not governing permeability in the swales as much as was thought. Instead, it is likely that plant root macropores in these swales or variable soil compaction (swales are up to 50 years old) was such a dominant factor in these swales that it partially overcomes the soil texture effect on the saturated hydraulic conductivity.

2.4 Peak flow rate ratio and peak discharge time span ratio

To quantify the peak reduction and peak delay which is realized by a bioswale, respectively the peak flow rate ratio and peak discharge time span ratio are used. As the design of the bioswale and climate conditions both influence these two metrics, the values from different bioswales are difficult to compare. Li et al. (2009) researched 6 under-drained bioswale locations in Maryland and North Carolina. The median peak flow rate ratios (R_{peak}) found for the swales were 0.14 (CP), 0.10 (L2), 0.04 (L1), 0.02 (SS), and < 0.01 (G1 and G2). Davis (2008) monitored 2 bioretention facilities, the median peak ratios were 0.40 for Cell A and 0.48 for Cell B. Results from a field bioretention study at the New Hampshire Stormwater Center have indicated an average R_{peak} of 0.15 (UNHSC 2006).

Li et al. (2009) found the median R_{delay} values ranged from 200 (SS and G1), 13 (G2), 22 (CP), to 4 (L1) and 3 (L2). Interesting to note is that the bioswales with the highest peak reductions (CP, L1 and L2) have the lowest peak delays. Davis (2008) found a median delay ratio of 2 for Cell A, indicating a peak that arrived two times later than that of the influent peak. The same value for Cell B was 2.7, demonstrating an even longer delay. An average center-of-mass delay of 615 min was reported for the bioretention facility at New Hampshire (UNHSC. 2006). Geerling (2014) measured a median outflow delay of 21 min, while the median outflow delay measured by Donkers (2010) for the same bioswale is 23 min. This slight difference is likely caused by the different weather occurring in the two monitoring years.

2.4.1 Effect of initial moisture content

Using initial water contents ranging from 10.5% to 12% (3 - 72 hours dry period), Barber et al. (2003) showed that the peak reduction is larger for lower initial water contents. However, this was only visible between the 11% and 10.5% initial moisture content giving a peak reduction of respectively 64% and 98%. This effect only impacted the hydraulic performance during smaller storms. The hydraulic performance of the ditch for larger storms is not sacrificed or improved based on initial water content of the media. On the other hand, initial conditions resulting from a week of hot summer weather is expected to have much greater and improved impacts on the hydraulic performance of the ditch.

Li et al. (2009) found that the antecedent dry weather period (ADWP) did not appear to affect R_{peak} . However, Donkers (2010) did observe a decrease in peak reduction related to high initial moisture contents (median peak reduction of 74% for shallow groundwater against 79% for all events). This might be due to different climates that govern the study sites (The Netherlands against North Carolina and Maryland), or how the initial moisture conditions were defined (groundwater levels against ADWP). In the Netherlands, groundwater tables tend to be high (affecting the unsaturated permeability of the soil above) and water is not drained easily. As such, a previous storm has a longer effect on the groundwater table, and thus the moisture content of the bioswale. Barber et al. (2003) also found that lower initial moisture contents result in a higher peak delay time (97 minutes against over 120 minutes), again only for smaller storms.

Donkers (2010) and Geerling (2014) also agreed that the outflow delay seemed to increase slightly with a deeper groundwater level. Donkers (2010) found a median peak delay of 21 minutes for event with shallow groundwater, against a median of 23 minutes for all events. As this is only a very small difference, it should not be weighed to heavy.

2.4.2 Effect storm size and distribution

A trend of decreasing peak reduction with increasing storm duration was found by Barber et al. (2003) (67% against 56% for respectively a 1 hour and 6 hour storm duration) and Li et al. (2009). This is caused by an increase in bioswale soil water content in the larger or higher intensity storms. An increase in water content results in an increase in the hydraulic conductivity. They both also found a decrease in the peak reduction with increasing storm size. One would expect greater peak reduction and spreading of the hydrograph, as the inflow increases and the outflow is reaching its limits. It seems that the increase in the hydraulic conductivity overpowers this effect for these studies. However, this drop in peak reduction tends to flatten out at larger storm sizes. At this point, the bioswale is almost completely saturated and the hydraulic conductivity is nearing its maximum value. It is possible that the peak reduction will go up again for even larger storms, as the increase in inflow (larger inflow peak) can no longer be compensated with an increase in hydraulic conductivity (almost constant outflow peak). Li et al. (2009) also concluded that the rainfall intensity did not appear to affect the peak reduction. An increasing peak delay with storm duration was found by Barber et al. (2003) (17.5% against 30% for respectively a 1 hour and 6 hour storm duration) and Geerling (2014). This is reasonable since the storm intensity decreases with longer storm durations. A decrease in storm intensity reduces the water content in the vicinity of the pulse and the corresponding effective hydraulic conductivity causing greater lag between peaks. Recall that unsaturated hydraulic conductivity decreases rapidly with small decreases in water content. Barber et al. (2003) and Geerling (2014) found that the peak delay time decreases with increasing storm size. The drop in peak attenuation tends to flatten out at larger storm sizes. Once saturation is reached, the hydraulic conductivity cannot increase any more, causing the peak delay time to approach a minimum.

2.4.3 Effect of media and depth

Barber et al. (2003) simulated the effects of different media on the hydraulic performance. USDA sand gave the highest peak reduction for a 2 hour storm (76%) compared to 43% for the model sand and 28% for gravel. Barber et al. (2003) claims that larger peak reductions are a result of finer medias tending to retain water better. As both the N parameter of these soils (1.59, 3 and 4.41, determine the shape if the pF-curve) and the K_s (0.006 m/s, 0.05 m/s and 1.0 m/s) could both explain this trend, it is a little early to say that only the storage characteristics of the media plays a part here. Following Davis (2008) and Li et al (2009), the depth of the media also plays an important role. The bioswales with a deeper media show a greater peak reduction. This can be found when comparing the peak reduction of Cell A with a depth of 1.2 m against that of the 0.9 m deep Cell B (Davis 2008), and when comparing G1, G2 and SS with a depth of 1.2 – 0.9 m against the other bioswales (0.5-0.8 m) (Li et al. 2003). This also gives the storm water more room to be stored, just as the finer media. Barber et al. 2003 found that peak delay time is dependent on the effective hydraulic conductivity. This can be seen when comparing the USDA sand (85 minutes), model sand (40 minutes) and gravel (20 minutes) for a 2 hour storm. Again, it is not ruled out that the N parameter doesn't play a part as well.

Following Barber et al. (2003), finer soils having lower hydraulic conductivities produce greater peak delay. In general, the level of peak reduction was highly dependent on the unsaturated properties of the soil. This effect decreases for increasing storm sizes. Davis (2008) found that the bioswale with lower media depth provided a higher peak delay, although the reason for this is not clear. As this bioswale did show a higher peak reduction, it might be an unexpected high hydraulic conductivity causing this effect. Li et al. 2009 however did find that the bioswales with more depth (G1 and G2) had larger peak delays.

2.5 Volume reduction

As for the peak reduction and peak delay, the volume reduction also depends on the bioswale design and the local climate conditions. As such, directly comparing results from different researches has limited value. To still get some idea of what influences the volume reduction, the factors influencing the volume reduction will be considered in more detail.

2.5.1 Effect of initial moisture content

Geerling (2014) found no influence from deep or shallow groundwater on the volume reduction in the field data, which corresponds with Donkers (2010). However, Geerling (2014) modelled the volume reduction for deep and shallow groundwater as well, and found that the volume reduction should be greater for deep initial groundwater (10%). Li et al. (2009) found that the ADWP did not influence the volume reduction, agreeing with the field research of Donkers (2010) and Geerling (2014).

2.5.2 Effect of storm size and distribution

Davis et al. (2011) found complete or significant reduction in runoff volume for small storm events. The four observed swales captured the smallest 40% of monitored storm events, reducing total runoff volume for an additional 40% of events, and performed as flow conveyance with negligible volume attenuation for the largest 20% of events. This agrees with Traver and Prokop (2003), Ermilio and Traver (2006), Davis (2008), Li et al. (2009) and Hatt et al. (2009). Modest or even negligible volume attenuation during large or intense storms was also found by Schueler (1994) and Deleticm (2006).

The maximal storage capacity of bioswales is the cause of this variable performance pattern. As runoff volume is reduced through infiltration, little volume attenuation occurs once the soil becomes completely saturated. Barber et al. (2003) also found that the storage in the soil was dependent on the intensities of the input hydrograph. As such it can be stated that when the bioswale media becomes saturated, all additional volume reduction is depended on the infiltration into the surrounding native soil.

2.5.3 Effect of media and depth

Davis (2008) showed that bioswales with a greater media depth provide a larger volume reduction (0.23 against 0.18, respectively Cell A and Cell B), which is agreed on by Li et al. (2009) who found that G1, G2 and SS had a media volume reduction of < 0.01, <0.10 and 0.10 against the other bioswales (0.36 - 0.6). For under-drained systems, the performance is more complex. The volume management will mainly depend on the available percolation to the surrounding soils, so a range of values is expected. The design parameter that produces the greatest impact to the volumetric management is the moisture holding capacity of the media.

2.6 Clogging top-soil

The major potential problem with any infiltration practices, in general, is the accumulation of sediments which results in clogging of the infiltration pores. This in turn leads to failure of the facility, as there is not enough space available anymore for the next storm as water from the previous storm is still present.

2.6.1 High initial failure rate

There have been previous surveys of infiltration facilities that found high decrease in infiltration capacity within a relatively short time frame. One such study focused on field inspections of infiltration facilities located in Maryland (Lindsey et al. 1992). Two separate rounds of field inspections were carried out 4 years apart. At the time of the first inspection the infiltration facilities were relatively new (2 years). The conclusion of the first inspection was that 67% of the facilities were not functioning as intended. Many of these failures were attributed to “poor design, inappropriate soils, and compaction of soils resulting from poor or careless construction practices” (Lindsey et al. 1992). The follow-up survey of most of the same infiltration facilities found that only 49% were functioning after an additional 4 years of operation. Many of the observed problems were related to the accumulation of sediment. This is likely a mistake in the construction, as significant sediment input is to be avoided by placing a grass-filter or sand/sediment catchers before the inflow of the runoff.

Sabourin et al. (2008) evaluated the performance of grass swales over 20 years, they found that the infiltration rates of 2006 were an order of magnitude lower than those in 1998. However, not all studies concerning bioswales find clogging (Emerson and Traver 2008; Boogaard et al. 2006; Geerling 2014). Even though they considered about the same time span as Lindsey et al. (1992).

2.6.2 Equilibrium in the top-soil

Multiple studies have shown that initially, hydraulic conductivity will rapidly decline (about 50% decrease) and then tend towards a constant value. Lewis et al. (2008) found a saturated hydraulic conductivity of 1.25 cm/d for 3 bioswales after construction, which decreased to 0.1 cm/d in half a year and then increased again in 10 months till between the 1 cm/d and 1.46 cm/d (though the last part of the increase was likely also aided by higher temperatures). The effects of suspended solids loading, mechanical compaction, rain drop impact on bare soil, and rapid wetting can all potentially have a negative impact on the infiltration process (Houston et al. 1999; Assouline 2004; Siriwardene et al. 2007).

However, there are soil characteristics and natural processes that can equally help maintain and improve the ability of a soil surface to infiltrate water over time (Benson et al. 2007). Soil organic matter content has been documented to help maintain and improve both the structure and hydraulic properties of soil (Barzegar et al. 2002; Carter 2002; Fuentes et al. 2004; Lado et al. 2004). The establishment of vegetation through the action of root growth and die off has also been shown to maintain or even improve the hydraulic characteristics of soil, mainly through the creation of larger more continuous macropores (Archer et al. 2002; Le Coustumer et al. 2007, Traver et al. 2007; Lewis et al. 2008; Li and Davis 2008). The mechanical action related to freeze-thaw processes has also been experimentally demonstrated to increase the hydraulic conductivity of soil (Asare et al. 1999).

The macropores are easy flow paths for infiltrating water, they impact retention time and contribute to improving infiltration rates. This was likely also the reason for the high hydraulic conductivities observed by Ahmed et al. (2015), in old roadside bioswales. These hydraulic conductivities were much larger than what could be expected for their respective textural soil classes, and thus likely governed by macropores.

2.7 Conclusions from literature review

When considering the current literature available on the hydraulic performance of bioswales, the following can be concluded. There is not a simple performance value that can be ascribed to bioretention, the hydrologic performance will vary from site to site, and within a site for different rainfall events. This means that when constructing a design, the specific hydrological and soil conditions of the area of application should be considered. When applying the same design under the same conditions, they should function reasonably consistent with each other. There are goals available to measure bioswale performance against (LID goals, aiming to recreate the hydraulic behaviour of undeveloped land), using peak reduction, peak delay and volume reduction. Davis (2008) experienced distortion from the definition from volume reduction, adjustment of the term seems needed. In addition, these terms do not always capture the complete behaviour of the discharge curve. As such, other metrics should be considered as well to contribute to a more complete description.

Considering the peak reduction, peak delay, volume reduction and emptying time, the following conclusions can be made.

- The emptying time depends on the water level in the bowl and the permeability of the soil medium.
- Not only the textural class of the soil is determining for the permeability, but also the macropores created by biological activity after 2 years.
- The hydraulic conductivity is strongly temperature depended, which results in a lower saturated hydraulic conductivity in cold conditions than in warm conditions.
- The bioswale soil media and storm size all influence the emptying time, peak delay, peak reduction and volume reduction.
- The initial conditions strongly effected the saturated hydraulic conductivity, the peak delay and peak reduction were only effected during small storms.
- The storm distribution was shown to influence the peak reduction and peak delay, no information was available concerning the effect on the emptying time and volume reduction.

3 Case study description

Now the knowledge already present regarding the hydraulic functioning of bioswales has been treated, and the common metrics and appurtenant goals have been given, the case study area which will be considered in this research can be discussed. This chapter will start by describing the conditions present in Rotterdam, which are likely to influence the hydraulic behaviour of the bioswales. This is followed by a description of the current standard bioswale conceptual design of the municipality of Rotterdam, based on previous research, maintenance and safety considerations. Using this design, 5 bioswales in Rotterdam are selected for the monitoring program. Lastly, the selected bioswales are discussed including their drainage levels and soil properties.

3.1 Conditions in Rotterdam

Most of the native soil in Rotterdam can be defined as river clay or peat. Only the parts which are artificially heightened usually have a sand foundation. This is mostly done around the river Meuse which runs through the city, and as foundation underneath roads and houses. The green area's in the suburbs are almost never lifted (and as such don't have a sand foundation), only close to the river this might be the case. It is also possible that previous groundwork has been done in that area (foundation of an old road, rubble processing, agricultural ground, etc.). However, for bioswales in green areas in Rotterdam, the native soil will almost surely be clay, usually with underlying peat. In addition, the deep polders like Alexanderpolder, Schiebroek and Hillegersberg-Noord also have seepage, which needs to be drained as well. The drainage depth in Rotterdam is usually only 1-1.2 meter below the (set) surface level. This already leaves little room available for storage underneath the surface, to which the following factors also contribute:

- Strong capillary soil (clay) holds water above the groundwater level, reducing storage available in the soil.
- Green areas are usually already lower than the set surface level, and as such are even closer to the groundwater.
- Some slope toward the bioswale is needed to collect the stormwater from the connected surface area.
- Bowl depth of the bioswale also needs to be constructed

3.2 Rotterdam bioswale conceptual design

The city of Rotterdam has decided to disconnect as much stormwater from the (combined) sewer system as possible. Disconnecting stormwater from the sewer system can be accomplished in multiple ways, of which the most promising solutions are being worked out in building blocks. One of these building blocks is the Rotterdam bioswale, which design is tailored to the conditions in Rotterdam. This is a conceptual design (Klapwijk, 2018), based on maintenance demands, safety considerations and recommendations from Boogaard (2006). Due to the low permeability native soils, infiltration from the swale to the surrounding soil is assumed to be negligible. As such, all the water in the bioswale is assumed to be discharged using the underlying drain. This means the bioswale only has a storing and delaying function, no volume reducing function. In addition, it is assumed that during a storm event, storage only takes place in the bowl of the bioswale. The part which infiltrates during the storm is neglected.

Sizing of the swale bowl

When designing a bioswale, maintenance also plays a part. To be able to mechanically mow the grass, a bottom width of 1.2 m or more is needed, and the slope of the sides should be 1:3 or less. A maximum water depth of 30 cm is set, in accordance with Boogaard (2006). In addition, the bioswale should empty within 24-48 hours. This in order to ensure the storage is available again for the next storm, and to ensure the water quality (especially in summer). In addition, the condition of the vegetation is better maintained.

Sub-surface structure

Underneath the sides, no ground improvement is applied. Underneath the flat bottom of the bioswale, a 20 cm thick layer of drainage sand (2/3) and compost (1/3) is constructed. With this composition, both the need for sufficient permeability and plant growth are facilitated. Underneath this layer, another layer of at least 20 cm is constructed consisting solely of drainage sand. This layer continues till the drainage case with drain, the drainage case should be at least 70 cm wide. The permeability of the first soil layer is 0.5 m/d, the second layer has a permeability of at least 1 m/d.

Drainage

A drainage pipe underneath the bioswale discharges the infiltrated water, this drain has an internal diameter of at least 250 mm. This size is not needed to ensure sufficient discharge, but to assist inspection and maintenance when needed. In addition, an overflow is installed to control the maximum water level in the bowl of the bioswale. The drain and overflow can be connected to a surface water body, a DIT-sewer or separated sewer system, or a combined sewer system (in that order of preference).

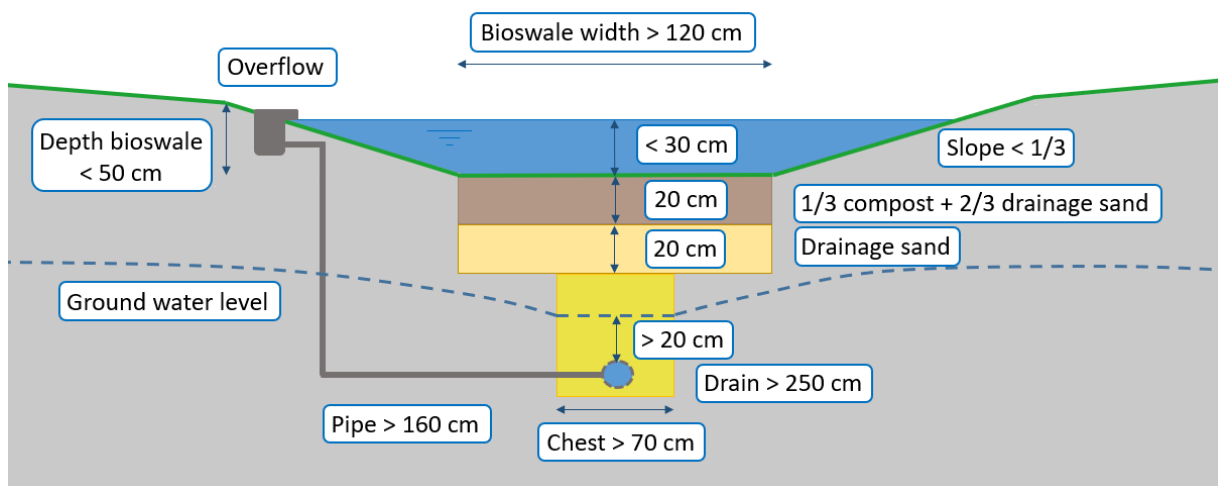


Figure 7: Conceptual design bioswale of the municipality of Rotterdam

3.3 Bioswales selection

Within the municipality of Rotterdam, there is no database present for bioswales. Instead, they are usually categorized as grass-fields by the green-maintenance department. To create an overview of the bioswales which currently exist in the city of Rotterdam, information was gathered from project managers and the authors of the conceptual designs. After gathering design data of the bioswales and visiting them in the field, a selection was made. A large part was excluded as (1) they were not there anymore or were never constructed, (2) they did not even remotely resemble a bioswale or (3) they were changed completely due to failure. In addition, it became clear that the design drawings were often incomplete and/or did not match the bioswales found in the field. As there was no registration system in place, a large number of old design documents were still in circulation, and adaptations made during construction were not registered or not updated. In order to obtain the most accurate drawings, the public works department was approached which did lead to acquiring revision drawings. The remaining bioswales were then selected on their location (polder conditions), and how well they represented the current conceptual design.

As such, bioswales in native sandy soils and/or with deep groundwater tables were put aside, as well as bioswales with multiple drains or garden-like vegetation. In order to execute the measurements, the bioswale should be safely accessible for both personnel and water trucks. As such, swale located in busy roads and confined inner-gardens are not considered. At last, the size of the bioswale also plays a part. The swale should be filled in a short amount of time, as the water truck takes time to re-fill this excludes large bioswales.

In total, 5 bioswales were selected. They resembled the conceptual design reasonably, but still have some interesting differences. Of the chosen bioswales, 2 have a free-flowing drain and 3 a submerged drain. In addition, one of the bioswales is constructed as an overflow of the DIT-system (Drainage, Infiltration, Transport), and has a very different design and vegetation from the other four bioswales.

3.4 Description bioswales

3.4.1 Location selected bioswales

All 5 selected bioswales are located in the (inner-)gardens of the Zeno-neighbourhood, which is located in district IJselmonde in the south of Rotterdam. Figure 4 below gives the locations of the 5 bioswales, including their drains (red dashed line) and the manholes to which the drains lead, where the discharge measurements will be done. As the drains are attached to an unperforated PVC transport pipe after leaving the bioswale, this pipe is drawn as an uninterrupted line. The source water is also shown, this is the surface water body from which the water is collected by the water truck for the storm simulations.

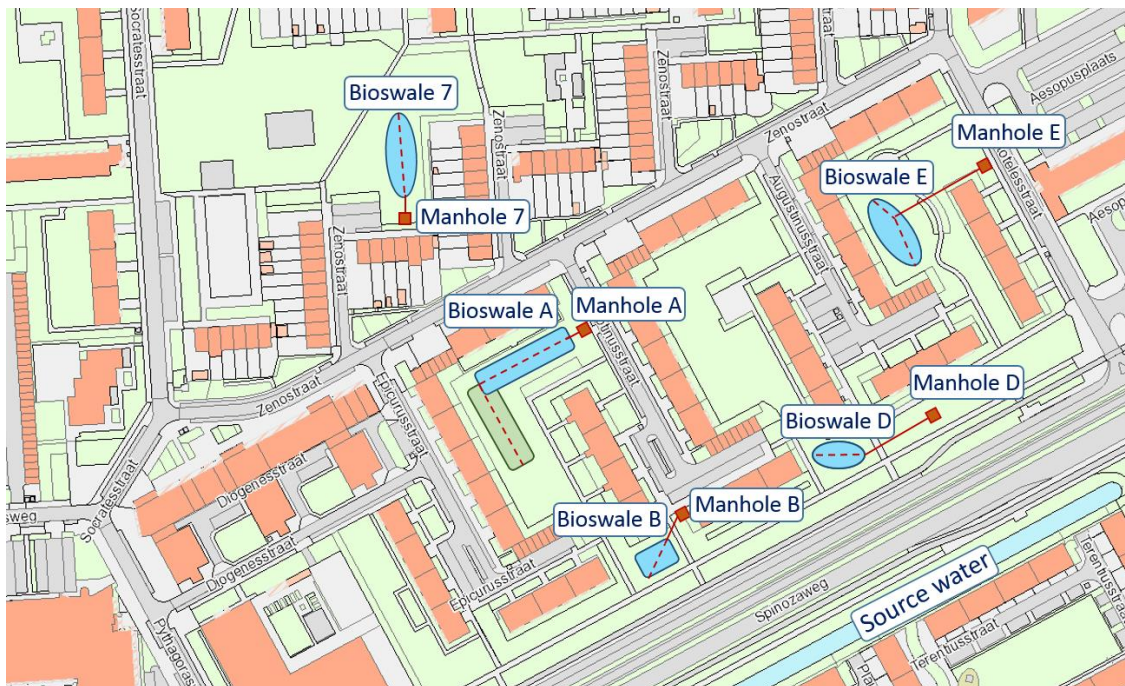


Figure 8: Location bioswales including their drains and manholes

3.4.2 Inner-gardens description

In 2017, the inner-gardens were taken under reconstruction after complains concerning water-nuisance and an observed decrease in surface level. The paths through the gardens were set back to their original level (-1.5 m NAP), and ground improvement was done in the gardens using basalt grit and compost to a depth of 0.5 m from the surface. Soil which came available during reconstruction was processed in the garden top-soil as well, raising the surface level (Municipality of Rotterdam, 2017)

Beneath the improved soil-layer sits a layer of medium loamy-silty clay, which starts at about -2.55 m NAP. Some rubble can sometimes be found here as well, usually after the first 30 cm. At a depth varying between -2.9 and -4.0 m NAP, a loam layer begins. The set drainage level of the area is -2.60 m NAP, the set surface level is -1.50 m NAP (Beindorff, 2014). The pressure level of the water in the aquifer is -1.5 to -1.6 m NAP. This results in seepage from the groundwater in this aquifer through the clay layer at a rate of 0.1 to 1 mm/day. The houses of this neighbourhood are founded on concrete poles, lower groundwater levels pose no risk to them.

The downspouts from the houses are not connected to the bioswales but to the sewer system. There were plans for disconnection, but none have been implemented at this time. However, experience has shown that these (older) downspouts tend to break-off at surface level, from which the water would flow to the bioswales. In the field, this was not observed. Most run-off comes from the mainly grassed gardens. Normally, it is expected that rainwater infiltrates here and run-off is only generated during high-intensity storms. However, due to the extremely poor permeable native soil, runoff occurs very quickly after the start of a storm. This matches the water nuisance mentioned by inhabitants, for which the bioswales were partially constructed.

3.4.3 Selected bioswale description

The above surface part and drainage pipes of all the bioswales were well-documented in the revision. However, even the revision did not always meet with field observations. There was very little information concerning the soil-composition of the bioswale, which needed to be determined in the field. The field work consisted of 2 drillings near the drain for every bioswale, 1 at the edge of the sandbed and 1 in the native soil. Further information on the bioswales came from pictures taken during construction, height measurements done in 2018 and work descriptions.

Bioswale A

This bioswale was constructed in the spring of 2017, and as such is 2 years old at the time of this field survey. In the original design the swale followed the corner of the garden, see the design drawing in Appendix 1. However, from field visits and depth-data, it became clear that the part around the corner (part 2) was slightly different. This part was not nearly as deep as part 1, and little to none ground improvement was done in the top-layer. Even so, the sandbed and drain underneath were constructed following the design. During the filling of this bioswale, water collected in the bowl of part 1 but part 2 remained dry. In addition, no significant reaction was seen in the groundwater level in the sandbed of part 2. As such, the lower half of the swale is considered a bioswale on its own, part 2 will not be considered any further.

The swale bottom lays at -2.0 NAP while the surrounding garden starts at -1.6 m NAP. The garden has a slight slope to the bioswale (from -1.5 to -1.6 m NAP), to convey the stormwater. The walkway through the garden is paved and dewateres to the bioswale as well. The swale bowl was constructed fluently, as can be seen in Figure 10 and the height map in Appendix 1. The top-layer of the bioswale is improved at the bottom above the sandbed, the sides and the rest of the bottom are the same as the top-soil of the garden. Underneath the top-layer at the bottom is a sandbed consisting of drainage sand, which is followed by a clay layer. The exact depth of the drain was not checked in the field, according to pictures taken during construction the bottom of the drain should be located 10-20 cm from the bottom of the sandbed.

The groundwater level next to the drain was found to be at -2.4 m NAP, which is 20 cm higher than it should have been (as it should be the same as the set drainage level). The drain is connected to the DIT-sewer (Drainage Infiltration Transport) and should maintain the set drainage level.

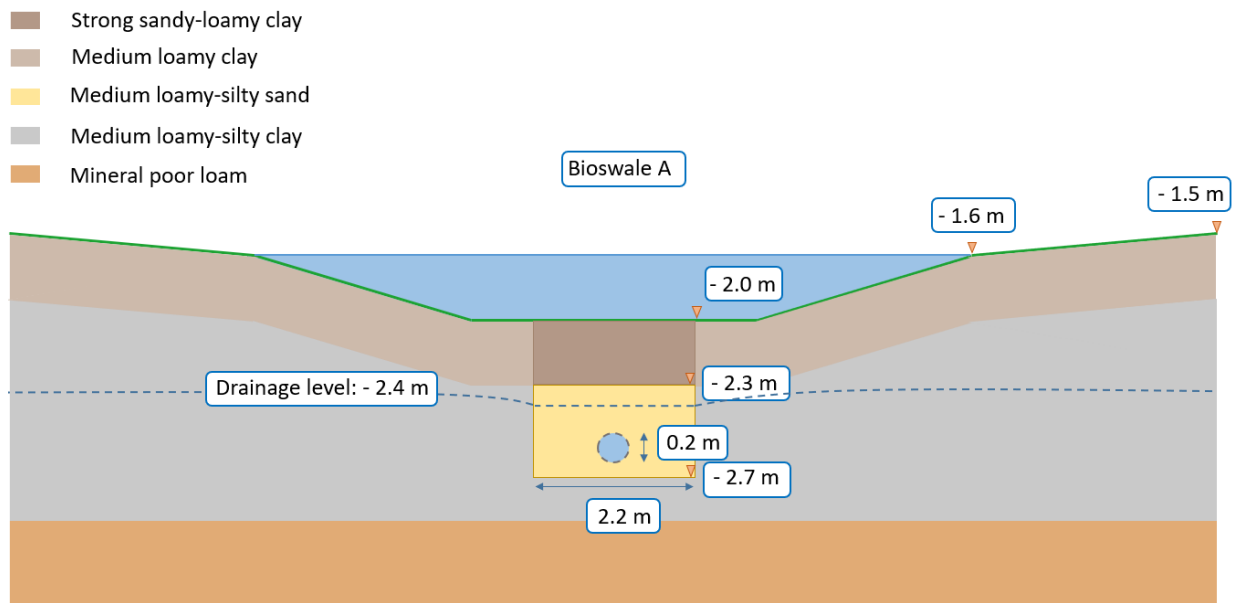


Figure 9: Schematization cross-section bioswale A



Figure 10: Picture bioswale A after filling

Bioswale B

This bioswale is located at the outside of the Zeno-neighbourhood and is one of the two smaller bioswales. It was constructed at the same time (spring 2017) as bioswale A. The shape of the bowl is well defined and fits the design reasonably well. The swale bottom lays at -1.9 m NAP while the surrounding garden starts at -1.6 m NAP. The garden has a slight slope to the bioswale (from -1.5 to -1.6 m NAP), to convey the stormwater (see the height map in Appendix 1). The walkway surrounding the garden at 3 sides is paved and dewateres to the bioswale. The top-layer of the bottom with the sandbed underneath is improved with sand and compost, the sides and the remaining bottom are the same as the rest of the green-area. About 20 cm underneath the top-layer at the bottom starts the drainage sand.

This layer has a depth of 70 cm and contains the drainage pipe, with the drain bottom at 10-20 cm from the bottom of the sandbed. Unlike the drain of bioswale A, this drain is connected to an end-manhole of a combined sewer system and is free-flowing. The bottom of the drain lays at -2.60 m NAP, which is the set drainage level for this area. The groundwater level in the sandbed is at drainage level, the groundwater at the edge of the bioswale in the native soil lays at -2.55 m NAP.

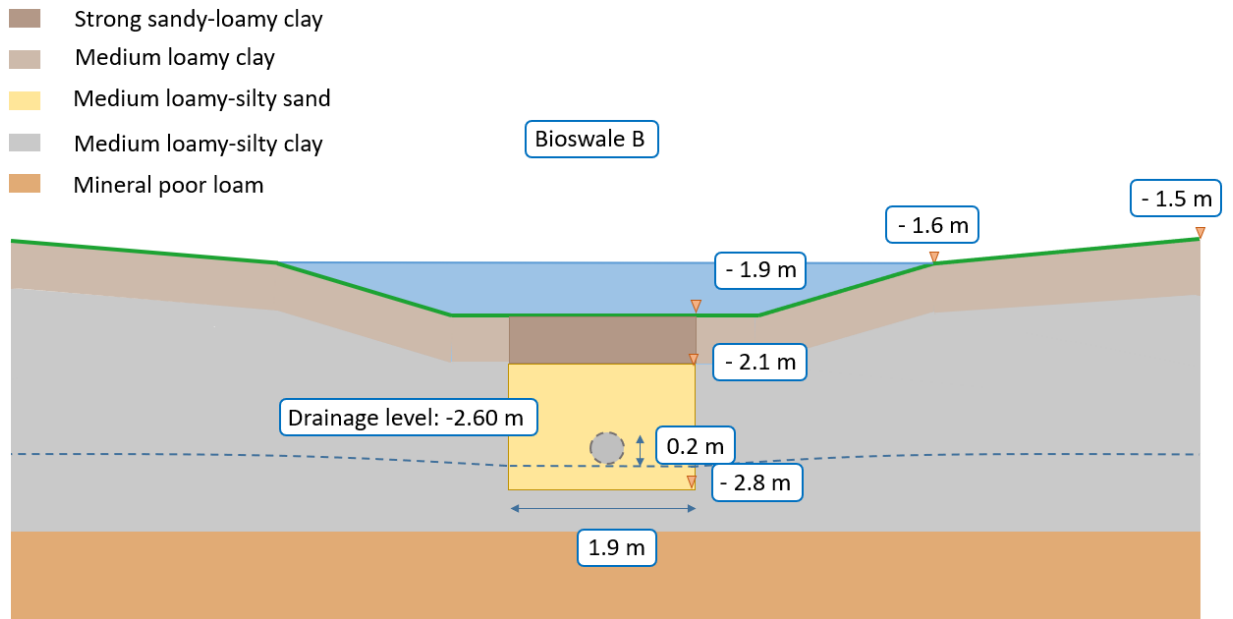


Figure 11: Schematization cross-section bioswale B



Figure 12: Picture bioswale B after filling

Bioswale D

This bioswale is located at the outside of the Zeno-neighbourhood and is one of the two smaller swales. It was constructed at the same time (spring 2017) as the previous bioswales. The shape of the bowl is reasonably defined and fits the design very well. The swale bottom lays at -1.9 m NAP while the surrounding garden starts at -1.6 m NAP. The garden has a slight slope to the bioswale (from -1.5 to -1.6 m NAP), to convey the stormwater from the surrounding grass (see the height map in Appendix 1). The walkway surrounding the garden at 3 sides is paved and dewateres to the bioswale. The top layer above the sandbed is improved with sand and compost, the sides and the remaining bottom are the same as the rest of the garden. The drainage sand starts about 20 cm underneath the top-layer of the bottom. This layer has a depth of 70 cm and contains the drainage pipe which bottom lays at 10-20 cm from the bottom of the sandbed. Like the drain of bioswale B, this drain is connected to the end-manhole of a combined sewer system and is free-flowing. The bottom of the drain lays at -2.60 m NAP, which is the set drainage level for this area. As such, the groundwater level next to the drain is at the set level. In dry conditions, the groundwater in the native soil directly next to the sandbed is at -2.60 m NAP as well. It should be noted that the groundwater outside the bioswale is not measured for this swale, but a slight slope to the drain can be expected. This would fit with the drain discharge data, as the drain keeps discharging during dry conditions.

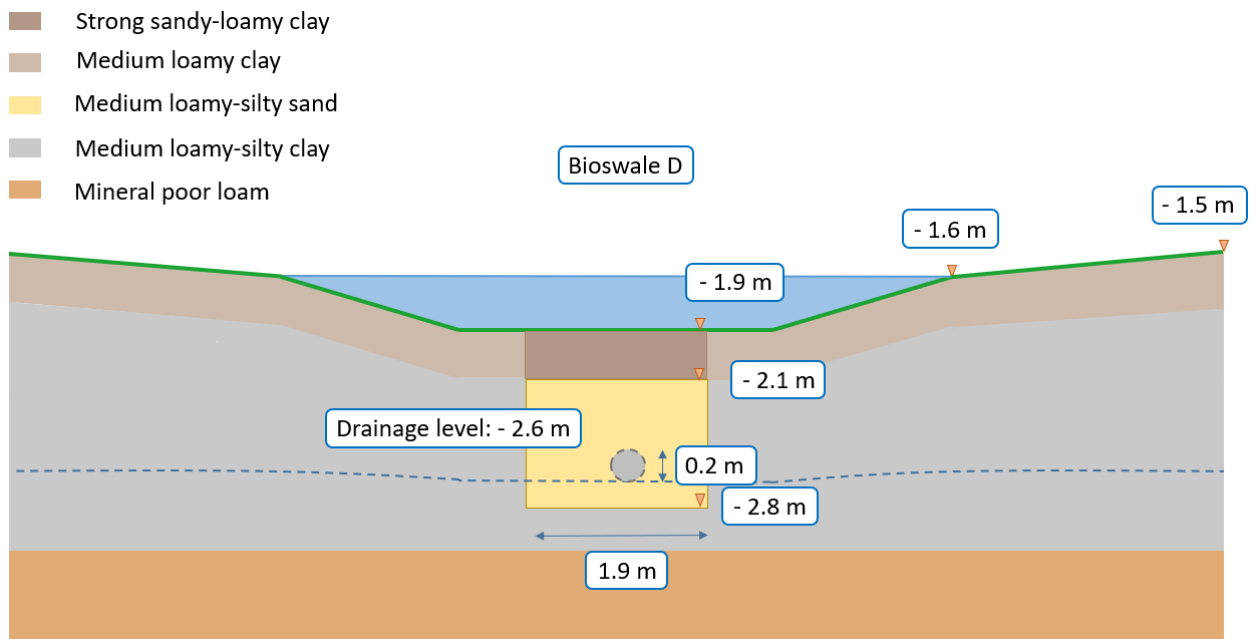


Figure 13: Schematization cross-section bioswale D



Figure 14: Picture bioswale D after filling

Bioswale E

This bioswale was constructed at the same time as the other bioswales (spring 2017). The bioswale bowl is also constructed fluently and has a less clear shape than the previous bioswales which can be seen in the height map in Appendix 1. It has less depth than bioswale A, but is much wider. The swale bottom lays at -1.9 m NAP while the surrounding garden starts at -1.6 m NAP. The garden has a slight slope to the bioswale (from -1.5 to -1.6 m NAP), to convey the stormwater. The walkway through the garden is covered with gravel and dewaterers to the bioswale as well. The top-layer of the bioswale is improved at the bottom above the sandbed, the sides and the rest of the bottom are the same as the top-soil of the garden. This means they are slightly improved and consist mainly of peat and clay. Underneath the top-layer at the middle of the bottom is a sandbed consisting of drainage sand, with a drain located inside. The bottom of the drain should be located at 10-20 cm from the bottom of the sandbed. The native soil surrounding the bioswale was found to be loam or clay, depending on the location. There was also rubble found in these soils. The groundwater level next to the drain is located at -2.3 m NAP, which is again higher than the set -2.6 m NAP. As for the previous swales, the groundwater in the native soil close to the bioswale showed a lower level (-2.43 m NAP). The drain is connected to the DIT-sewer and should maintain the set groundwater level. In the original design, there was also a bioswale at the other side of the path through the garden. However, this second bioswale was removed from the plans as it could not be constructed around the large trees present in that part of the garden. As a result, this side of the garden often experiences water nuisance due to rainfall. Especially around the trees where the surface level is lower, ponds form and can remain for days.

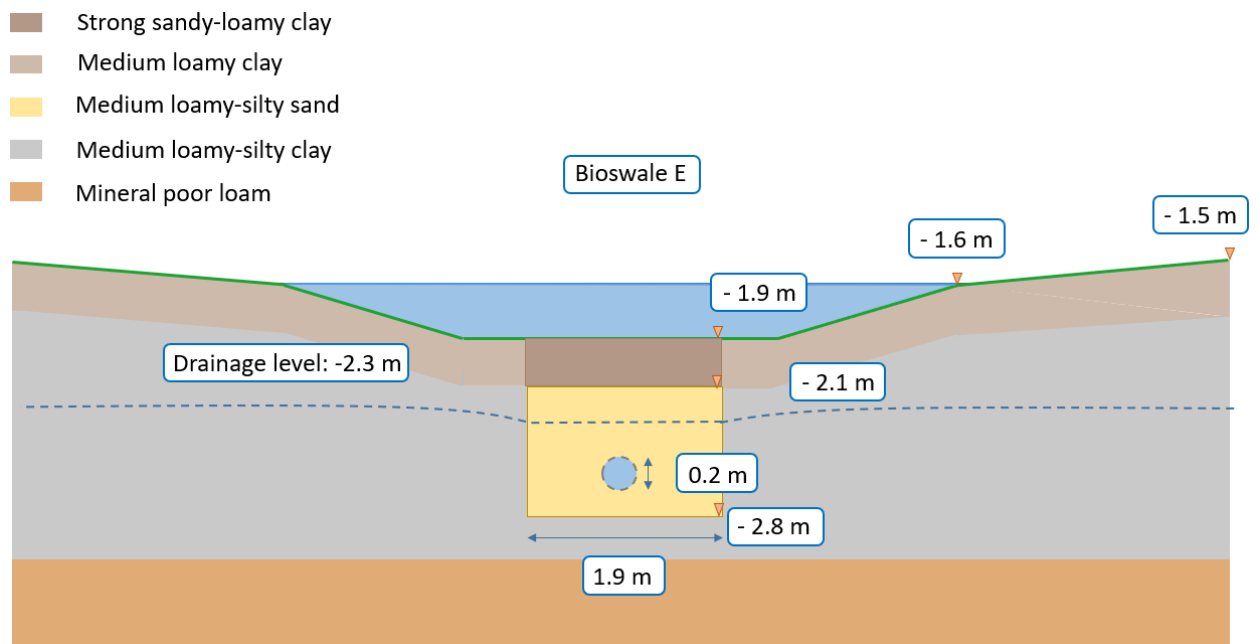


Figure 15: Schematization cross-section bioswale E



Figure 16: Picture bioswale E after filling

Bioswale 7

This bioswale is quite different from the other bioswales in the Zeno-neighborhood. It was constructed 2014, and thus 5 years old during the measuring campaign. It was designed to deal with both the stormwater from the surrounding garden and function as overflow basin for the DIT-sewer of the neighborhood. Due to miscommunication, a dike was constructed around the bioswale in order to retain the water from the overflow, since the surface level of the swale bottom was slightly higher (10 cm) than that of the surrounding garden. Therefore, the stormwater from the garden could not enter the swale, and instead gathered in the lower spots of the garden and could remain there for days.

The surface level of the bioswale bottom lays at about -1.83 m NAP, the dikes -1.55 m NAP and the lowest area directly next to the bioswale -1.95 m NAP (see the height map in Appendix 1). The bottom of the bioswale has a 20 cm layer consisting of a mixture of clay, compost and sand. Lumps of clay were found in the top of the sandbed, suggesting some re-use of native soil took place here. The groundwater level measured next to the drain is -2.50 m NAP, close to the set drainage level. However, the groundwater level in the native soil is much higher (40 cm), suggesting the drain is draining quite a large area. This is supported by the discharge data of this bioswales, as it has the largest discharge of all the swales in dry conditions.

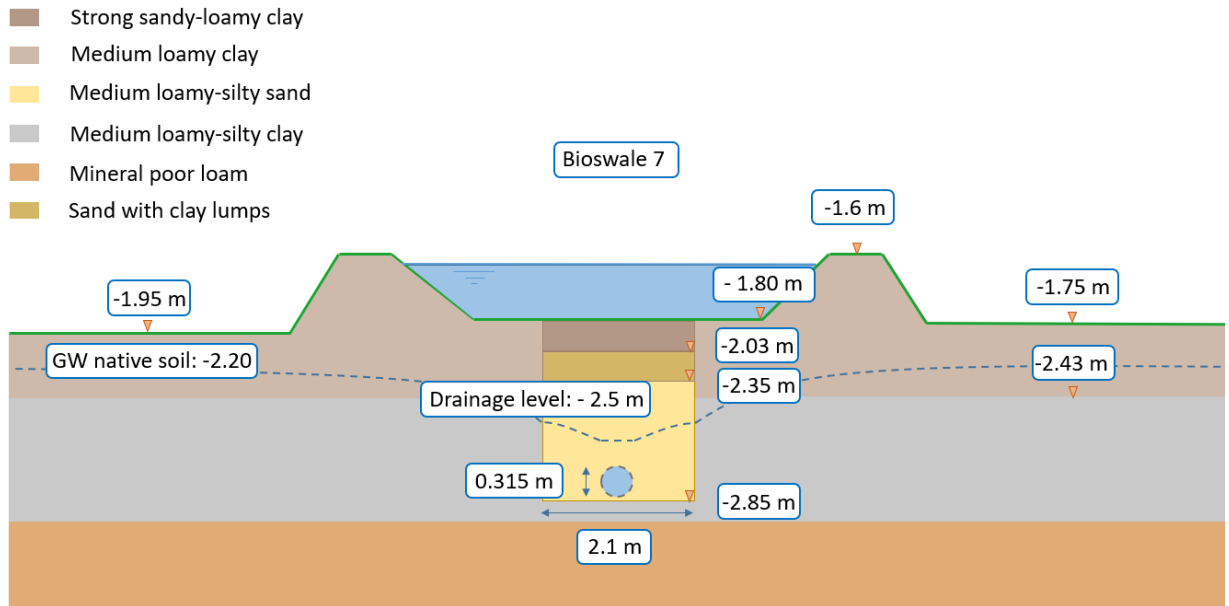


Figure 17: Schematization cross-section bioswale 7



Figure 18: Picture bioswale 7

4 Method and materials

As the case study area has been discussed in the previous section, the monitoring method and materials shall now be treated. To start, the 4 storms which will be simulated are discussed including the simulation periods. This is followed by the measuring equipment used, such as the discharge measuring device and the water level measuring devices. Afterwards, the laboratory tests for the soil properties and the modeling program are explained. This chapter ends with the introduction of some (new) metrics, to better describe the hydraulic behavior of the bioswales.

4.1 Storm simulations

In this field survey, the hydraulic functioning of bioswales in Rotterdam will be investigated. To this end, 4 storms will be simulated by filling the bioswales manually. As the literature study has shown that storm size and distribution can affect the hydraulic behavior, the simulation storms have different sizes and distributions to see the effect in polder conditions. The findings on the influence of the initial moisture conditions from the literature review were more diverse. As such, dry and wet initial conditions are considered in this research as well. The manual filling is done using a tractor with a water tank of 10 m³ (see Figure 17), which is filled at a near surface water body. To protect the vegetation and soil, a protective canvas was used during filling. The 4 storms simulated are defined by filling time and water volume, they are not directly linked to rainfall intensities. As the inflow to a bioswale depends just as much on the connected surface area, and this area can differ greatly per bioswale, it was decided to not simulate the runoff process in relation to the bioswale.

The measuring period ranges from the 18th of February till the 2nd of July. The 4 simulations for every bioswale were completed within 25 days of each other or less. Bioswale A was measured between 21st of March and the 17th of April, Bioswale B between the 15th of May and the 2nd of July, bioswale D between the 18th of February and the 9th of March, bioswale E between the 15th of May and the 2nd of July and bioswale 7 between the 12th of March and the 19nd of March.



Figure 19: Tractor with water tank

4.1.1 Heavy dry storm (1): Short large intensity storm in dry conditions

This storm fills the bioswale to a large extent in 1 hour. The simulation takes place in dry conditions, having an antecedent dry weather period (ADWP) of approximately 5 days (excluding very small events). This storm simulation is comparable with an intense, but short storm after a dry weather period. It will show the hydraulic performance in case of extreme rainfall in dry initial conditions, as well as the effect of the initial moisture content when compared with storm 2.

4.1.2 Heavy wet storm (2): Short large intensity storm in wet conditions

This storm fills the bioswale bowl bioswale to a large extent in 1 hour as well. However, this will be done under wet conditions. The bioswales have either experienced rainfall within 20 hours before the simulation or the simulation was done right after storm simulation 1. This storm simulation is comparable with an intense, but short storm in wet conditions. It will show the hydraulic performance in case of extreme rainfall in wet conditions, as well as the effect of the initial moisture content when compared with storm 1.

4.1.3 Double peak storm (3): Two successive storms

This storm first partially fills the bioswale ($> \frac{1}{2}$ total storm inflow of storm 1). After some time, depending on the infiltration capacity of the bioswale, the swale is filled again. The second filling is done while there is still water inside the swale from the first filling, how much differs per simulation. Both the first and second inflow occur within 1 hour. This storm simulation will show the effect of storm distribution, as the same water volume is used as in storms 1 and 2.

4.1.4 Medium storm (4): Medium intensity, long duration storm

This storm has a much smaller volume than the other 3 storms ($< \frac{1}{2}$ storm 1) and has a duration of 2 hours. By comparing the results from this storm with storm 1, the effect of storm size on the hydraulic behavior can be quantified. In addition, as this is the only storm with a long duration inflow, it would be interesting to see the effect on the shape of the discharge hydrograph. As most of the storm events in The Netherlands will have a greater resemblance to this storm than to the other storms, it will also give an idea about the hydraulic behavior which can usually be expected.



Figure 20: Filling of bioswale D

4.2 Measuring equipment

This section has been devoted to the measuring devices which will be used in this monitoring campaign. First, the discharge measuring device which has been designed for this campaign is treated. A more extensive overview of this device can be found back in Appendix 2.

Following the discharge device, the water level measuring instruments for both surface water and ground water measurements are discussed including their placement in the bioswales.

4.2.1 Discharge measurements

In order to quantify the hydraulic behavior of the bioswales, the discharge from the drains is measured for each storm simulation. With this data, metrics like the peak reduction, peak delay and volume reduction can be determined and bioswale performance can be evaluated. The outflow from the bioswales takes place from the drainage pipes, these dewater onto the local sewer system. Two of the drains discharge onto the combined sewer system and are free-flowing, three discharge on the DIT-sewer and are submerged. This makes discharge measurements challenging, as a portable device is needed which can measure both free-flowing and pressurized flows. As a satisfying solution could not be found in the existing measuring devices, a new device was designed, constructed and laboratory tested. More information concerning the development process of this new discharge measuring device can be found in Appendix 2.

Discharge measuring device

The developed discharge measuring device is applicable for drains and other clean-water pipes connected to a manhole. As this manhole is closed off from all other pipes, this should not cause problems for the remaining sewer system. A frame with pumps and floaters is put inside the manhole, the pumps outflow is connected to a tipping bucket. When the drain discharges, the water level in the manhole increases since the outflow has been blocked. This activates the floaters, which are set to the original water level, which in turn activated the pumps. When the water level decreases to the original level again, the floaters deactivate the pumps. The water which is pumped up by the pumps is counted by the tipping bucket, which tips every 3 liters. The discharge from the bioswale is determined by combining the number of tips for 10 minutes. Figure 21 below shows the discharge measuring set-up in the field, a schematization is given in Figure 22 for a submerged drain. The situation for a free-flowing drain is only slightly different, this can be found back in Appendix 2 showing both situations. Here, the design and functioning of the discharge measuring device will be explained in more detail as well.

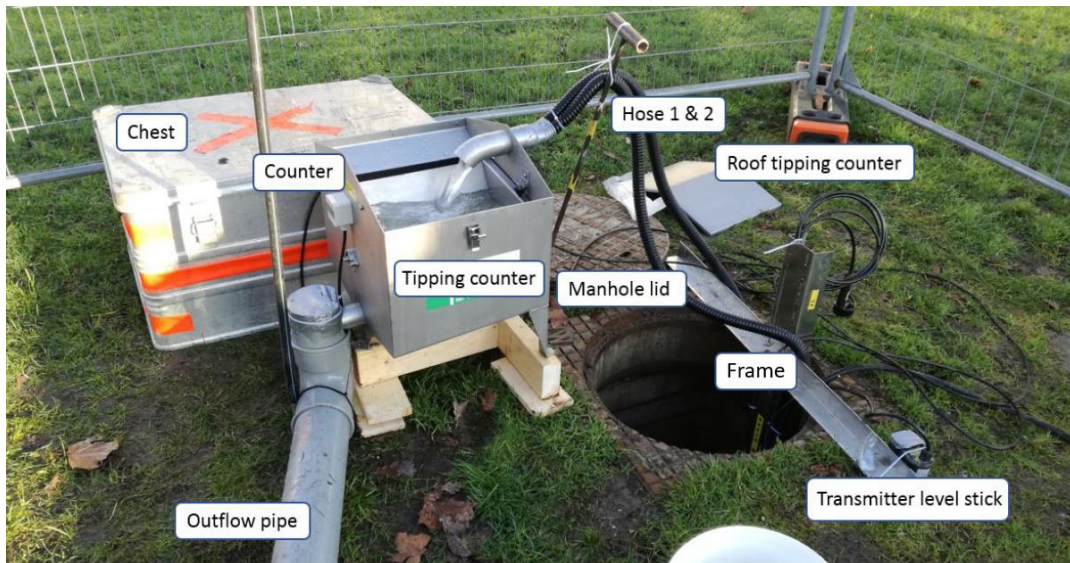


Figure 21: Discharge measuring device in the field

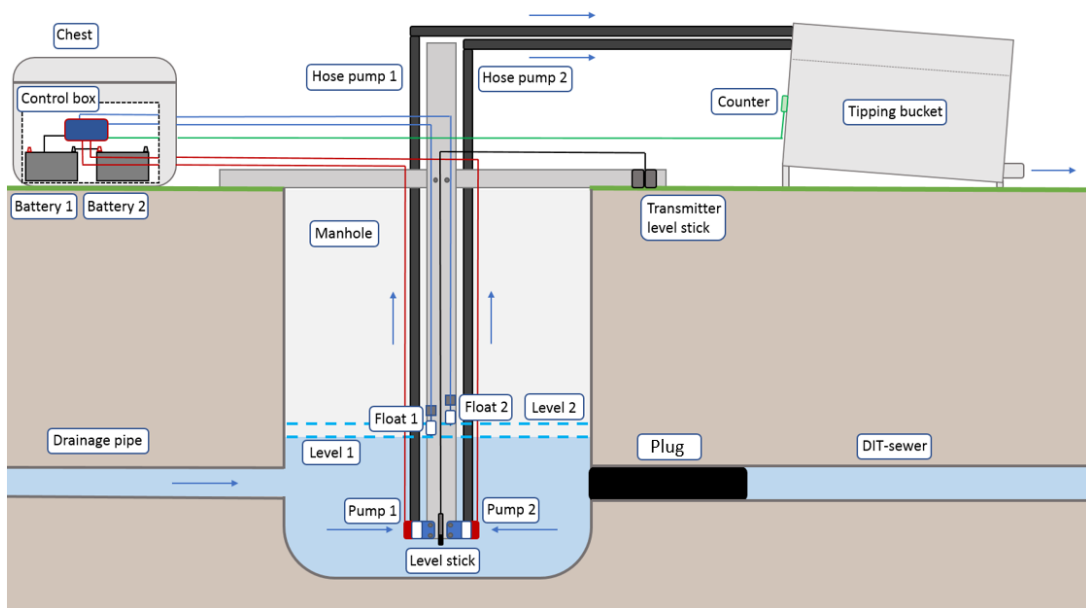


Figure 22: Discharge measurements submerged drain

4.2.2 Groundwater and surface water level measurements

In order to determine the emptying time of the bioswale, the water level in the bioswale needs to be measured during the storm simulations. To this end, 2 divers are placed inside the bioswale bowl. They are placed as far apart as possible, while still ensuring they are located at the lowest area(s) in the bioswale. The groundwater levels are measured with level sticks, only in bioswale B divers are used as well. To correct these absolute pressure measurements, the air pressure is recorded in the laboratory of the VLG where there is a constant temperature of 20 degrees Celsius. The off-set of the divers was determined using dry measurements of the respective diver. All pressure sensors have a measuring interval of 1 measurement per minute.

Placement of divers and piezometers

The divers measuring the water level in the swale bowl are pressed into the topsoil, so as only the top part (with pressure sensor) remains above the surface level. This method ensures that the divers are not moved during or in-between simulations. The height of the piezometers above surface level were measured by hand, as well as the length of the wire/cable of the divers/level sticks from the top of the piezometer to the pressure sensor. This data was used to determine the depth of the groundwater relative to the surface level. The piezometers were scheduled to be measured relatively to NAP as well (with spirit level), this could not be done as they were removed prematurely. The pressure measuring sensors in the piezometers were installed at least 24 hours before the simulations were started for the specific bioswale, and were not removed between simulations. As the data from the level sticks could be retrieved using a Bluetooth connection and mobile application, the functioning of the equipment could be monitored without removing them. The piezometers were constructed in two rounds, so that questions arising from the first measuring round could influence the placement of the piezometers for the second round.

The first round consists of bioswales A, D and 7, the second round of bioswales B and E. From the first round, it became clear that the groundwater table was influenced much more and further away from the drain than expected, as such bioswales B and E have an extra piezometer further away from the others. It was also found that the groundwater level away from the drain was lower than close to the drain, this also made a measurement further away from the drain more interesting. Figures 23 and 24 below show the placement of the piezometers for bioswale D, an overview for all the bioswales and the placement of a piezometer in detail can be found back in Appendix 3.

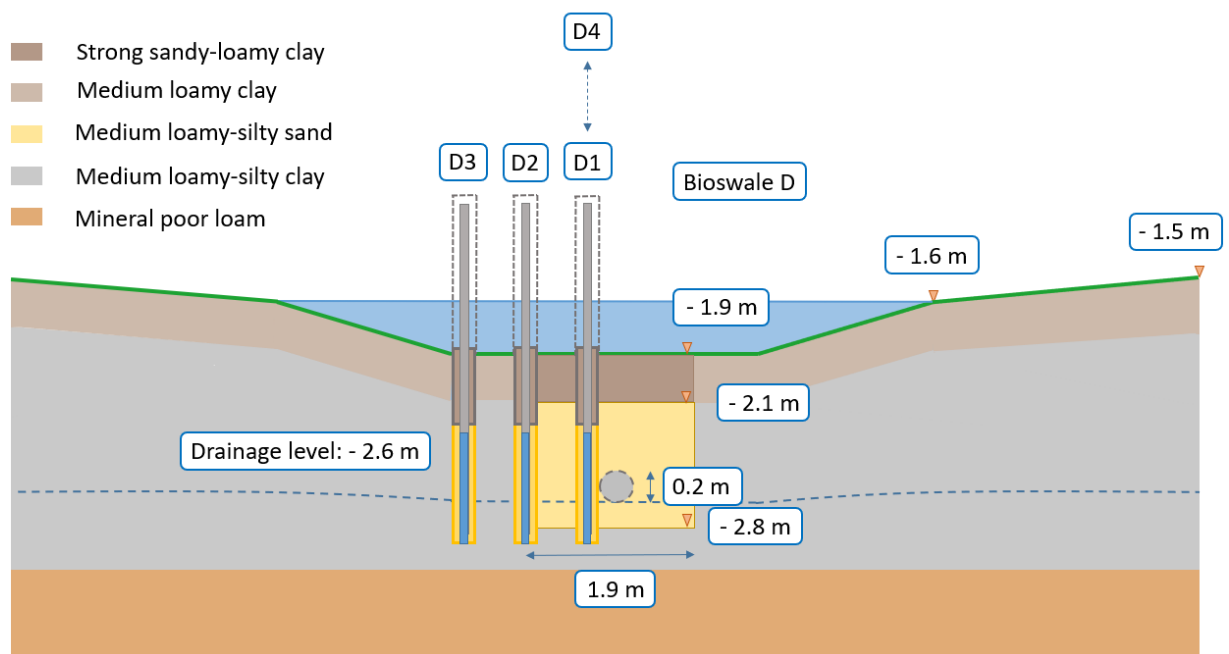


Figure 23: Piezometers bioswale D in cross-section

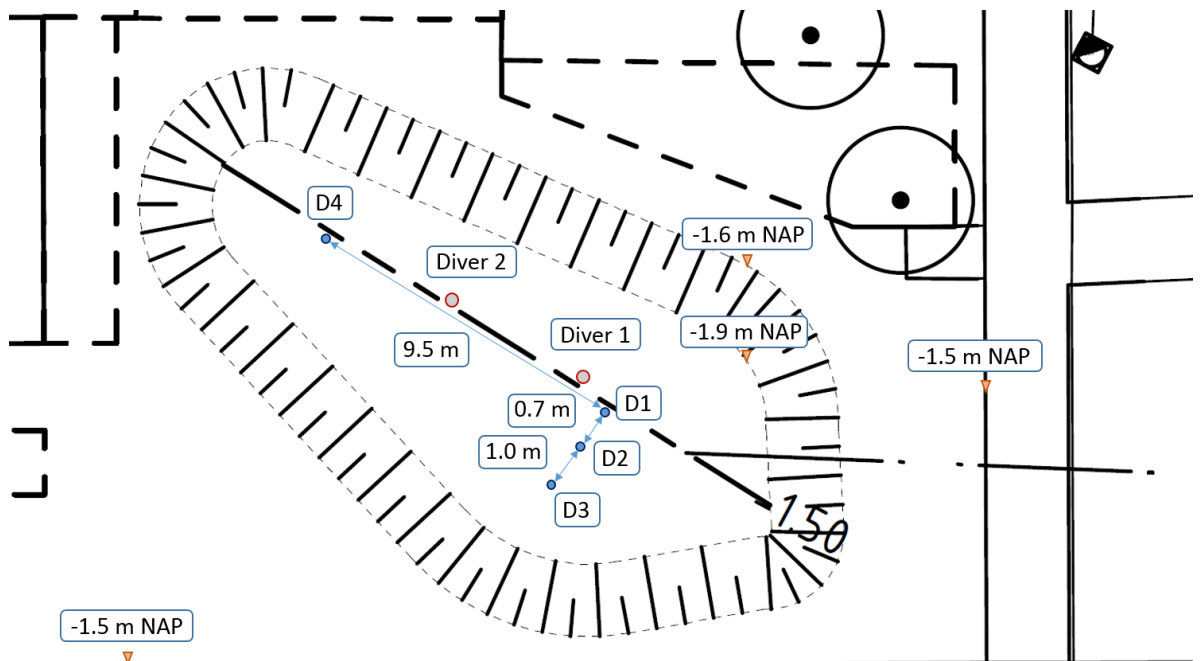


Figure 24: Piezometers and divers bioswale D in plane-view

Piezometer 1

This piezometer is placed next to the drain and is used to determine whether the topsoil or drain governs the infiltration at this location. If the groundwater level reaches the surface level here, all infiltration is limited by the drain. This piezometer also gives a good indication of the set drainage level of the bioswale drain. All bioswales have this piezometer, noted as A1, B1, D1, E1 and 71.

Piezometer 2

This piezometer is placed at the edge of the sand layer, to determine the bulging of the groundwater in the sandbed. If the groundwater at the edge of the sandbed reaches the surface level during infiltration, it shows that the drain partially limits the infiltration. All bioswales have this piezometer, noted as A2, B2, D2, E2 and 72.

Piezometer 3

This piezometer is placed just inside the native soil (mostly clay), to determine if this low-permeability soil plays a part in the infiltration process. As the native soil has very low permeability, this piezometer is placed only 0.5 inside this layer to ensure a reaction is observed. All bioswales have this piezometer, noted as A3, B3, D3, E3 and 73.

Piezometer 4

This piezometer is placed next to the drain like piezometer 1, but on the other side of the bioswale. In addition to serving as a back-up for piezometer 1 as it proves difficult to locate the drain in the field, it also indicates if the infiltration is equal over the bioswale length. As bioswale B is very small, it is only equipped with piezometer 1. The piezometers in the other bioswales are A4, D4, E4 and 74.

Piezometer 5

This piezometer is placed at the edge of the bioswale bowl, to determine what the groundwater increase is here. As little effect was expected, only bioswale E and bioswale B have this piezometer, since they were constructed in the second measuring round. However, as bioswale E is the largest bioswale with the most permeable native soil, and bioswale B has the longest emptying time, these might be the most interesting bioswales to observe. These piezometers are named E5 and B5. In addition, a piezometer was placed in bioswale A, in the sandbed of part 2. Though this part of the swale is not receiving any water, the drain and sandbed do run through both parts. As such, for a good evaluation it needs to be determined if part 2 experiences any effects of the filling from part 1, and as such influences the hydraulic behavior. This piezometer is called A5.

4.3 Soil-parameters determination by laboratory experiments

In order to help explain results from the storm simulations, and make recommendations concerning soil-application in bioswales, the soil-hydraulic properties need to be determined. Several tests were done in the laboratory for the different soils inside and surrounding the bioswale, using the results the soil-hydraulic parameters can be determined using the neural-network prediction function of Hydrus 2D/3D.

4.3.1 Laboratory experiments

During the placement of the piezometers in the bioswales, two soil samples were taken from the top and two from the sandbed to be analyzed in the laboratory of the VLG. These soils were disturbed during sampling. In addition, undisturbed samples were taken from the native soil next to the bioswales. This was done by hammering a case into the soil, which was then retracted with the soil sample and sealed off. For bioswales A, B, D and E, two soil samples of the top-layer and one sample from the sandbed were analysed by means of: (1) a sieving-curve including sand, silt and loam percentage, and (2) burning to determine the organic content. In additions, for two sandbed samples per bioswale, the saturated hydraulic conductivity (K_s) and the dry bulk density (BD) were determined. For bioswale 7, 2 samples from the top-soil were analyzed and none for the sandbed. At last, the undisturbed soil-samples of the native soil next to every bioswale were analyzed with a K_s -test for undisturbed, cohesive soils.

The following methods are used:

K_s disturbed: Permeability constant head following the NEN 5123.

K_s undisturbed: Permeability constant head following the NEN 5124.

Organic content: RAW 2015, test 28 ('gloeiverlies')

Soil-texture: Sieving curve following NEN-EN-933-1

Dry-bulk density: Determining wet and dry volume weight following NEN 5111

4.3.2 Soil-parameter determination

In order to estimate the soil hydraulic parameters from the soil textural data retrieved from the laboratory tests, the neural network prediction of Hydrus 2D/3D is used (Model 3: percentage sand, silt and clay + dry bulk density). This prediction determines:

Soil residual water content (θ_r) (cm³/cm³)

This is defined as the water content for which the gradient $d\theta/dh$ becomes zero.

Soil saturated water content (θ_s) (cm³/cm³)

This is the water content of the soil when it has been completely saturated, which is equal to the porosity.

Shape parameter (α) (>1, [1/cm])

This scale parameter is inversely proportional to mean pore diameter and the air-entry value of the pF-curve. When the mean pore diameter increases, this scale parameter decreases.

Shape parameters of the soil water characteristic (n) (>1, [-])

This parameter is a measure of the pore-size distribution and influences the shape (slope) of the pF-curve. When the suction force of a soil increases, the n increases as well.

Saturated hydraulic conductivity (K_s) (cm/d).

Describes the ease with which water can move through the pore spaces or fractures of a saturated soil.

In order to predict these parameters, Hydrus 2D/3D was coupled with the Rosetta Lite DLL (Dynamically Linked Library) developed by Schaap at the U.S. Salinity Laboratory (Schaap et al. 2001). Rosetta implements pedo-transfer functions (PTFs) which predict van Genuchten's (1980) water retention parameters and the saturated hydraulic conductivity (K_s) from the soil textural distribution and bulk density. The prediction uses 2134 samples for water retention parameters (θ_r , θ_s , α , and n) and 1306 samples to determine K_s (Schaap et al. 2001).



Figure 25: Pictures K_s -test disturbed samples in laboratory

4.4 Hydrus 2D/3D calibration

In order to explain the behaviour observed during the monitoring program, Hydrus 2D/3D is calibrated using the discharge data from the monitoring campaign. The soil hydraulic parameters obtained using this method are likely the most reliable.

4.4.1 Formula used in the model

The soil hydraulic parameters which will be calibrated are the soil residual water content (θ_r), the soil saturated water content (θ_s), the shape parameters (α and n), and the saturated hydraulic conductivity (K_s). The model uses the retention function of van Genuchten (1980) to determine the water content at different depths:

$$\theta(h) = \theta_r + \frac{\theta_s - \theta_r}{(1 + (\alpha h)^n)^{1-1/n}}$$

Where $\theta(h)$ is the volumetric water content (cm^3/cm^3) at the suction h (cm, taken positive for increasing suction). Combining this equation with Mualem's (1976) pore-size model yields:

$$K(S_e) = K_0 S_e^L (1 - (S_e^{n-1})^{1-1/n})^2$$

Where the effective saturation (S_e) is computed as:

$$S_e = \frac{\theta(h) - \theta_r}{\theta_s - \theta_r}$$

K_0 is a fitted matching point at saturation (cm/d) while L (-) is an empirical parameter (Mualem 1976). It was shown that K_0 and L were poorly related to the dry bulk density and soil texture (Schaap et al. 1998), and thus can better be determined in a different way. Schaap and Leij (2000) found that fitted K_s values were usually one order of magnitude smaller than the K_s , and the fitted L were often negative having an optimal value of -1, instead of the value of 0.5 which is usually assumed. However, a $K_0 < K_s$ leads to a untenable situation near $S_e = 1$ or $h = 0$ cm, as such only $L = 0.5$ will be adapted to $L = -1$ (Schaap et al. 2001).

4.4.2 Input data of the model

As complete discharge data was only available for bioswales A, D and E, only these swales are modelled. As the model is 2D, only a cross-section of each bioswale can be considered. These cross-sections are taken from the lowest part of the bioswale, which is (close to) the location of piezometers 1, 2 and 3. To get the discharge data for the whole bioswale, the discharge from the cross-section is multiplied with the bioswale length. As the shape of the bioswales is organic, the actual cross-section is not constant over the bioswale length. This should be kept in mind when interpreting the results and calibrating the model.

The discharge data from storm 1 is used to calibrate against, as this storm has the best discharge data available from the field-survey for all three bioswales. As the modeling and calibration turned out to be quite time-consuming (and automated calibration failed), the other storms are not included in the calibration. As Hydrus 2D/3D cannot correct the water layer height with the infiltrated volume, the water level decrease from the storm simulation is used as input for the ponding depth against time.

Since the depth of the water layer relative to the surface level differs over the cross-section, the water level is divided into 4 different heads relative to 4 different surface levels (4 was the maximum number for variable pressure heads).

Besides calibrating soil hydraulic parameters in order to fit the discharge data, the (calibrated) model also gives a deeper understanding of the processes which influence the hydraulic performance of the bioswale. If those processes are not represented correctly in the model, the results will not meet the field-data. This will give more insight in the contribution of macropores and the less-improved bioswale sides to the infiltration. It will also help to explain the shape of the discharge curve and of course will help determine the soil hydraulic properties of the different soils. Hydrus gives a graphical overview of the flow velocities in the soil, the soil moisture content and the pressure head. Figure 26, 27 and 28 give a preview of the results to illustrate the functioning of the model.



Figure 26: Bioswale E, flow velocities 0.36 days into the storm simulation

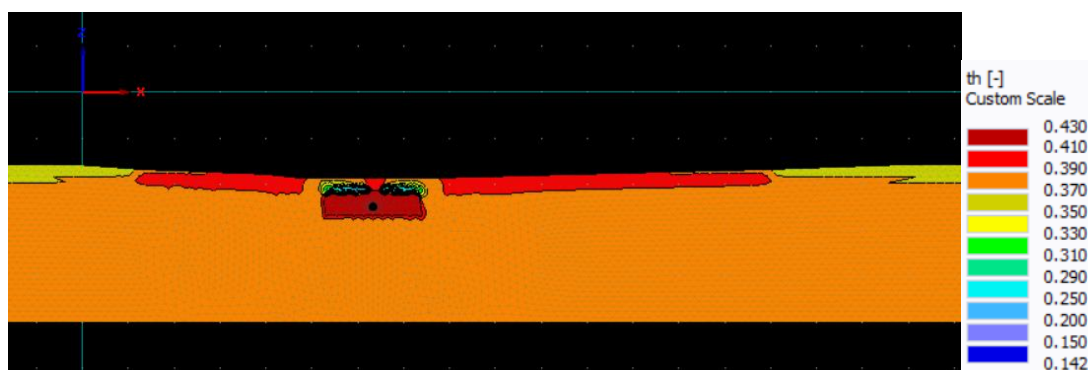


Figure 27: Bioswale E, water content 0.36 days into the storm simulation

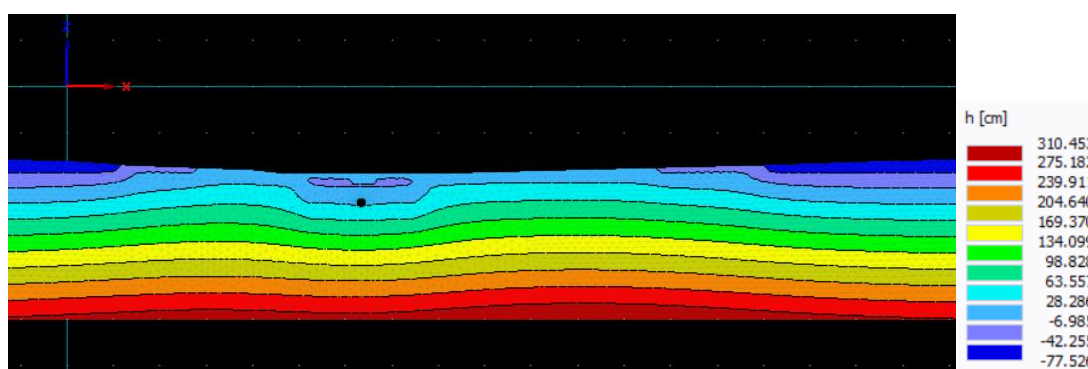


Figure 28: Bioswale E, pressure head 0.36 days into the storm simulation

4.5 Adaptations metrics

As it was found in the literature study that additional metrics would help to describe the hydraulic behavior of a bioswale more completely, this chapter will propose a few of such metrics. In addition, some alterations will be done as well to existing metrics to better describe the obtained results.

4.5.1 Altering existing metrics

Some alterations have been made to better represent the hydraulic behavior of the bioswales considered in this research. As the outflow can last much longer than 24-hours (also experienced by Davis 2008), the outflowing volume ends when the discharge is below 95% of the peak discharge, corrected for the natural discharge. This time-frame can be shortened when natural rainfall soon after the storm simulation starts to contribute to the discharge.

$$f_{v-95\% \text{ peak}} = \frac{V_{\text{out-95\% peak}}}{V_{\text{in}}}$$

V_{in} is the input storm water volume to the bioswale; and $V_{\text{out-95\% peak}}$ is the corresponding outflow volume leaving the cell (outflow till the discharge < 95% peak discharge).

As the storms are artificially simulated, different interpretation for the parameters used to construct the peak delay and peak reduction are also needed. The swales are officially filled over the course of one hour. However, the real filling-time usually lays between the 30 and 70 minutes, and occurs in 1-3 inflow peaks of 10 m³ (depending on swale size). As simplification, the inflow is taken to always occur over 1 hour, and the peak is taken to occur in the middle of the storm (after 30 minutes).

4.5.2 New and less-known metrics

Beside the previous mentioned metrics, there are more ways to describe the hydraulic functioning of a bioswale. One very important metric is the emptying time of the swale, as most countries have determined a guideline value for this (Boogaard 2016). This is the time it takes for the bioswale bowl to empty again, once it has been filled.

$$T_{\text{emptying}} = T_{\text{start ponding}} - T_{\text{end ponding}}$$

In addition, one completely new and two less well-known metrics will be used as well. The new metric is the peak delay at the first effluent peak $R_{p1 \text{ delay}}$, the less-known metrics are the outflow delay $t_{q\text{-out-start}}$ and the total delayed volume V_{delay} (Donkers 2010). The first effluent peak is not a peak in the true sense of the word, since it does not lay between two lower points. However, after this first peak a strong decrease in the slope of the discharge graph is observed as illustrated in Figure 26. The absolute peak follows much later but is not much higher (~6%). This begs the question which peak should be considered when evaluating the peak delay time. As both the peak delay ratios are depended on the time when the peak occurs in the storm event, the peak delay time (time between the start of the storm and peak in the discharge) is also noted.

$$R_{p1 \text{ delay}} = \frac{t_{q\text{-peak1-out}}}{t_{q\text{-peak-in}}}$$

The outflow delay (T_{delay}) is the time between inflow and resulting outflow from the drain. This is also referred to as the reaction time of the bioswale and gives more insight in the delay which is realised by the swale. The total delayed volume (V_{delay}) is the volume which does not discharge during the storm event. As such, this is the volume which does not add to the water which the urban water system needs to convey during the storm event.

$$T_{delay} = T_{inflow} - T_{outflow} \quad V_{delay} = V_{in-t_storm} - V_{out-t_storm}$$

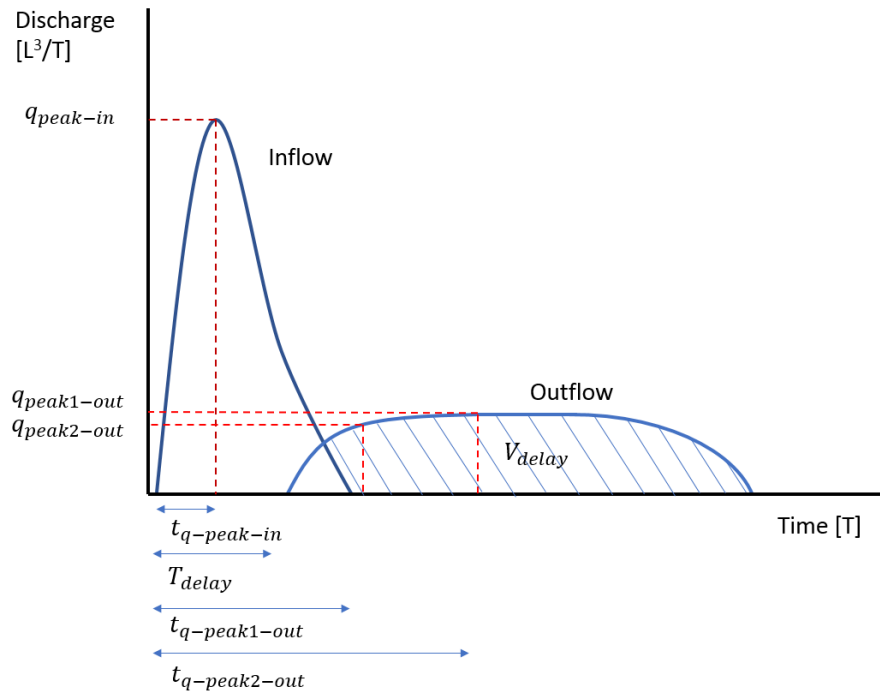


Figure 27: Representation metrics in a hydrograph

5 Results

With the case study area and methods and materials known, the results of the measuring campaign will be covered. This chapter is divided into three sections. The first section considers the observations made in the field, the second section the results of the measurements of the 5 bioswales ordered per storm simulation and the last section the results from the laboratory tests and modeling exercise. A complete overview of all the simulated storms and their results can be found back in Appendices 4 and 5.

5.1 Field observations

During the monitoring campaign, some interesting field observations were made which could potentially help explain the hydraulic behaviour or result in recommendations. The main observations include severe iron-oxidation on the measuring equipment, the state of the vegetation per bioswale throughout the measuring campaign and the state of the grassland where no swale was constructed.

5.1.1 Iron-rich seepage

From the drainage report (Municipality of Rotterdam, 2014) on the groundwater situation in the Zeno-neighbourhood, it could already be concluded that there was seepage occurring in this part of Rotterdam. This is quite standard in polder-conditions, as the drain of the bioswale will not only discharge the infiltrated stormwater, but groundwater as well.

During the monitoring period, severe iron-oxidation took place on the measuring equipment. This was the result of Fe^{2+} ions from the anaerobic-groundwater reacting with the oxygen inside the air. This resulted in an orange-brown scaling on the measuring equipment including the level sticks, hoses, tipping bucket, floaters and pumps (Figure 27). Especially the scaling on the floaters became a problem, as too much iron-oxidation inhibited the floats from moving. This sometimes resulting in a failure of the discharge measuring device. Since the drains of bioswales A, E and 7 lay beneath the groundwater table, they should not suffer from iron oxidation related clogging as no oxygen is present in the drains. However, as the drains of bioswales B and D are free-flowing and lay partially above the groundwater table, it is very likely that they will suffer from clogging due to iron oxidation in the future.



Figure 28: Oxidised iron in outflow pipe and on pump

5.1.2 Vegetation health

Vegetative quality of the surrounding green-area

Overall, the vegetation in the bioswales didn't seem to suffer much from the storm simulations. The quality of the grass was usually about the same as the grass of the surrounding green-area, or even slightly better (see the pictures in Appendix 1). The reason for this seems the lay with the native soil of the green-area. As this soil is very impermeable and has strong capillary forces, and the soil surface is bumpy allowing not all the stormwater to be conveyed to the bioswale, water is likely to remain on the surface and in the soil for quite some time after rainfall. As such, the grass in the bioswale might experience less water nuisance than the surrounding area during smaller storms, as the swale having an improved top-soil drains much quicker. The vegetation quality of bioswales B and D both inside and outside the swales are clearly worse than for the inner-gardens of bioswales A and E. This can be explained by the very large trees on one side and tall buildings on the other, capturing most of the direct sunlight. In addition, leaves and small branches from the trees accumulate on the grassed area.

Vegetative quality inside the bioswales

When considering the vegetative quality, bioswale E scores the highest. It is followed by bioswale A, which shows more weeds but is still well-covered. Bioswale D was completely covered and had no bare spots, but the grass was less tick than for bioswales A and E. This is likely due to the shortage of sunlight in inflow of leaves and branches, which is staffed by the state of the grass outside the bioswale being of the same quality. Bioswale 7 was completely overgrown with weeds and high-grass. The different grass specie had been placed there according to the design, though the weeds are likely a results of the bioswale being inaccessible to mechanical mowing due to the dike surrounding it. It is surely not the result of water ponding, since an overflow event should only occur once a year according to the design. Only one bioswale had clearly worse vegetational health than the surrounding grass, namely bioswale B (Figure 28). At the lowest part of this bioswale, little to no vegetation was present at all. This condition became significantly worse after the storm simulations. Large parts of the bioswale surface had no, or clearly drowned, vegetation. The large trees and buildings surrounding the bioswales played a role for this bioswale as well, though it does not explain the difference in quality between the grass in- and outside the bioswale.



Figure 29: Vegetation damage in bioswale B

Non-constructed bioswale

Interesting to note, was the quality of the grass in an inner-garden without a bioswale. There was a bioswale planned here, but due to old trees (and their roots) present, the swale was removed from the design. After rainfall, this area stands almost completely underwater, as it lies slightly lower than the elevated roads around it. Especially around the trees, where the surface level is at its lowest, water can pond for days. The same was observed for the low-laying area at the side of bioswale 7, where water could not flow into the bioswale as the swale was higher than the surrounding area. This again illustrates how impermeable the grass-land is in this polder, even after some ground improvement has been done.

5.2 Bioswale storm simulations

In this section, the most important results of the monitoring campaign will be discussed. As the monitoring of all 4 storms is only complete for bioswales A, D and E, these swales are discussed together in detail. For every storm, a table with the most important resulting metrics is provided for each of these bioswales. Only the graph of bioswale E is shown in this section, the graphs for all the bioswales can be found back in Appendix 5 and the complete tables in Appendix 4. The results for bioswales B and 7 are treated separately after bioswales A, D and E, the complete results can also be found back in Appendix 4 (tables) and Appendix 5 (graphs).

During the installation of the measuring equipment and processing of the data, the following was discovered. One of the divers placed in bioswale A failed in between storm simulations. Even though this diver was placed in a deeper part of the bioswale compared to the second diver, it cannot be used to compare water levels from different storms. As such, the other diver is used. This means that the actual water level in bioswale A is about 6.29 cm higher than reported. All discharge data is corrected for the baseflow, when this is present. Since the bioswale has an organic shape, estimating the location of the drain in the field proved difficult. When considering the groundwater data, it seems that piezometer E2 lays closer to the drain than piezometer E1, as the groundwater reaction is smaller. The same likely happened for bioswale B, as piezometer B2 also showed a weak reaction than piezometer B1. Lastly, it is known that piezometer A4 lays closer to the drain than piezometer A1, as the drain was found when installing piezometer A4.

5.2.1 Heavy dry storm (1): Discharge

The ascending dry period for bioswales A, D and E were respectively 20 hours (2 mm), 7.36 days (13 mm) and 2.92 days (2.5 mm). For bioswale D, during the simulation a small rainfall event was reported of 2 mm about 1/3 into the emptying time. No influence on the water level in the swale bowl could be observed from the water level decrease, it is unclear whether this event took place. The baseflows of bioswales A, D and E are respectively 1.0 l/min, 0.12 l/min and 0.0 l/min. The graph of bioswale E is given in Figure 29 below, the complete tables and graphs (ordered per storm) for all the bioswales can be found back in respectively Appendix 4 and 5. Bioswale A was measured on 26/03/2019, bioswale D on 18/02/2019 and bioswale E on 15/5/2019. The graph in Figure 30 below gives the water level in the bioswale (*Diver 1* and *Diver 2*), the groundwater levels at various locations (*E1 - E5*) and the discharge from the drain (*Discharge*). The time taken as 0 is the moment the inflow begins, all the water levels are relative to the bioswale bottom which lays roughly at -1.8 m NAP.

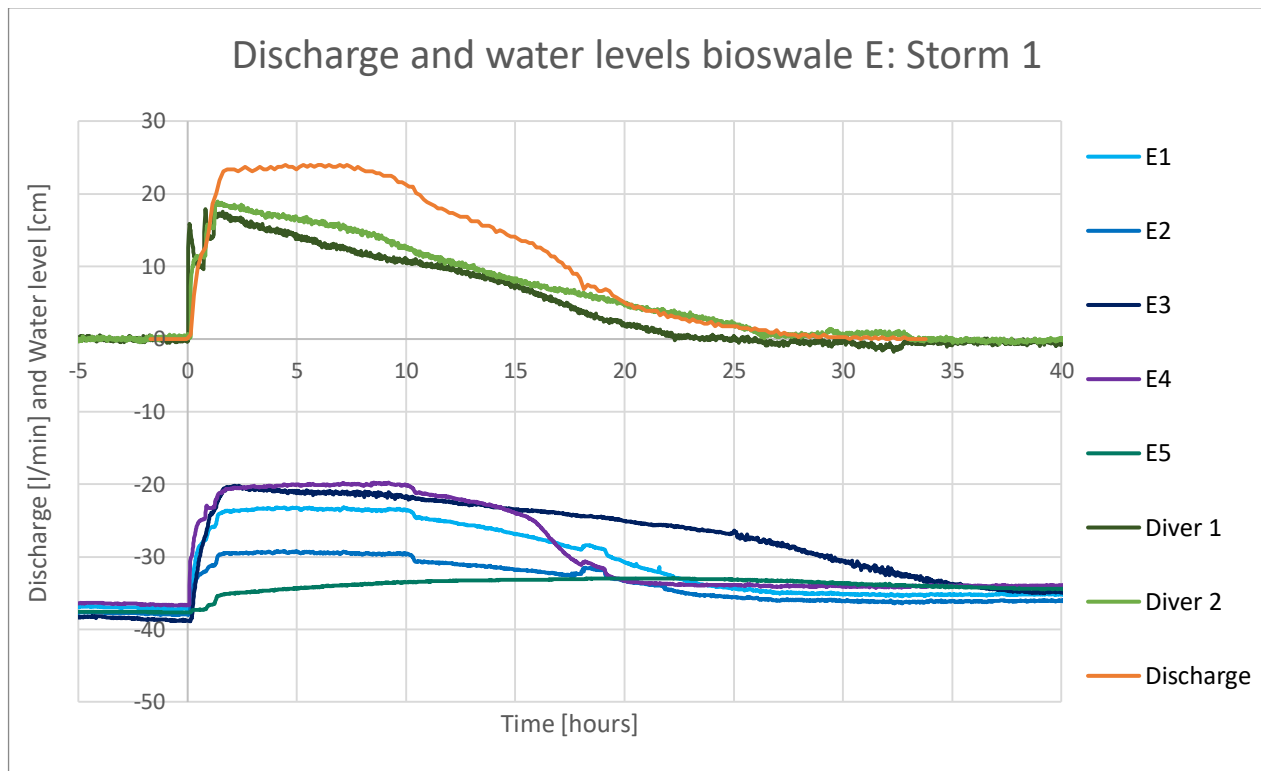


Figure 30: Heavy dry storm (1) bioswale E

Emptying time

In the last part of the graph of bioswale E, the decrease in water level is much slower than in the first part of the graph. In addition, one of the divers is dry way before the other one, even though they are both in low points. None of the bioswales are able to empty within 24 hours, though bioswale A gets close. They do all empty within 48 hours.

Peak reduction and delay

All bioswales show a clear fast first and absolute second peak in the discharge. Though these two outflow peaks roughly have the same magnitude (5-7% difference), they are widely separated in time. The peak reduction is highest for bioswales D, which has the longest emptying time as well. Since the emptying time depends on the discharge (and infiltration to the surrounding soil), this seems logical. The LID goal for peak reduction was to reach a value of 0.33 [-] or less, while the goal for peak delay was 6 [-] or more. As can be concluded from the data in Table 1 below, these goals are easily met by all three bioswales when considering the absolute peak discharge. However, if we look at the fast peak, the peak reduction is still extremely good but the peak delay takes a deep dive. In case of bioswale E, even under the LID goal of 6 (and just above for bioswale A).

Volume reduction and delay

The volume reductions of all three swales are quite low. This was to be expected, as the literature study showed that the volume reduction decreases when the inflow increases. In addition, the native soil (clay) is very impermeable, and not well suited for infiltration. Taking this into account, the achieved volume reductions (0.68 to 0.82) are actually much higher than expected. From all the bioswales, swale E has the highest volume reduction. This can be explained by both the large infiltration area of the swale and the more permeable native soil (more rubble and peat mixed with the clay). The delayed volumes are extremely high (99.6 – 98.0 %), this is the combined effect of the very large peak reduction which strongly limits the outflow both during and after the storm simulation, and the short storm duration. As the bioswales react quickly to the inflow (discharge increases after 3-14 minutes), the strat delay is quite low.

Table 1: Discharge data Heavy dry storm (1)

Heavy dry storm (1)	Bioswale A	Bioswale D	Bioswale E
T_{average} [°C]	10.44	6.75	15.92
h_{water} [cm]	20.4	22.6	18.6
T_{emptying} [hour]	29.3	38.4	26.4
$R_{\text{p1 peak}}$ [-]	0.028	0.021	0.047
$R_{\text{p2 peak}}$ [-]	0.029	0.023	0.048
$t_{\text{q-peak1-out}}$ [min]	299	191	118
$t_{\text{q-peak2-out}}$ [min]	539	911	328
$R_{\text{p1 delay}}$ [-]	10.0	6.4	3.9
$T_{\text{p1 delay}}$ [hour]	4.98	3.18	1.97
$R_{\text{p2 delay}}$ [-]	18.0	30.4	10.9
$T_{\text{p2 delay}}$ [hour]	8.98	15.18	5.47
f_v [-]	0.8	0.8	0.7
V_{delay} [%]	99.0	99.6	98.0

5.2.2 Heavy dry storm (1): Groundwater

From the groundwater data, a clear pattern can be observed. Near the drain, the groundwater will only increase slightly (about 2-5 cm). The strong reaction from the groundwater in the sandbed of bioswale E is most likely caused due to the placement of the piezometer, which is assumed to be further away from the drain (drain ends earlier than the bioswale). At the edge of the sandbed, the groundwater can increase much more (about 13-25 cm). This increase is the strongest in bioswale A, which also has quite a wide sandbed. The largest effect is shown by the piezometers just inside the native soil, which shows an increase between the 18 and 59 cm. The piezometers outside the bioswale only show a groundwater increase of 4.6 to 7.75 cm. Interesting enough, almost all piezometers seem to react simultaneously to the water in the bioswale. Only the groundwater outside does react slower compared to the groundwater inside the bioswale. As the piezometers could not be measured using spirit level as was originally planned, the absolute depth of the groundwater levels are prone to a much larger error (> 5 cm) than the relative groundwater changes (< 0.5 cm).

Table 2: Groundwater changes Heavy dry storm (1)

Heavy dry storm (1)	Bioswale A	Bioswale D	Bioswale E	Bioswale B
h_{water} [cm]	20.37	22.58	18.64	25.39
T_{emptying} [hours]	29.3	38.4	26.43	36.33
dh_{p1} [cm]	7.7	1.67	13.67	16.02
dh_{p2} [cm]	25.06	13.17	8.51	4.48
dh_{p3} [cm]	23.35	29.16	18.43	58.84
dh_{p4} [cm]	3.11	1.8	16.53	-
dh_{p5} [cm]	0.15	-	4.6	7.75

5.2.3 Heavy wet storm (2): Discharge

The ascending dry period for bioswales A, D and E were respectively 19 hours (4 mm), 6.46 days (and rainfall occurred during the simulation, 13.8 mm), and 2.64 days (simulated directly after the Heavy dry storm). The baseflows for bioswale A, D and E were respectively 0.8 l/min, 0.2 l/min and 0.0 l/min. The graph of bioswale E is given in Figure 31 below, the complete tables and graphs for all the bioswales (ordered per storm) can be found back in respectively Appendix 4 and 5.

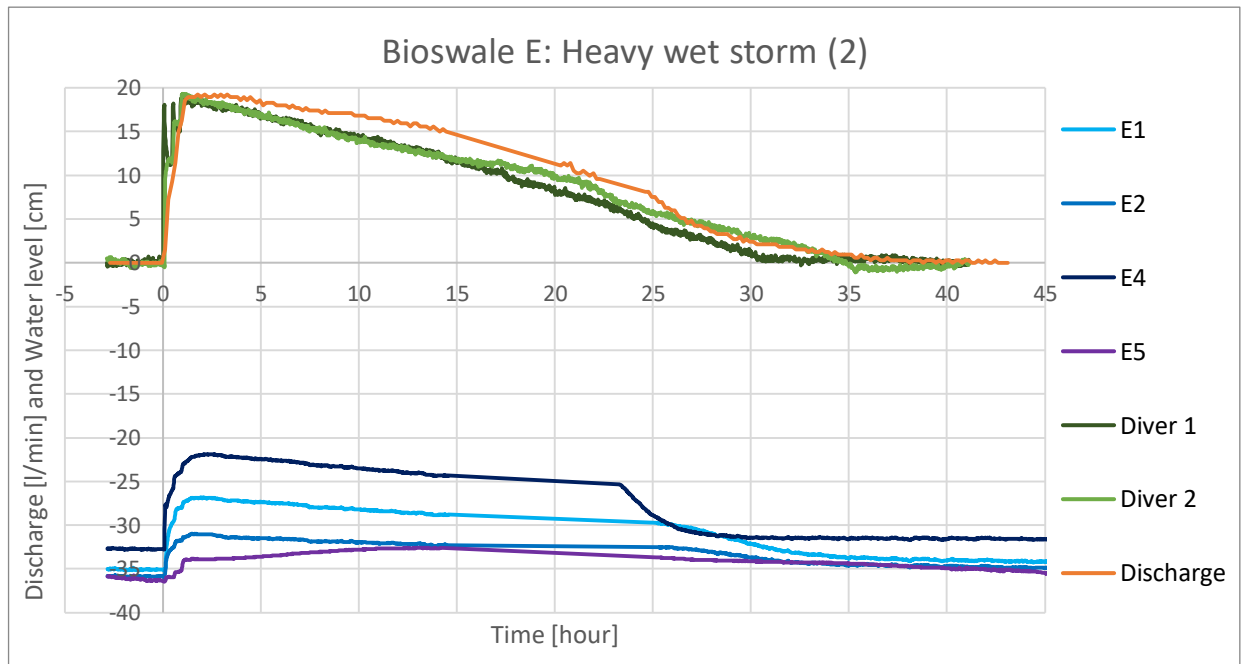


Figure 31: Heavy wet storm (2) bioswale E (E3 failed)

Emptying time

It is immediately clear that all three bioswales have a longer emptying time in wet conditions than in dry conditions (6.5 % to 32.6 %). However, during the simulation of storm D, a significant rainfall event (13.8 mm) occurred halfway into the simulation. In addition, something seems to limit the peak discharge during this storm which will be covered in the discussion. The emptying time of bioswale E was affected the least, likely since no real rainfall had occurred for 2.64 days.

This storm was simulated in the tail of the Heavy dry storm simulation, in an effort to simulate the wet conditions. However, this does seem to have much less effect than a real rainfall event. None of the bioswales are able to empty within 24 hours, bioswale D not even within 48 hours (though the extra inflow plays a role here).

Peak reduction and delay

The peak reductions for all three bioswales are higher in wet conditions than in dry conditions. Though this only differs 5% for swales D and A, it is a much larger difference for bioswale E (16.8%). Both bioswale A and D still meet the LID goals for peak reduction and peak delay, for both the fast and slow (absolute) discharge peak. Bioswale E meets the required peak reduction for both peaks easily but does not reach a sufficient peak delay for either peaks. The peak delays for bioswale E are larger in the wet situation, the peak delays of bioswale D shorter and bioswale A differs per peak.

Volume reduction and delay

The volume reduction for both bioswale D and E decreases (7.6 % and 41.2 % respectively), though bioswale D likely has an even higher reduction as the additional inflow is unknown. As bioswale E had the most volume reduction to begin with, it seems logical wet conditions can decrease this significantly. Bioswale A on the other hand, has more volume reduction in wet conditions (5.9 %). None of the bioswales reach the LID goal of 33% or more volume reduction. The delayed volume is still extremely large, which is the combined effect of the very large inflow and large peak reduction. The delayed volume is slightly smaller for bioswales A and E, and slightly larger for bioswale D. However, these differences are so small that they were found to be insignificant.

Table 3: Discharge data Heavy wet storm (2)

Heavy wet storm (2)	Bioswale A	Bioswale D	Bioswale E
T_{average} [°C]	11.20	7.91	18.82
h_{water} [cm]	20.5	21.9	19.1
T_{emptying} [hours]	38.9	49.2	35.2
$R_{\text{p1 peak}}$ [-]	0.026	0.017	0.038
$R_{\text{p2 peak}}$ [-]	0.028	0.020	0.038
$t_{\text{q-peak1-out}}$ [min]	242	367	88
$t_{\text{q-peak2-out}}$ [min]	620	803	118
$R_{\text{p1 delay}}$ [-]	8.1	15.3	2.9
$T_{\text{p1 delay}}$ [hour]	4.03	6.12	1.47
$R_{\text{p2 delay}}$ [-]	20.7	33.5	3.9
$T_{\text{p2 delay}}$ [hour]	10.33	13.38	1.97
f_v [-]	0.77	0.81	0.77
V_{delay} [%]	98.7	99.7	97.9

5.2.4 Heavy wet storm (2): Groundwater

For all bioswales, the groundwater reacts stronger for the Heavy dry storm (1) than for the Heavy wet storm (2). This is most likely since the groundwater is higher at the start of this simulation due to rainfall before the simulation, which could be taken from the piezometer in the native soil. As mentioned before, all bioswales (especially bioswales D and B) have a longer emptying time compared to the Heavy dry storm. Even though the water in the bioswale bowl is present for much longer, the groundwater increase is still less than for the Heavy dry storm.

Table 4: Groundwater changes Heavy wet storm (2)

Heavy wet storm (2)	Bioswale A	Bioswale D	Bioswale E	Bioswale B
h_{water} [cm]	20.51	21.85	19.07	20.21
T_{emptying} [hours]	32.02	49.18	35.23	54.73
dh_{p1} [cm]	9.81	1.39	8.27	7.64
dh_{p2} [cm]	28.66	10.11	4.88	1.4
dh_{p3} [cm]	29.78	22.74	-	37.74
dh_{p4} [cm]	4.37	1.4	10.92	-
dh_{p5} [cm]	0.2	-	3.82	0.93

5.2.5 Two-peak storm (3): Discharge

During this storm the same amount of water is fed to the bioswales as in the Heavy dry storm (1) and Heavy wet storm (2). Only now, it is given in two separate peaks. The ascending dry period for bioswales A, D and E were respectively 2.08 days (1.5 mm), 3.83 days (0.8 mm) and 23 hours (14.2 mm). During the storm simulation in bioswale E, rainfall occurred in the middle of the storm (1.8 mm). The baseflows for bioswale A, D and E were respectively 0.36 l/min, 0.0 l/min and 0.0 l/min. The graph of bioswale E is given in Figure 32 below, the graphs for all the bioswales (ordered per storm) can be found back in Appendix 4.

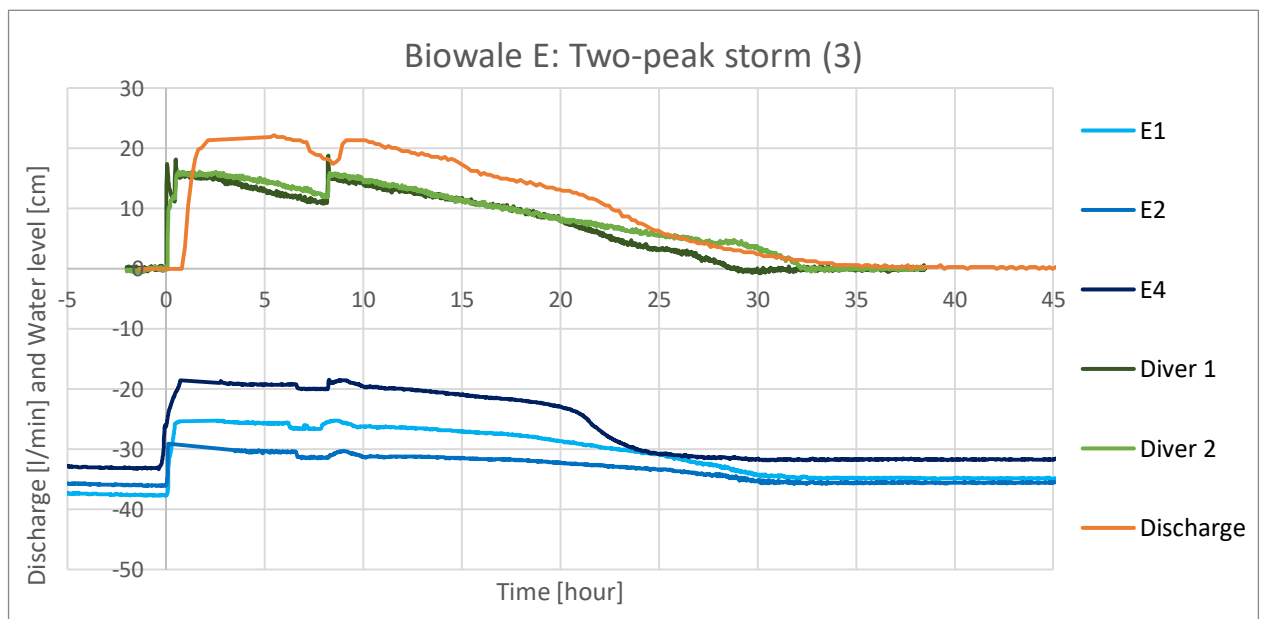


Figure 32: Two-peak storm bioswale E

Emptying time

As was expected, the emptying time of bioswale A and D were larger than their emptying time during the dry conditions. Since the same volume of water needs to be infiltrated, but with a lower head, it takes longer (respectively 38.2 % and 10.0 %). However, for bioswale E the emptying time is even slightly shorter (1.8 %) compared to the dry conditions, even though the conditions were relatively wet. This might be explained by the vegetation, which became more active in the 2 weeks between the measuring of storm 1 and storm 3, or the rising temperatures. None of the bioswales empty within 24 hours, though they do all stay within 48 hours.

Peak reduction and delay

The peak reduction for all bioswales is worse than for the Heavy dry storm (1), which could be expected since the peak inflow is much smaller. The R_{peak} of the Two peak storm (3) is respectively 23.01%, 103.1% and 47.24% larger than the R_{peak} for the Heavy dry storm (1) for bioswales A, D and E. In addition, the peak reduction for the absolute peak resulting from the second inflow is respectively 30.58%, 6.49% and 50.0% smaller than that of the absolute peak from the first inflow for bioswales A, D and E. The peak delays of the absolute peak for bioswale D and A are much smaller than during the Heavy dry storm (1), the absolute peak delay of bioswale E is roughly the same for both storms. Another interesting thing to see is that, though bioswales A and E have both a fast and slow absolute peak for the first filling, they only have an absolute peak during the second filling.

Volume reduction and delay

The volume reductions for bioswales A and D are better than for the Heavy dry storm (1) (respectively 3.5 % and 46.5 %). However, it should also be considered that bioswale D had an extra 18 hours to infiltrate, due to a failing discharge measuring device. On the other hand, the volume reduction of bioswale E decreased drastically (-45.5 %). This is very likely due to the rainfall occurring during the simulation. A sudden increase in the water level near the end of the simulation confirms this. The volume delay is much worse than for the previous storms. This is a result of (1) two storms of 1 hour which results in 2 hours of outflow occurring during rainfall and (2) during the second rainfall event the discharge is around its highest value.

Table 5: Discharge data Two-peak storm (3)

Storm 3	Bioswale A	Bioswale D	Bioswale E
T_{average} [°C]	13.01	7.99	18.47
h_{water1} [cm]	17.4	14.0	15.8
h_{water2} [cm]	12.9	16.1	15.7
T_{emptying} [hours]	44.1	43.3	32.5
$R_{p1.1 \text{ peak}}$ [-]	0.032	0.040	0.062
$R_{p1.2 \text{ peak}}$ [-]	0.035	0.043	0.064
$R_{p2.1 \text{ peak}}$ [-]	-	0.042	-
$R_{p2.2 \text{ peak}}$ [-]	0.049	0.046	0.128
$t_{q\text{-peak1.1-out}}$ [min]	146	243	148
$t_{q\text{-peak1.2-out}}$ [min]	256	430	289
$t_{q\text{-peak2.1-out}}$ [min]	-	138	-
$t_{q\text{-peak2.2-out}}$ [min]	109	427	38
$R_{p1.1 \text{ delay}}$ [-]	4.87	8.10	4.93
$T_{p1.1 \text{ delay}}$ [hour]	2.43	4.05	2.47
$R_{p1.2 \text{ delay}}$ [-]	8.53	14.33	9.63
$T_{p1.2 \text{ delay}}$ [hour]	4.27	7.17	4.82
$R_{p2.1 \text{ delay}}$ [-]	-	4.6	-
$T_{p2.1 \text{ delay}}$ [hour]	-	2.3	-
$R_{p2.2 \text{ delay}}$ [-]	3.6	14.2	1.3
$T_{p2.2 \text{ delay}}$ [hour]	1.82	7.12	0.63
f_v [-]	0.75	0.74	0.82
V_{delay} [%]	72.3	72.2	76.7

5.2.6 Two-peak storm (3): Groundwater levels

All groundwater increases are determined from the groundwater level before the storm simulations. Interesting to see is that the groundwater levels reach their maximum value much quicker during the second peak than during the first peak. This is likely due to the soil being already largely saturated. Even though the first inflow is much less than the inflow during the Heavy dry storm (1), the reactions are very mixed. For bioswales A, E and B, piezometer 1 shows a lower increase in groundwater level, but bioswale D a higher one. Piezometers 2 and 3 show a lower increase for all four bioswales. For piezometer 4, bioswale D is the only bioswale showing a higher groundwater table increase (supporting piezometer 1). Interesting to see, is that the piezometers at the edge of bioswale B barely react at all, while this piezometer for bioswale E still shows a clear reaction. This might be due to clogging of the swale bottom, partly due to previous storm simulations. When comparing the groundwater reaction to the first and second inflow peak, it shows that these reactions are usually very similar in magnitude. The largest differences occur in the piezometers 2 and 3 of bioswale A, the reactions are respectively 23.4 % and 13.9 % lower which matches with the lower water level. At last, the groundwater does reach its peak much sooner after the second filling than after the first filling, as can be seen in Appendix 4.

Table 6: Groundwater changes storm 3

Two peak storm (3)	Bioswale A	Bioswale D	Bioswale E	Bioswale B
h_{water1} [cm]	17.37	14.01	15.8	20.21
$dh1_{p1}$ [cm]	7.25	2.32	9.2	7.64
$dh1_{p2}$ [cm]	21.66	12.84	5.2	1.4
$dh1_{p3}$ [cm]	23.06	22.75	25.14	37.74
$dh1_{p4}$ [cm]	2.43	2.59	12.69	-
$dh1_{p5}$ [cm]	0.21	-	2.4	0.93
h_{water2} [cm]	12.88	16.11	15.7	20.87
$T_{emptying}$ [hours]	44.13	43.3	30.65	124.23
$dh2_{p1}$ [cm]	8.88	2.36	8.82	6.89
$dh2_{p2}$ [cm]	16.59	12.57	4.86	1.75
$dh2_{p3}$ [cm]	17.55	23.68	18.13	40.71
$dh2_{p4}$ [cm]	2.76	2.54	12.51	-
$dh2_{p5}$ [cm]	0.31	-	0	0

5.2.7 Medium storm (4): Discharge

Before the simulation, bioswale A, D and E had respectively been dry for 3.13 days (0.45 mm), 2.38 days (0.2 mm) and 1.41 days (0.5 mm). The Rotterdam weather station (344) reported some rainfall during the simulation (0.8 mm) of bioswale D but this was not reported by the VLG weather station or observed in the field. According to the VLG station, no rainfall occurred for bioswale E for 10 days. In this period, the Rotterdam station (344) does reports some rainfall but less than 1 mm in total. The graph of bioswale E is given in Figure 32 below, the graphs for all the bioswales (ordered per swale) can be found back in Appendix 4.

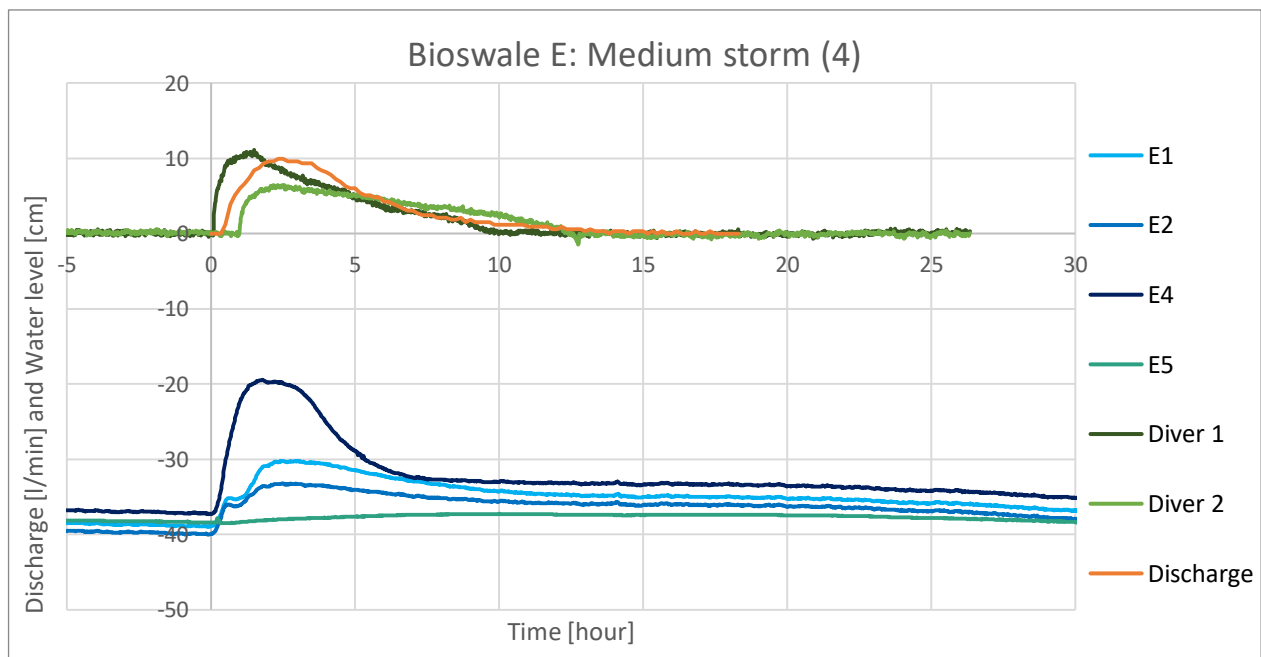


Figure 33: Medium storm (4) bioswale E

Emptying time

The emptying time of all three bioswales is short compared with the heavy storms. This was to be expected, since the inflow was much smaller. Even though the inflow to bioswale A is higher than in bioswale E, the emptying time of bioswale E is larger. It was found before that when the water level in bioswale E is low, the infiltration becomes much slower. The emptying time is 35.49, 31.51 and 34.51 % of the emptying time for the heavy dry storm (1) for respectively bioswales A, D and E. As expected, the infiltration takes relatively longer at lower water levels, due to a lower hydraulic head and less infiltrating surface. The emptying times vary between 10.4 and 12.1 hours, well within 24 hours.

Peak reduction and delay

The reduction in peak outflow compared to Heavy dry storm (1) for bioswales A, D and E is respectively: 55.74 %, 46.41 % and 56.05 %. It seems that the peak outflow is strongly depended on the water level in the swale bowl for all three bioswales. Interesting to see is that both bioswale A and E only have one (absolute) peak, while bioswale D still has a fast and slow peak (thought less pronounced). The R_{peak} of bioswales A, D and E are much less than during the Heavy dry storm (1), they become respectively 353.6 %, 661.7 % and 456.0 % the R_{peak} of the Heavy dry storm (1). The absolute peak delay is reduced significantly for bioswales A, D and E, with respectively 93.60 %, 72.39% and 75.92 % compared to the Heavy dry storm (1). It is noted that the performance of bioswale A seems to decrease the most at lower water levels in the bowl.

Volume reduction and delay

As the inflow for these storms was quite difficult to determine, the volume reduction should not be valued to high. The volume reduction of bioswales A and E seem to improve quite a lot, with 42.29 % and 39.59 % respectively. The volume reduction of bioswale D even seemed to decrease drastically (-48.15 %) compared to storm 1, which is highly unlikely. The inflow was not measured for this storm simulation in bioswale D, but data from the same hose was used which was retrieved when measuring bioswale A. However, it is possible that these were different hoses or that a second hose was connected to the first in order to reach bioswale A. The delayed volume is quite high for this storm as well, though not as good as for the two heavy large storms (especially for bioswale A). Though the storm duration (2 hours) reduced the delayed volume, the low inflow resulted in a low head in the bioswale (main driving force of infiltration) which again resulted in a low discharge. This likely reduces the negative effect of the longer storm duration on the delayed volume.

Table 7: Discharge data Medium storm (4)

Medium storm (4)	Bioswale A	Bioswale D	Bioswale E
T_{average} [°C]	10.08	6.26	16.36
h_{water} [cm]	11.39	7.82	6.22
T_{emptying} [hours]	10.4	12.1	11.42
$R_{p1 \text{ peak}}$ [-]	-	0.16	-
$R_{p2 \text{ peak}}$ [-]	0.13	0.17	0.25
$t_{q\text{-peak1-out}}$ [min]	-	263	-
$t_{q\text{-peak2-out}}$ [min]	69	503	144
$R_{p1 \text{ delay}}$ [-]	-	4.38	-
$T_{p1 \text{ delay}}$ [hour]		4.38	
$R_{p2 \text{ delay}}$ [-]	1.15	8.38	2.4
$T_{p2 \text{ delay}}$ [hour]	1.15	8.38	2.4
f_v [-]	0.65	0.91	0.55
V_{delay} [%]	90.9	96.6	96.8

5.2.8 Medium storm (4): Groundwater measurements

As could be expected, all groundwater reactions are much less severe than for the Heavy dry storm (1). Since the inflow is much lower, the water level in the swale bowl is low and the groundwater reaction is small. The only outstanding data is from piezometer 4 in bioswale E, it reacts just as strongly as for the Heavy dry storm (1). This can partially be explained by the way the bioswale was filled, as the inflow point was located at piezometer 4. This can also clearly be found back in the water level data, as the water level at piezometer 4 reacts much quicker and reaches a higher level (Figure 32). However, this still doesn't explain why the groundwater level increased even more than for the Heavy dry storm (1). Micropores resulting from vegetational activity should also have been visible in the other piezometers, more local biological activity (worms, birds) might play a role here. The effect of such a small storm on the groundwater level outside the bioswale is minimal.

Table 8: Groundwater changes Medium storm (4)

Medium storm (4)	Bioswale A	Bioswale D	Bioswale E	Bioswale B
h_{water} [cm]	11.39	7.82	6.22	-
T_{emptying} [hours]	10.4	12.1	11.42	-
dh_{p1} [cm]	2.44	1.16	8.87	-
dh_{p2} [cm]	13.16	4.64	6.68	-
dh_{p3} [cm]	13.84	14.32	-	-
dh_{p4} [cm]	1.65	1.21	17.8	-
dh_{p5} [cm]	0.08	-	1.23	-

5.2.9 Bioswale 7: Discharge

This bioswale has such a high permeability, it was not possible to simulate the 4 storms. Even after adding 40 m³ in 1.5 hour, no water layer had formed on top of the soil. In addition, the discharge measuring device could not keep up with the outflowing volume. To still get some insight in the hydraulics of this swale, a very low inflow was simulated (Small storm (5)) at a local low-point in the bioswale, to limit the infiltrating surface. This is the same area in which the piezometers 71, 72 and 73 are located. During the simulation, the infiltrating surface grew from 12.6 m² at the start to 22.77 m² near the end of the simulation. With this data, it becomes immediately clear that this bioswale has an extremely large permeability. The emptying time is only 1 hour longer than the storm duration, and 40% of the outflow occurs during the storm event itself. The R_{peak} is very high, while the R_{delay} and emptying time are very low. The volume reduction is low as well, which was unexpected as by far the largest part of the bioswale experienced no ponding and this soil should have been available for storage. On the other hand, the delayed volume was higher than expected. It is likely though that for longer storms this can become really low as the peak reduction is low.

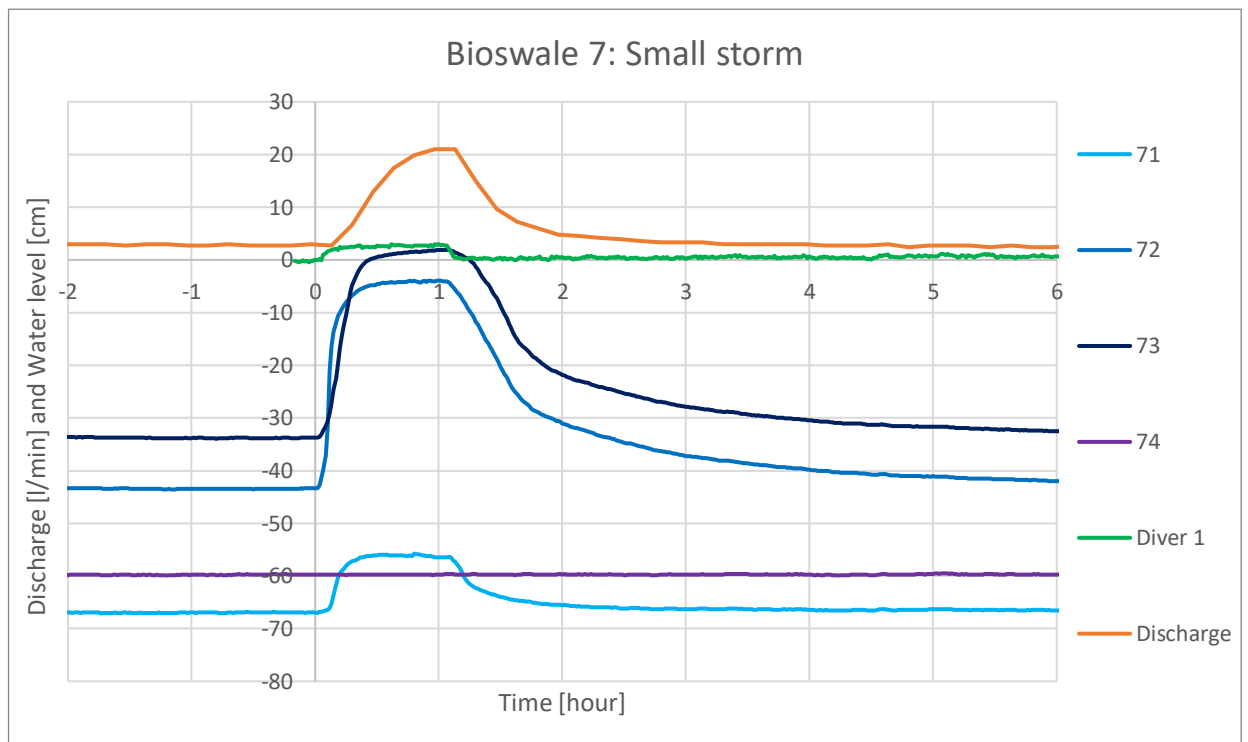


Figure 34: Small storm bioswale 7

Table 9: Discharge data Small storm

Small storm (5)	Bioswale 7
T _{average} [°C]	9.22
h _{water} [cm]	2.76
T _{emptying} [hours]	1.15
R _{p1 peak} [-]	-
R _{p2 peak} [-]	0.66
t _{q-peak1-out} [min]	-
t _{q-peak2-out} [min]	58
R _{p1 delay} [-]	-
R _{p2 delay} [-]	1.93
f _v [-]	0.67
V _{delay} [%]	73.05

5.2.10 Bioswale 7: Groundwater measurements

The piezometers in bioswale 7 show very extreme reactions. The groundwater level in the clay even almost reaches the water level in the swale bowl, near the end of the storm. This might be due to leakage in the piezometer, but piezometer 2 shows almost the same (extreme) effect. Also, piezometer 1 reacts extremely strong for its location next to the drain. If the piezometers are working correctly, it shows that the drain in this bioswale does become limiting, and as such governs the infiltration for the soil located about a meter from the drain. Only the piezometer 4 doesn't respond at all, which is logical as it is located at the other side of the bioswale from the side of infiltration.

Table 10: Groundwater changes Small storm (5)

Small storm (5)	Bioswale 7
h _{water} [cm]	2.76
T _{emptying} [hours]	1.15
dh _{p1} [cm]	10.85
dh _{p2} [cm]	39.25
dh _{p3} [cm]	35.47
dh _{p4} [cm]	0

5.2.11 Summary findings bioswale monitoring

When considering the factors that influence the hydraulic behaviour of the bioswales, the following can be concluded.

- The peak reduction was lower in the wet conditions
- The peak reduction increases with increasing storm size (for medium to large storms)
- The peak reduction decreases with increasing storm duration

- The peak delay gave varying results, but decreases with increasing initial moisture content when the difference was large enough.
- The peak delay increases with increasing storm size (for medium to large storms)
- The peak delay decreases with increasing storm duration

- The delayed volume is slightly higher for the dry conditions.
- The delayed volume increases with increasing storm size
- The delayed volume decreases (strongly) with increasing storm duration

- The volume reduction is higher in dry initial conditions than in wet initial conditions when the moisture holding capacity of the native soil is not too high.
- The volume reduction is much larger for smaller storms
- The volume reduction is slightly better for long duration storms

- The emptying time is larger for the wet conditions, with an average difference of 25%
- The emptying time is shorter for smaller storms
- The emptying time is much longer for long duration storms (21%)

The groundwater at the edge of the bioswales didn't increase with more than 6 cm in clay and peat soils, it is not likely that surrounding structures or green will suffer from this. The groundwater in the native soil within the bioswale reacted the strongest to the large storms (usually 20 - 40 cm) and is likely responsible for most of the volume reduction. The groundwater rise at the edge of the sandbed remains low (usually 10 - 25 cm), the groundwater next to the drain only increases with a few centimeters.

5.3 Field estimated saturated hydraulic conductivity

Using the infiltration data from the bioswales of the two heavy storms (1-2), the saturated hydraulic conductivity is calculated for bioswales A, B, D and E which can be found in Table 15. As we assume the sandbed to have a very high permeability, which is staffed by the soil-texture data and the saturated hydraulic conductivity determined in the laboratory, the top-layer should govern the saturated hydraulic conductivity of the layers combined, and thus the K_s -total of the bioswales. Emerson and Traver (2008) showed that the temperature of the infiltrating water can have a strong effect on the K_s , as it influences the dynamic viscosity of the water. The average temperature during simulations for bioswales A, D and E were respectively 11.18, 7.23 and 17.39 degrees Celsius. This results in a dynamic viscosity of respectively 0.012639, 0.0142 and 0.010683 (g/cm*s). When this effect is corrected for, it reveals that bioswales A, D and E respectively have the highest permeability top-soil (Table 11). Interesting enough, this is the same order as the saturated hydraulic conductivity resulting from the neural network prediction of Hydrus, though all the values were much to high (122.1, 118.4 and 111.8 cm/d respectively). In addition, where the field found K_s -values are in a similar range (16.9 - 14.0 cm/d), those found using the neural network prediction have a large spread (150.5 – 34.09 cm/d).

Table 11: K_s from infiltration data of two heavy storms

K_s from field-data	Bioswale A	Bioswale B	Bioswale D	Bioswale E
$T_{average}$ [°C]	10.82	15.00	7.33	17.37
K_s [cm/d] Heavy dry storm (1)	16.59	16.60	13.97	16.89

5.4 Laboratory tests

5.4.1 Soil texture top-layer

The soil-texture data of the top-layer shows that there can be large differences between samples taken inside the same bioswale (Table 12). This is mostly present in the gravel, sand and silt fractions, the loam content is quite stable. One bioswale which really separates itself from the others is bioswale 7. It has an extremely low sand-gravel fraction (49.4 %) and a very high silt and loam content in one of the two samples. The other sample is much more in line with the other bioswales. This indicates that the part of the soil-layer which is improved is quite small, and that the un-improves soil is very impermeable. When leaving out the first soil sample of bioswale 7, bioswale B has the lowest sand-gravel fraction by far (65.1 %), followed at a distance by bioswale E (78.7%), bioswale D (80.6 %), bioswale 7 (80.7%) and bioswale A (82.3 %). On the other hand, bioswale E has the highest organic content by far (11.2 %), compared to the bioswales other bioswales (6.1 % – 6.4 %). This might be the result of the peat soil which is closer to the surface for bioswale E. This soil likely came free during construction of the bioswale and was processed again in the top-layer.

Table 12: Soil-texture results top-layers for samples 1 and 2

Soil texture	Bioswale A	Bioswale B	Bioswale D	Bioswale E	Bioswale 7
	Top-layer	Top-layer	Top-layer	Top-layer	Top-layer
Gravel [%] [>2 mm]	7.3	2.1	7.9	2.5	3
	2.5	1.6	2.4	1.2	4.4
Sand [%] [2-0.063 mm]	73.4	65.8	69.5	71.5	46.4
	81.4	60.7	81.4	82.2	76.3
Silt [%] [0.063-0.002]	13.9	23.1	18.5	22.7	39.1
	10.9	26.2	12.7	13.2	15.1
Loam [%] [<0.002]	5.4	9	4.1	3.3	11.6
	5.2	11.5	3.4	3.3	4.1
Organic content [%]	6.4	5.6	6.9	11.1	6.7
	6.4	6.6	5.4	11.2	-
D10 [mm]	0.014	0.003	0.009	0.004	0.002
	0.012	0.002	0.015	0.014	0.010
D50 [mm]	0.197	0.148	0.206	0.204	0.063
	0.220	0.109	0.210	0.235	0.254
D70 [mm]	0.294	0.237	0.321	0.314	0.201
	0.311	0.198	0.313	0.325	0.355

5.4.2 Soil-texture sandbed

As could have been expected, the main fraction of all the samples is sand (Table 13). There is little ‘pollution’ with other fractions and the organic content is very low. The sand and gravel fraction from low to high is; bioswale D (92.3%), bioswale B (95.6 %), bioswale A (96.6 %) and bioswale E (98.1%). In addition, the organic content of bioswale D is the highest of the bioswales, though for such low contents this could easily be caused by heterogeneity in the soil. All things considered, the sandbeds seem to be realised according to design. No accumulation of small, infiltrated particles is indicated by this data.

Table 13: Soil-texture results sandbeds

Soil properties	Bioswale A	Bioswale B	Bioswale D	Bioswale E
	Sandbed	Sandbed	Sandbed	Sandbed
Gravel [%] [>2 mm]	2	0.9	3.3	0.6
Sand [%] [2-0.063 mm]	94.6	94.7	89	97.5
Silt [%] [0.063-0.002]	2.7	3.3	5.3	1.5
Loam [%] [<0.002]	0.7	1.1	2.5	0.4
Organic content [%]	0.7	0.6	1.7	0.6
D10 [mm]	0.125	0.125	0.124	0.130
D50 [mm]	0.240	0.243	0.259	0.279
D70 [mm]	0.320	0.309	0.351	0.350

5.4.3 Soil (hydraulic) properties

Determining the soil hydraulic properties of a soil is difficult and costly. As such, only the sand-layer was tested, as determining the saturated hydraulic conductivity (K_s) in the laboratory for non-cohesive soils is easier and less costly than cohesive soils (top-layer). The K_s shows large variety within the same bioswale (Table 13). As the samples are quite homogeneous when looking at the textural classes, this was somewhat unexpected. When considering the K_s for the consolidated soils, respectively bioswale E (15.0 m/d), bioswale B (9.9 m/d), bioswale A (7.1 m/d) and bioswale D (4.7 m/d) have the highest values. These values are quite high, even for drainage sand. The bulk-density is very constant, not only when considering different samples from the same bioswale but also when comparing all samples. Bioswale A has the highest bulk density (15.05 KN/m³), followed by bioswales D and E (14.55 KN/m³) and bioswale B (14.5 KN/m³).

Table 14: Saturated hydraulic conductivity and bulk density sandbed for sample 1 and 2

Soil properties	Bioswale A	Bioswale B	Bioswale D	Bioswale E
	Sandbed	Sandbed	Sandbed	Sandbed
K10 unconsolidated [m/d]	13.82	15.55	3.89	25.92
	6.83	13.82	9.5	13.82
K10 consolidated [m/d]	9.5	10.37	2.94	22.46
	4.75	9.5	6.48	7.52
BD unconsolidated [KN/m ³]	14.5	13.9	13.7	14.5
	14.4	13.7	14.4	13.4
BD consolidated [KN/m ³]	15.1	14.6	14.2	14.9
	15	14.4	14.9	14.2

5.5 Hydrus 2D/3D results

5.5.1 Neural network prediction results

The results of the neural network prediction of the soil hydraulic parameters can be found in Table 14 for the 2 samples of the top-layers and in Table 15 for the sandbeds. According to the prediction, the top-layer of bioswale A should have a much higher saturated hydraulic conductivity than the other bioswales. The top-layer of bioswale B has the lowest permeability, which seems to match with field observations. The saturated hydraulic conductivity values for the sandbed are very high, with the exception of bioswale D.

Table 15: Soil-hydraulic parameters for the top-layers following the neural network prediction

Soil-hydraulic parameters	Bioswale A	Bioswale B	Bioswale D	Bioswale E
	Top-layer	Top-layer	Top-layer	Top-layer
θ_r [-]	0.046	0.040	0.035	0.032
	0.043	0.044	0.040	0.039
θ_s [-]	0.385	0.386	0.390	0.394
	0.383	0.386	0.386	0.387
α [1/cm]	0.041	0.034	0.044	0.044
	0.039	0.027	0.042	0.043
n [-]	1.712	1.418	1.607	1.522
	1.915	1.398	1.957	1.930
K_s [cm/d]	102.50	45.55	86.31	78.72
	141.71	34.09	150.50	144.80

Table 16: Soil-hydraulic parameters for the sandbed following the neural network prediction

Soil-hydraulic parameters	Bioswale A	Bioswale B	Bioswale D	Bioswale E
	Sandbed	Sandbed	Sandbed	Sandbed
θ_r [-]	0.051	0.052	0.060	0.053
θ_s [-]	0.374	0.392	0.391	0.390
α [1/cm]	0.032	0.033	0.034	0.032
n [-]	3.928	3.735	3.071	4.255
K_s [cm/d]	975.40	936.77	574.35	1267.86

5.5.2 Results from modelling

When the model of the cross-sections were constructed according to the available soil texture data and depth profiles, the discharge curve could only be mimicked to a certain extent when calibrating the soil hydraulic properties. The automated calibration option gave even worse results, if it didn't stop before the calibration was fully done. It proved especially difficult to mimic (1) the fast response of the discharge curve, (2) the two different peaks of the discharge curve, and (3) the end-section of the discharge curve.

The fast response could only be approached by giving very low α and n values (0.01 and 1.3 respectively) to both the top-layer and the sandbed, which is highly unlikely as these values are usually reserved for clay-soils. In addition, when using these parameters to simulate storm 4 of bioswale D, the model didn't match the field-data at all. As such, another explanation was sought after that could explain the fast response. From the literature study it had become clear that macropores originating from biological activity can play an important role in the infiltration process of bioswales (Archer et al. 2002; Le Coustumer et al. 2007, Traver et al. 2007, 2008; Lewis et al. 2008; Li and Davis 2008; Ahmed et al. 2015). This was simulated by giving a small section of the top-layer a very high K_s . This solved the problem of matching the fast response, in addition it became clear that bioswale D relies the strongest on macropores and bioswale A the least (Tables 17 to 19). This also resulted in 2 peaks in the discharge curve. The first peak being the result of the macropores (structural permeability), and the second (slow) peak of the textural permeability starting to aid the infiltration as well.

The only remaining issue is the end-section of the discharge curve. As this is only a problem for bioswales D and E, it is assumed to be a result of the organic shape of these bioswales (inconsistent cross-section). The model is a cross-section of the bioswale (2D), the discharge is calculated by multiplying the result of the 2D model with the bioswale length. Bioswale A is the only swale with a constant cross-section, which would explain why the model fits this bioswale much better than bioswales D and E (Appendix 6).

The model also showed that the less-improve sides do play a part at the start of infiltration, when the pressure head is high. However, this quickly decreases to a very low contribution. This can be seen in Figure 35 and 36.

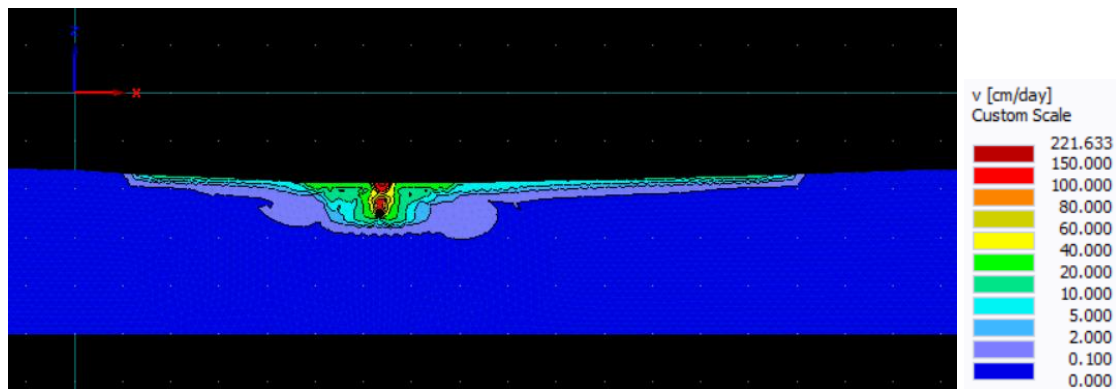


Figure 35: Bioswale E, flow velocity after 0.04 days

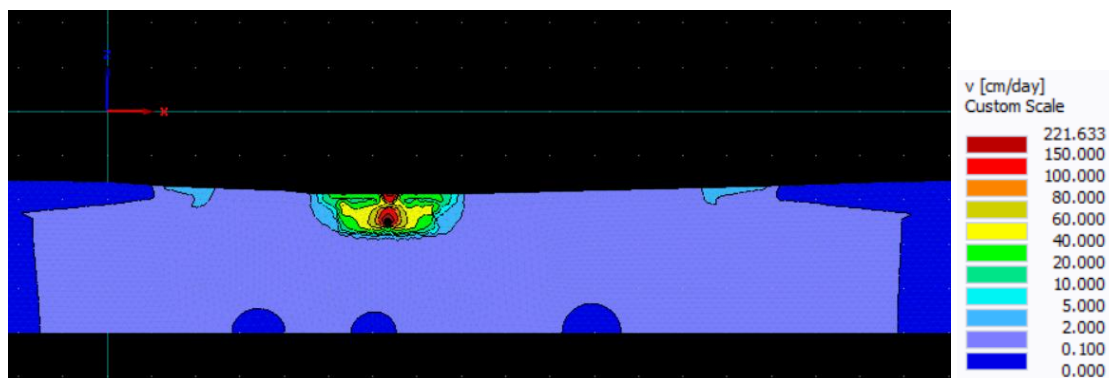


Figure 36: Bioswale E, flow velocity after 0.2 days

To determine whether the water infiltrating through the improved top-soil above the sandbed or that the less-improved soil and native soil are responsible from the groundwater level increase in the native soil, the water layer on top of the less-improved soil funded on the native soil was removed in the model. This resulted in Figure 37 below, and shows that both top-soils contribute to the increase in groundwater level in the native soil.

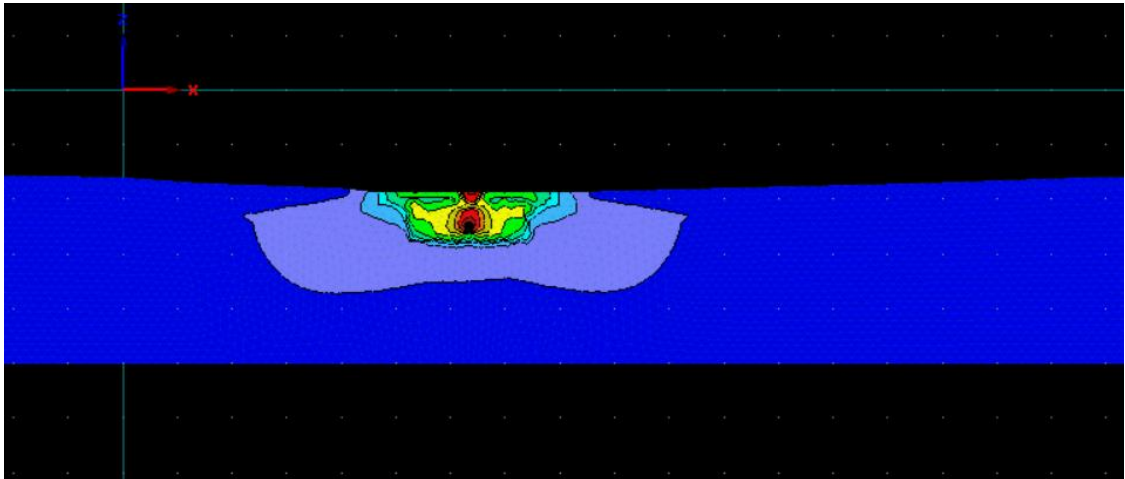


Figure 37: Bioswale E, flow velocity only resulting from water on the improved top-soil

5.5.3 Calibrating soil-hydraulic properties in Hydrus 2D/3D

The discharge data of the heavy dry storm (1) is used to calibrate the soil-hydraulic properties (θ_r , θ_s , α , n and K_s) for bioswales A, D and E. The resulting soil-hydraulic parameters can be found in Tables 17 to 19.

Table 17: Soil-hydraulic properties bioswale A, calibrated

Bioswale A: Soils	θ_r [-]	θ_s [-]	α [1/cm]	n [-]	K_s [cm/d]
Improved top-layer	0.095	0.41	0.12	2	12
Slightly improved top-layer	0.095	0.41	0.019	1.31	4
Sandbed	0.045	0.43	0.08	3.5	750
Native soil	0.068	0.38	0.008	1.3	2
Macropores	0.078	0.43	0.01	1.3	42

Table 18: Soil-hydraulic properties bioswale D, calibrated

Bioswale D: Soils	θ_r [-]	θ_s [-]	α [1/cm]	n [-]	K_s [cm/d]
Improved top-layer	0.1	0.39	0.059	1.48	13
Slightly improved top-layer	0.1	0.38	0.027	1.23	2.88
Sandbed	0.045	0.43	0.145	2.68	800
Native soil	0.068	0.38	0.008	1.3	2
Macropores	0.057	0.41	0.124	2.28	205

Table 19: Soil-hydraulic properties bioswale E, calibrated

Bioswale E: Soils	θ_r [-]	θ_s [-]	α [1/cm]	n [-]	K_s [cm/d]
Improved top-layer	0.1	0.39	0.07	1.6	13
Slightly improved top-layer	0.095	0.41	0.019	1.31	3
Sandbed	0.045	0.43	0.145	2.68	800
Native soil	0.068	0.38	0.008	1.3	2
Macropores	0.045	0.43	0.145	2.68	175

6 Discussion

6.1 Hydraulic functioning of bioswales: Effect of factors

As mentioned in the literature and in the method, there are a number of goals set for bioretention facilities. These were the peak reduction ($R_{peak} > 0.33$), peak delay ($R_{delay} > 6$) and volume reduction ($f_v > 0.33$) from the literature, and the emptying time ($T_{empty} < 24$ hours) from the method. All bioswales perform well when considering the peak reduction and peak delay for the larger storms, and less well for the small storm. On the other hand, the volume reduction and emptying for the small storm is quite good in contrast to the big storms. Table 19 below gives a quick overview concerning which factors influence the bioswale performance. A negative sign means that the metric is influenced negatively (less peak reduction), a positive sign the opposite (more peak reduction). A zero means that the effect observed is not significant or very diverse for each bioswale, an N means that there is no data concerning the influence of this factor.

Table 20: Factors influencing bioswale performance

Factors	R_{peak}	$R_{p1\ delay}$	$R_{p2\ delay}$	f_v	T_{empty}	$V_{delayed}$
Storm size increase	++	+	++	--	--	0/-
Storm duration increase	-	-	--	+	-	--
Wet initial conditions	-	-	--	0/-	-	0/-
Temperature increase	-	-	-	N	+	N
Ks soil increase	--	-	--	-	++	--
Capillary forces soil increase	-	-	--	N	N	-

Storm size increase

Thought a larger storm event gives a very good peak reduction and peak delay, it also resulted in a low volume reduction and long emptying time. Barber et al. (2003), Li et al. (2009) and Donkers (2010) on the other hand found a decrease in the peak reduction with increasing storm size. However, this drop in peak reduction tends to flatten out at larger storm sizes. At this point, the bioswale is almost completely saturated and the hydraulic conductivity is nearing its maximum value. It is possible that the peak reduction will go up again for even larger storms, as an increase in inflow volume barely results in a higher hydraulic conductivity anymore. It is interesting that especially the absolute peak delay is influenced by the storm size, in the case of smaller storms the fast peak is usually not even present. This might be a result of the shorter ponding time and lower driving force (low water level), which don't provide enough time and/or force for the textural porosity to significantly contribute to the infiltration.

Storm duration increase

A longer storm duration has a negative influence on almost every metric, except for the volume reduction. This is likely a result of the longer emptying time leaving more time for infiltration to the native soil. As a longer storm has a lower peak intensity, the peak reduction ratio worsens. In addition, there is no more storage available in the soil to act as buffer and the conductivity is at its maximum. Barber et al. (2003) and Li et al. (2009) found a decreasing peak reduction with increasing storm duration as well. Due to the higher conductivity, the peak delay also worsens.

The absolute peak delay more than the fast peak delay, suggesting the absolute peak depends more heavily on the initial water content staffing the idea that this peak results from the (later) contribution of the smaller pores in the soil. As the storm duration is longer, the amount of discharge during this storm is also larger resulting in a lower delayed volume.

Wet initial conditions

As it proved very difficult to do simulations in wet conditions (without them being interrupted by natural rainfall), the results are more diverse. When comparing the two large storms, wet conditions seem to give a slightly higher peak reduction. However, when comparing the first and second peak of the Two-peak storm, the second peak has a worse peak reduction. This suggests that the initial conditions should be really wet to have a significant effect on the metrics. Barber et al. (2003) also found that the peak reduction decreases with increasing initial moisture content for smaller storms and Donkers (2010) did observe a large decrease in peak reduction with high initial moisture content.

Again, the effect in the absolute peak delay is much bigger, and the fast peak can usually not be observed since the soil is already completely saturated. Barber et al. (2003), Donkers (2010) and Geerling (2014) also found a lower peak delay in wet conditions.

Temperature increase, K_s and capillary forces

As has been previously discussed, temperature directly influences the K_s . As such, these factors will be discussed simultaneously. As the K_s determines how fast a liquid moves through a media, it greatly influences the emptying time, peak reduction and peak delay. However, the capillary forces in a soil (determining the pF-curve) also play an important role in the peak delay and peak reduction following the modelling exercise. Barber et al. (2003) found that the peak reduction was dependent on the storage characteristics of the media. For finer media, the peak reduction increased. As finer media usually also have a lower K_s and higher suction force, this description already combined these factors. However, they also claim that the peak delay time is dependent on the effective hydraulic conductivity and the peak reduction ratio on the soil storage characteristics. This while the modelling exercise showed that both factors influence both metrics.

6.2 Clogging

During this monitoring campaign, 2 examples of clogging were found. Namely were the Two-peak simulations for bioswale B and D. These cases were defined as clogging since the peak discharge reached were much smaller than for previous storms with the same water level, and did barely vary with water level during the storm (see Figure 21). As none of the bioswales emptied within 24 hours, and the simulations were quite intense, it is not strange that clogging could occur at the end of the simulation period. As bioswale D was measured in winter, and also underwent many failed simulations, the bioswale itself is likely constructed well. However, bioswale B was monitored in late-spring and had only undergone one previous simulation. This bioswale also has the lowest permeability and will likely need reconstruction if it is to function properly.

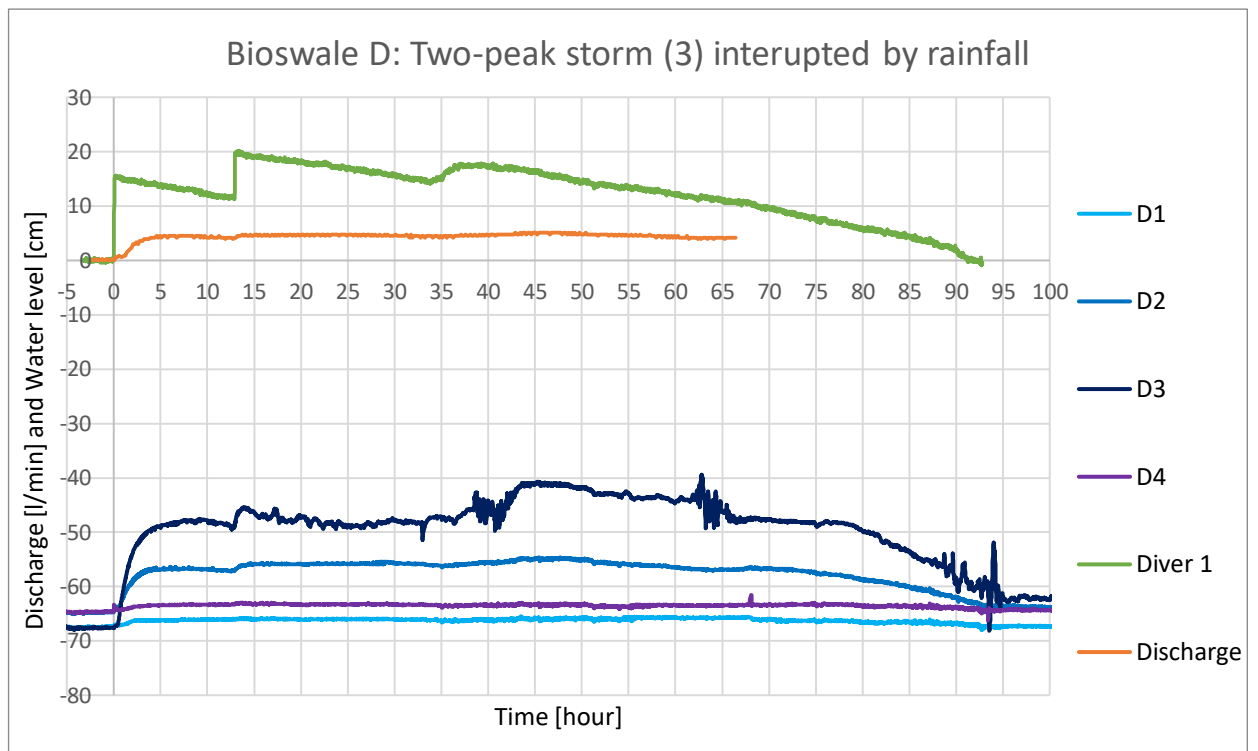


Figure 38: Clogging of the top-soil in Bioswale D

6.3 Structural and textural porosity

As discussed before, a lot of the discharge curves show two peaks. One fast peak, occurring quickly after the inflow, and one slow peak which takes much longer to occur. The fast peak is always lower than the slow, absolute peak, but usually not by much. As the fast peak does arrive much earlier, it might be much more important for the hydraulic impact on downstream water infrastructure. This absolute peak could be the result of (1) the soil media becoming completely saturated, (2) the un-improved part of the top-layer starts to contribute or (3) the surrounding native soil got saturated and doesn't suck water from the sandbed anymore. As the less-improved part of the topsoil lays on-top of the native clay soil, it is very unlikely this layer can contribute. Even when the macropores created by the grass help the water to the first 15-20 cm, it still has to move through the heavy clay to reach the drain. The native clay could suck water from the sandbed. However, as the groundwater is quite high, it is very unlikely there is any dry clay present, especially not at the depth of the sandbed. This leaves the option of the structural and textural porosities. As the grass roots usually go 15-20 cm deep, they help the water pass the first soil-layer resulting in the fast first peak. This also explains the fast response of the bioswales (between 2-14 minutes). When the water starts passing through the textural pores in the soil as well, the second peak occurs. Using this approach, the Hydrus model was calibrated as well.

6.4 Measuring approach and set-up

The discharge measuring device was very prone to failure, due to both the floaters and the needed batteries. As more robust floaters have been installed, the set-up would profit most from a connection to the electricity network at the monitoring location. As all the other pipes in the manholes were blocked, no water could flow from the outside DIT-system into the bioswale, which might have occurred during long-lasting dry conditions. At last, though the water level changes in the manholes were not notable due to the high accuracy floater, the water level which was set likely had an error of a few centimetres. The height of the piezometers was only measured by hand, as they were removed by accident before the precise measurements could take place. This results in a significant error, as the bottom of the swales were not flat and measuring the piezometer height within the tubes proved difficult. However, the piezometers did follow the reaction of the groundwater well, also in the clay soils. Lastly, it was observed that for bioswales A, D and 7, water discharged from the drain even when it had been dry for a number of days. This was expected for bioswales D and 7, but it is likely that the set drainage level of the pumps was set to low for bioswale A. The divers in the bioswale bowl performed well, though it proved quite difficult to locate the absolute lowest point in the bioswale, as they were shaped organically and sometimes more separated low areas could be defined.

Further, the Hydrus 2D/3D model showed that the saturated hydraulic conductivity tests done in the laboratory didn't give reasonable data and as such did not add to the research. The neural network prediction did not give reasonable values either, though the order of lowest and highest saturated hydraulic conductivity was correct. As it was shown that the macropores dominate the infiltration, it is not unreasonable for a prediction based on textural data to fail. However, as macropores add to the total permeability, the textural permeability should not have been higher. With processes as clogging and biological activity working against each other, it proves difficult to determine the hydraulic conductivity. The best method to approach this is still a full-scale measurements, with temperature correction when needed.

Conclusion

To contribute to a standard bioswale design which is applicable in polder conditions, 5 bioswales have been monitored on their hydraulic behavior. In order to determine the performance which can be expected from such bioswales under different circumstances, the following was researched: effect of (1) storm size, (2) storm distribution, (3) initial conditions, (4) temperature and (5) soil hydraulic properties. In addition, findings considering what is governing the infiltration will be discussed.

The LID goals for peak reduction ($R_{peak} < 0.33$), peak delay ($R_{delay} > 6$) and volume reduction ($f_v > 0.33$), as well as the maximum emptying time (24 hours), were tested. The goal for peak reduction was reached for all simulated storms, the goal for peak delay only by the large, short storms. Medium storms, and storms when there was still water in the swale did not meet this goal. The goal for volume reduction was only reached during the medium storms, as was the goal set for the emptying time. It might be difficult to reach the goal for peak delay for smaller storms (reducing permeability of the soil), while at the same time still reaching the emptying time goal for larger storms (larger permeability needed).

As two of the 5 bioswales experienced clogging during the monitoring campaign, an emptying time of 24 hours and not 48 hours should be maintained. This way the swales will also maintain function in autumn and winter, where there are more and longer rainfall events and little biological activity in the soil. One swale on the other hand had a much too large permeability, resulting in little delay or reduction. This was caused by the type of vegetation, as the soil was the same as that of the other bioswales. The vegetation consisted of high (dune) grass and large weeds, creating large and deep macropores resulting in a very high permeability.

It was found that the structural porosity governed the infiltration in all the bioswales, showing how important the right vegetation is. However, at the developing stage of the bioswale the textural porosity needs to provide the necessary permeability and thus should be high enough. Otherwise, the vegetation cannot develop well with bare-spots and clogging the result, as could be seen in Bioswale B. This textural porosity will decrease over time (clogging), while the structural porosity increases and restores the infiltration capacity of the bioswale. The top-layer of the bioswales should have a sand/gravel fraction of $> 80\%$, lower values showed problems with clogging.

Of the 5 bioswales, only bioswale 7 had a drain which was governing part of the infiltration. This was caused by the extremely high permeability of the soil above, and is unlikely to occur in properly designed swales.

All things considered, constructing bioswales in polder conditions will result in less volume reduction and a quicker and slightly stronger response from the drain. However, if the design is tailored to this (low permeability top-soil), the LID-goals can still be met for many storms. When designing a bioswale, a consideration needs to be made between reaching the LID-goals and reaching the emptying time.

Recommendations

8.1 Rotterdam bioswale

This research was set-up to contribute to the design of the Rotterdam bioswale, which is specially designed to function well in polder conditions. The following can be used:

Expected hydraulic functioning

The lowest volume reduction for the large, high intensity storms in wet conditions was 20%, this should be a save value to work with (average was 21.5% for wet conditions). When considering medium storms, the lowest volume reduction observed was 34.5%. For smaller storms, the volume reduction is expected to be even larger. However, the LID-goal ($f_v < 0.6$) is not reachable in Dutch Polder conditions except for the smallest of storms. As the peak reduction can be quite high, limited volume reduction should not pose a real problem.

The peak reduction can be very large, depending on the construction of the top-soil. When aiming at the 24 hours emptying time, a peak reduction of 90-95% should be reachable for extreme storms. For medium storms, the peak-reduction should be in the range of 75-85%. This is all within the LID-goal set for peak reduction. Smaller and longer storms have a lower peak reduction, as the inflow peak is smaller as well this is less of an issue.

The peak delay can vary a lot, results also depend on which peak (fast or slow) is considered. Since the peaks don't differ much in magnitude, it is recommended that the first fast peak is considered for the peak delay and the slow, absolute peak for the peak reduction. The peak delay goal ($R_{delay} > 6$) is never reached by the medium storms (4), and for roughly 45% of the large storms. However, as the peak reduction is quite large, this should not be problematic. The moisture content of the soil, hydraulic conductivity and media depth play a role here, as the moisture content of the soils is usually high and the media depth low (shallow groundwater) this is a difficult goal to reach in Rotterdam's polder conditions.

The emptying time should be no more than 24 hours, as the whole sewer system is expected to be empty again for the next storm. None of the large storms meet this goal, only for medium or small storms can this goal be reached. The permeability of the top-soil should be sufficient, either a larger sand-fraction is needed or no clay should be mixed in. When increasing the permeability, the peak reduction and peak delay decrease. As such, it should be considered which goals take priority.

Another way to quantify the hydraulic benefits is the volume delay, which gives the percentage of volume from the storm which is not discharged during the storm event. As such, the water infrastructure doesn't have to deal with this water when it already has to process the resulting discharge from other areas. The volume delay ranged from 70-99 %, with the worst volume delay occurring during a Two- peak storm (3) when the outflow from the first inflow peak contributed to the discharge which took place during the second inflow peak.

Design and construction recommendations

The current design of the Rotterdam bioswale should work decent, but a few improvements can be made.

- The goal of the drainage chest is to allow for the drain to be placed under the groundwater level. When the area has significant subsidence or a shallow drainage level, the drain can also be placed in the sandbed as long as it still lays underneath the groundwater table (top drain + 20 cm).
- Soil which is released during groundwork should not be mixed carelessly in the top-layer of the bioswale, as it can drastically decrease the infiltration capacity.
- The top-layer should be 20 cm deep, so the macropores from the grass-roots can ensure sufficient permeability over time.
- Weeds should be controlled, as they can impact the permeability of the top-layer. This might also mean that green-areas with little sunlight are not well-fit for bioswales.
- When the bioswale is placed in an area that is less-favorable for grass (little sun-light, large trees surrounding it), the textural porosity should be monitored extra carefully to ensure the grass doesn't suffer from ponding to much as well.
- The current design doesn't account for any volume reduction during rainfall, with the low permeability of the top-soil this is a good assumption.
- Instead of allowing the top-soil to govern infiltration, it could be decided to let the drain be the limiting factor by drastically decreasing the drain diameter. This way, the storage in the soil is maximally utilized. However, Hydrus 2D/3D does show that most of the soil is already near saturation with the current design, mainly due to the high groundwater level (Figure 17 and Figure 18).

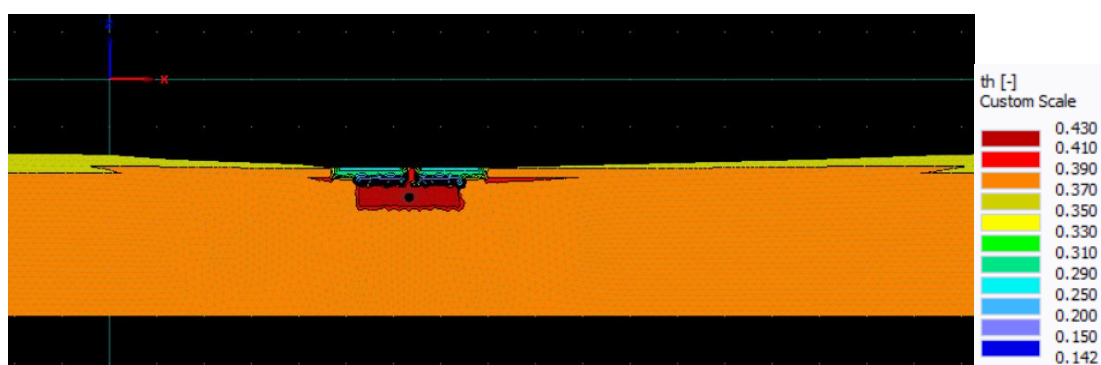


Figure 39: Bioswale E moisture content before the storm simulation

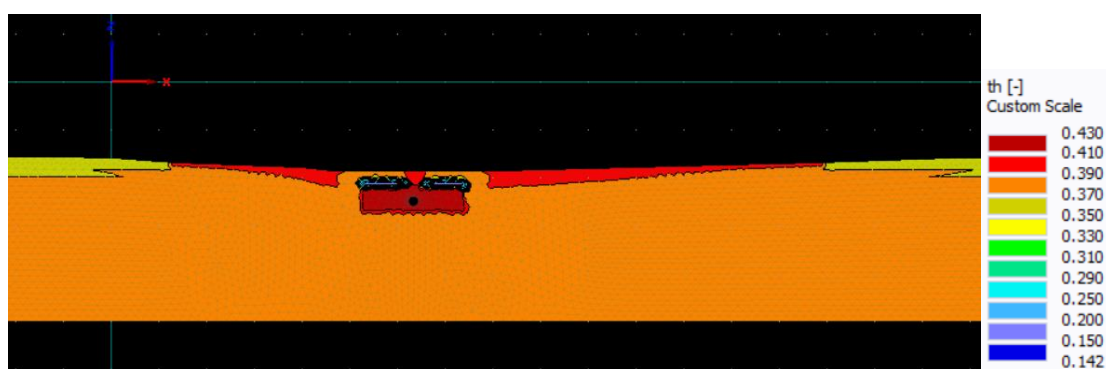


Figure 40: Bioswale E moisture content 0.04 days into the storm simulation

Direct action

Bioswale B is prone to clogging, as the top-soil has a too low sand fraction. This results in large bare spots on the bioswale bottom, which are not likely to recover on their own. The top-soil of this bioswale should be replaced, and have a sand-fraction of about 85%. This should be done just before the growing season, under dry conditions.

Bioswale 7 has a much to high permeability, the bottom lays to high and the surrounding dike prohibits water from the green-area to enter the swale. A complete reconstruction is needed of the groundwork, as well as different vegetation.

In the current register, bioswales are usually denoted as grass-land, sometimes with higher maintenance. However, it can nowhere be found that these grass-land are bioswales and are part of the water structures of the city. To ensure correct maintenance and allow for monitoring, it is strongly advised to add a category in the register for bioswales including revised design drawings.

8.2 Further research

- It would be recommended to research the emptying time for different storms, to see which storms give the worst performance. It was already shown in this research that two storms with the same volume as one storm give a much larger emptying time.
- When more diversity in the vegetation of bioswales is wanted, it should be carefully considered which plant-species are fitting of bioswales, creating sufficient but not to high permeability.
- The drains which lay above the groundwater table are likely to suffer from iron-oxidation. To determine the rate at which this occurs could be helpful for similar drains (Molière-neighborhood). As such it could be interesting to dig up the drains of bioswales B and D, and if possible connect them to the DIT-sewer instead of the combined sewer system.
- The recommended mix of drainage sand and compost for the top soil-layer (Boogaard, 2006) was mostly followed for the monitored bioswales, only some soil which was released during construction was used as well. Did the released soil cause the low permeability or did the prescribed composition not function well?

References

- Ahmed, F., Gulliver, J.S. and Nieber, J.L. (2015). "Field infiltration measurements in grassed roadside drainage ditches: Spatial and temporal variability." *J. Hydrol. Eng.*, 530, 604–611.
- Archer, N.A., Quinton, J.N., and Hess, T.M. (2002). Below-ground relationships of soil texture, roots and hydraulic conductivity in two-phase mosaic vegetation in south-east Spain. *Journal of Arid Environments*, 52(4), 535–553.
- Asare, S. N., Rudra, R. P., Dickinson, W. T., and Wall, G. J. (1999). "Effect of freeze-thaw cycle on the parameters of the Green and Ampt infiltration equation." *J. Agric. Eng. Res.*, 733, 265–274.
- Assouline, S. (2004). "Rainfall-induced soil surface sealing: A critical review of observations, conceptual models, and solutions." *Vadose Zone J.*, 3, 570–591.
- Barber, M., King, S., Yonge, D. and Hathhorn, W. (2003). "Ecology Ditch: A best management practice for storm water runoff mitigation." *J. Hydrol. Eng.*, 8(3), 111-122.
- Barzegar, A. R., Yousefi, A., and Daryashenas, A. (2002). "The effect of addition of different amounts and types of organic materials on soil physical properties and yield of wheat." *Plant Soil*, 247, 295-301.
- Beindorff, B.A. (2014). *Bemalingsadvies tbv rioolvervanging Zenostraat en geohydrologische advies tpv en omgeving van de wadi*. Municipality of Rotterdam.
- Boogaard, F.C. (2015). "Stormwater characteristics and new testing methods for certain sustainable urban drainage systems in The Netherlands." TU Delft. 97-117. ISBN: 978-94-6259-745-7.
- Boogaard, F., Bruins, G. and Wentink, R. (2006). "Wadi's: aanbevelingen voor ontwerp, aanleg en beheer". Ede: RIONED.
- Boogaard, F.G., Rozendaal, B., Pieter, G., and Steenbruggen, G. (2017). "Overschatten we het hydraulisch functioneren van wadi's en doorlatende verharding?" *H2O-Online*, 21 June 2017.
- Davis, A. P. (2008). "Field performance of bioretention: Hydrology impacts." *J. Hydrol. Eng.*, 13(2), 90–95.
- Bouwer, H. 1978. *Groundwater hydrology*. McGraw-Hill, New York.
- Carter, M. R. (2002). "Soil quality for sustainable land management: Organic matter and aggregation interactions that maintain soil functions." *Agron. J.*, 95, 38–47.
- Constantz, J., Thomas, C. L., and Zellweger, G. 1994. "Influence of diurnal-variations in stream temperature on streamflow loss and groundwater recharge." *Water Resour. Res.*, 30(12), 3253–3264.
- Davis, A. P., Hunt, W. F., Traver, R. G., and Clar, M. E. (2009). "Bioretention technology: Overview of current practice and future needs." *J. Environ. Eng.*, 135(3), 109–117.
- Davis, A.P., Stagge, J.H., Jamil, E. and Kim, H. (2011). "Hydraulic performance of grass swales for managing highway runoff." *Water res.*, 46, 6775-6786.
- Davis, A.P., Traver, R.G., Hunt, W.F., Lee, R., Brown, R.A. and Olszewski, J.M. (2012). "Hydrologic Performance of Bioretention Storm-Water Control Measures." *J. Hydrol. Eng.*, 17(5), 604-614.
- Donkers, E. (2010). *Swale filter drain system: Inflow–discharge relation*. TU-Delft repository.
- Driscoll, E., Shelley, P. E., and Strecker, E. W. (1990). *Pollutant loadings and impacts from highway stormwater runoff. Volumes I–IV*, FHWA/RD-88-006-9, Federal Highway Administration, Woodward-Clyde Consultants, Oakland, Calif.

- Duchene, M. McBean, E. A., and Thomson, N. R. (1994). "Modeling of infiltration from trenches for storm-water control." *J. Water Resour. Plann. Manage. Div., Am. Soc. Civ. Eng.*, 120(3), 276–293.
- Ellis, J. B., Harrop, D. O., and Revitt, D. M. (1986). "Hydrological controls of pollutant removal from highway surfaces." *Water Res.*, 20(5), 589–595.
- Emerson, C. H., and Traver, R. G. (2008). "Multi-year and seasonal variation of infiltration from stormwater best management practices." *J. Irrig. Drain. Eng.*, 134(5), 598–605.
- Energy Independence and Security Act. (2007). 110–140
(www.epa.gov/oaintrnt/stormwater/requirements.htm#eisa).
- Ermilio, J.R., and Traver, R.G. (2006). *Hydrologic and pollutant removal performance of a bio-infiltration BMP*. Proceedings of the 2006 world environmental and water resources congress. ASCE/EWRI. Omaha, Nb, USA. pp. 1–12.
- Federal Highway Administration (FHWA). (1996). "Evaluation and management of highway runoff water quality." *Pub. No. FHWA-PD-96-032*, U.S. Department of Transportation, Washington, D.C., June.
- Folkesson L, Bækken T, Brenčić M, Dawson A, François D, Kuřimská P, et al. (2009). Sources and fate of water contaminants in roads. *In Water in Road Structures*. Springer, Netherlands, 107–146.
- Fuentes, J.P., Flury, M., and Bezdicsek, D.F. (2004). "Hydraulic properties in a silt loam soil under natural prairie, conventional till, and no-till." *Soil Sci. Soc. Am. J.*, 68, 1679–1688.
- Geerling, H.R. (2014). "Infiltration swales: Quantitative performance on an urban catchment scale." TU Delft repository.
- Harrington, B. W. (1989). "Design and construction of infiltration trenches." *Proc., Urban Runoff Water Quality Control*, ASCE, New York, 290–304.
- Hatt, B.E., Fletcher, T.D., and Deletic, A. 2009. Hydrologic and pollutant removal performance of stormwater biofiltration systems at the field scale. *Journal of Hydrology*, 365(4), 310 –321.
- Heasom, W., Traver, R., and Welker, A. (2006). "Hydrologic modeling of a bioinfiltration best management practice." *J. Am. Water Res. Assn.*, 42(5), 1329–1347.
- Hillel, D. 1998. *Environmental soil physics*. Academic, San Diego.
- Houston, S. L., Duryea, P. D., and Hong, R. (1999). "Infiltration considerations for ground-water recharge with waste effluent." *J. Irrig. Drain. Eng.*, 125, 264–272.
- Hunt, W.F., Davis, A.P., and Traver, R.G. (2012). Meeting hydrologic and water quality goals through targeted bioretention design. *J. Environ. Eng.*, 138(6), 698-707.
- Hunt, W. F., Smith, J. T., Jadlocki, S. J., Hathaway, J. M., and Eubanks, P. R. (2008). "Pollutant removal and peak flow mitigation by a bioretention cell in urban Charlotte, NC." *J. Environ. Eng.*, 134(5), 403–408.
- Hunt, W. F., Jarrett, A. R., Smith, J. T., and Sharkey, L. J. (2006). "Evaluating bioretention hydrology and nutrient removal at three field sites in North Carolina." *J. Irrig. Drain. Eng.*, 132(6), 600–608
- van Genuchten, M.T. (1980). A closed-form equation for predicting the hydraulic conductivity of unsaturated soils. *Soil Sci. Am. J.*, 44, 892-898.
- Khan, U.T., Valeo, C., Chu, A., and van Duin, B. (2012). Bioretention cell efficacy in cold climates: Part 1 — hydrologic performance. *Can. J. Civ. Eng.*, 39, 1210 –1221.
- Klapwijk, A. (2018). *Wadi Bouwsteen: Ontwerpaspecten*. Municipality of Rotterdam.
- Jaynes, D. B. 1990. "Temperature variation effect on field-measured infiltration." *Soil Sci. Soc. Am. J.*, 54, 305–312.

Kluge, B., Markert, A., Facklam, M., Sommer, H., Kaiser, M., Pallasch, M., and Wessolek, G. (2016). "Metal accumulation and hydraulic performance of bioretention systems after long-term operation." *J. Soils Sediments*, 18, 431–441

Lado, M., Paz, A., and Ben-Hur, M. (2004). "Organic matter and aggregate size interactions in infiltration, seal formation, and soil loss." *Soil Sci. Soc. Am. J.*, 68, 935–942.

Le Coustumer, S., Fletcher, T.D., Deletic, A., and Barraud, S. (2007). Hydraulic performance of biofilters for stormwater management: first lessons from both laboratory and field studies. *Water Science and Technology*, 56(10), 93–100.

Lewis, J.F., Hatt, B.E., Deletic, A., and Fletcher, T.D. (2008). *The impact of vegetation on the hydraulic conductivity of stormwater biofiltration systems*. Proceedings of the 11th International Conference on urban drainage. ICUD, Edinburgh, UK. pp. 1–10.

Li, H., and Davis, A.P. 2008. Urban particle capture in bioretention media. I: Laboratory and field studies. *Journal of Environmental Engineering*, 134(6), 409–418.

Li, H., Sharkey, L., Hunt, W. F., and Davis, A. P. (2009). "Mitigation of impervious surface hydrology using bioretention in Maryland and North Carolina." *J. Hydrol. Eng.*, 14(4), 407-415.

Lindsey, G., Roberts, L. and Page, W. (1992). "Inspection and maintenance of infiltration facilities." *J. Soil and Water Cons.*, 47(6), 481–486.

McCuen, R. H. (2003). "Smart growth: Hydrologic perspective." *J. Prof. Issues Eng. Educ. Pract.*, 1293, 151–154.

Mualem, Y. (1976). A new model predicting the hydraulic conductivity of unsaturated porous media. *Water Resour. Res.*, 12, 512-522.

Municipality of Rotterdam (2017). *Zenostraat, gemeenschappelijke Tuinen*. Grondwerk herinrichting gemeenschappelijke tuinen en voortuinen. Municipality of Rotterdam.

Parker, J.K., McIntyre, D., and Noble, R.T. (2010). Characterizing fecal contamination in stormwater runoff in coastal North Carolina, USA. *Water Res*, 44(14), 4186–4194

Rawls, W.J., Brakensiek, D.L. and Miller, N. (1983). "Green-Ampt infiltration parameters from soil data." *J. Hydraul. Eng.*, 109(1), 62-70.

Ronan, A. D., Prudic, D. E., Thodal, C. E., and Constantz, J. 1998. "Field study and simulation of diurnal temperature effects on infiltration and variably saturated flow beneath an ephemeral stream." *Water Resour. Res.*, 34, 2137–2153.

Sabourin, J.F., and Wilson, H. C. (2008). *20 year performance evaluation of grass swale and perforated pipe drainage systems*. J.F. Sabourin and Associates Inc.

Schaap, M.G., Leij, F.J., and van Genuchten, M. T. (2001). Rosetta: a computer program for estimating soil hydraulic parameters with hierarchical pedo-transfer functions. *Journal of Hydrology*, 251, 163-176.

Schueler, T. R. (1987). "Controlling urban runoff: A practical manual for planning and designing urban BMPs." *Dept. of Environmental Programs*, Metropolitan Washington Council of Governments, Washington, D.C.

Schueler, T.R. (1994). "Performance of grassed swales along east coast highways." *Watershed Prot. Tech.*, 1(3), 122-123.

Siriwardene, N. R., Deletic, A., and Fletcher, T. D. (2007). "Clogging of stormwater gravel infiltration systems and filters: Insights from a laboratory study." *Water Res.*, 41, 1433–1440.

Traver, R.G., Davis, A.P., and Hunt, W.F. 2007. *Bioretention and bioinfiltration BMPs*. Stormwater: The journal for surface water quality professionals.

Traver, R.G., and Prokop, M. (2003). *Effectiveness of a bioinfiltration BMP*. Proceedings of the World water and environmental resources congress 2003 and related symposia. ASCE/EWRI, Philadelphia, Pa., USA. pp. 1.

University of New Hampshire Stormwater Center (UNHSC), (2006). *2005 Data Rep.*, CICEET, Durham, N.H.

Urbonas, B., and Stahre, P. (1993). *Stormwater: Best management practices and detention for water quality, drainage and CSO management*, Prentice-Hall, Englewood Cliffs, N.J.

Walsh, C. J., Roy, A. H., Feminella, J. W., Cottingham, P. D., Groffman, P. M., and Morgan, R. P. (2005). "The urban stream syndrome: Current knowledge and the search for a cure." *J. North Am. Benthol. Soc.*, 24(3), 706–723.

Appendix

Appendix 1: Height profile and pictures of dry swales, bioswales A, B, D, E and 7

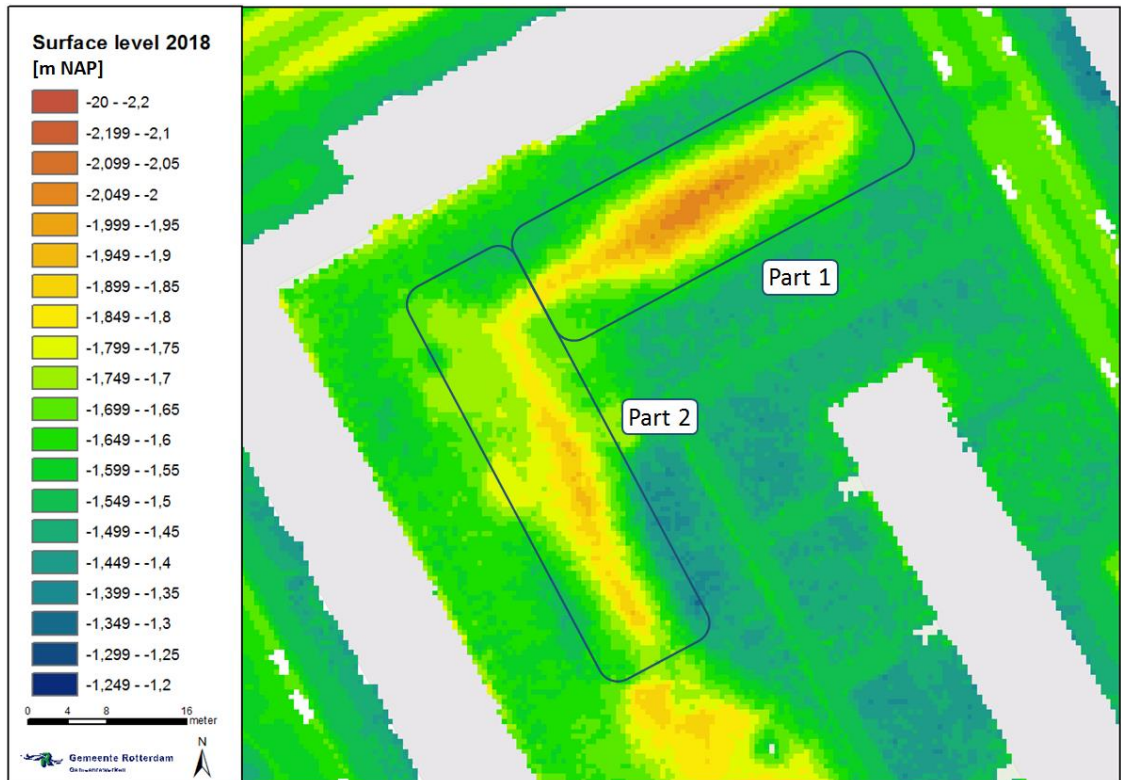


Figure 41: Depth profile bioswale A, clear height divide between sections



Figure 42: Picture bioswale A part 1, clear shape bioswale

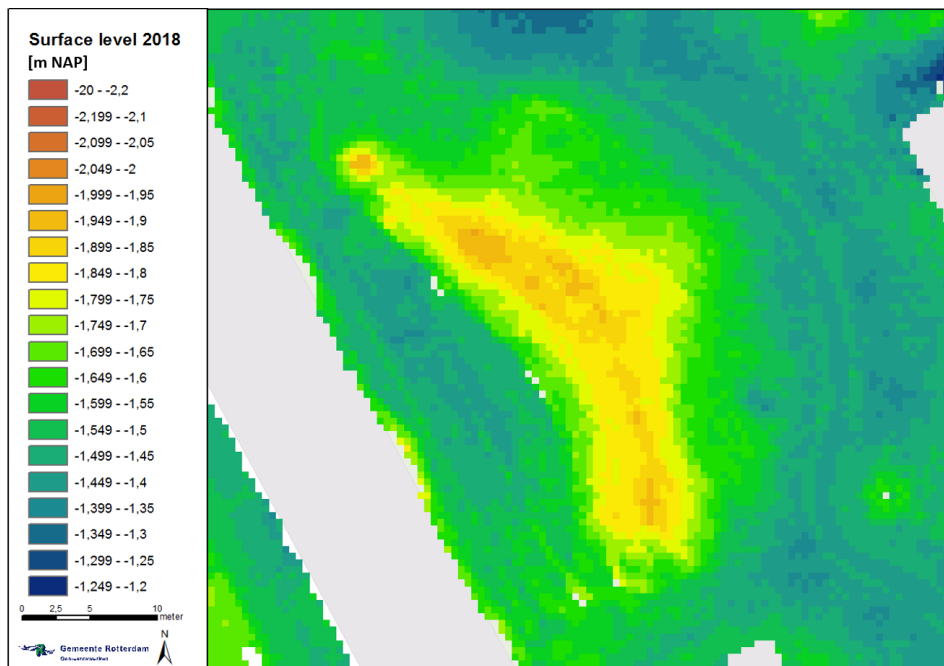


Figure 43: Depth profile bioswale E, multiple low point are visible



Figure 44: Picture bioswale E, organic shape bioswale

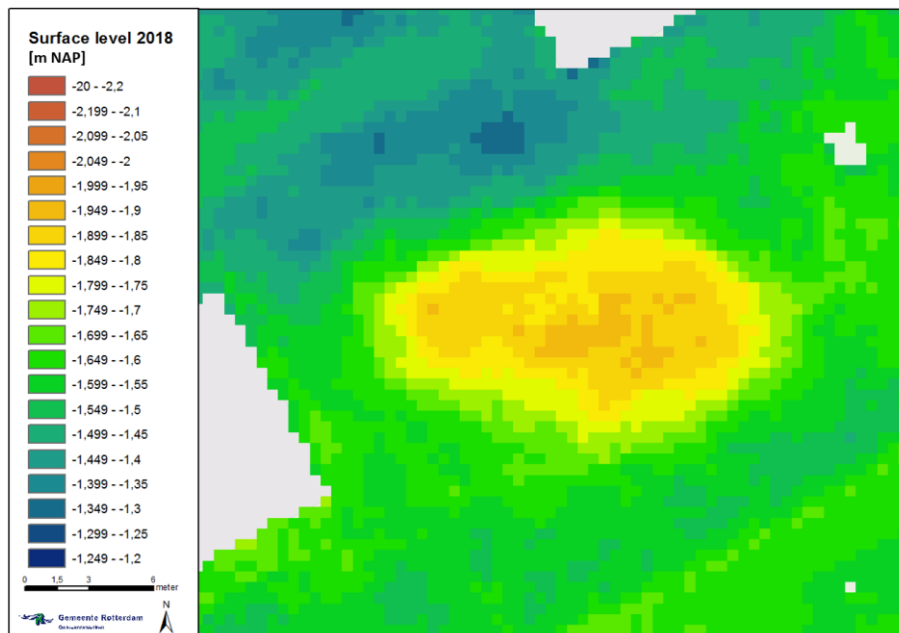


Figure 45: Depth profile bioswale D, clear shape



Figure 46: Picture bioswale D, little sun-light due to trees and buildings

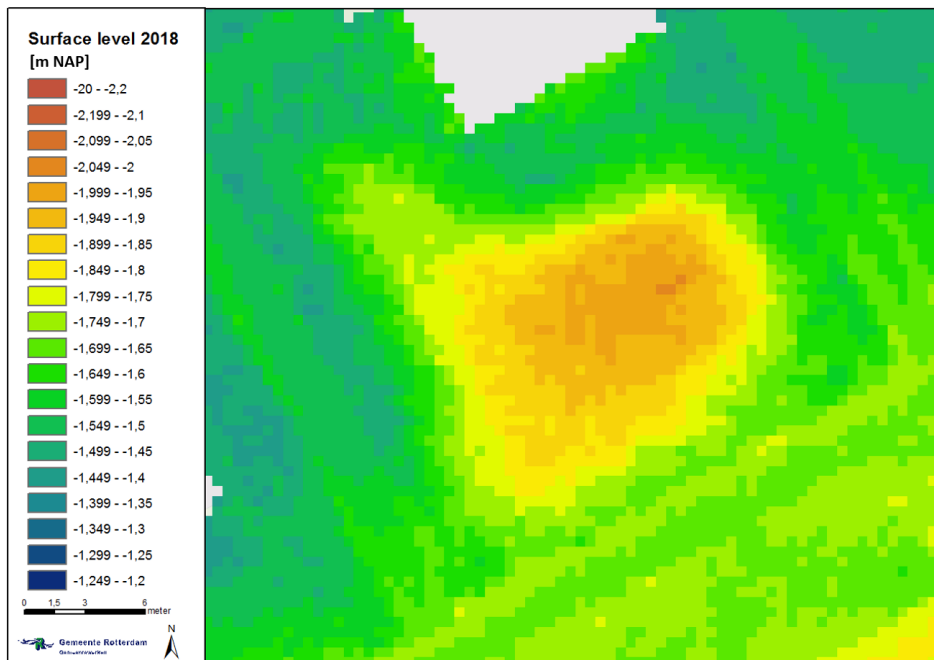


Figure 47: Depth profile bioswale B, clear slope to lowest point



Figure 48: Pictures respectively bioswale D and bioswale B

Observations in the field after natural rainfall, suggest that bioswale B empties much slower than bioswale D. Where bioswale D had a thin ice-layer where there had been water the previous day, all water underneath had drained. Bioswale B had an ice-layer as well, but all water underneath was still there.

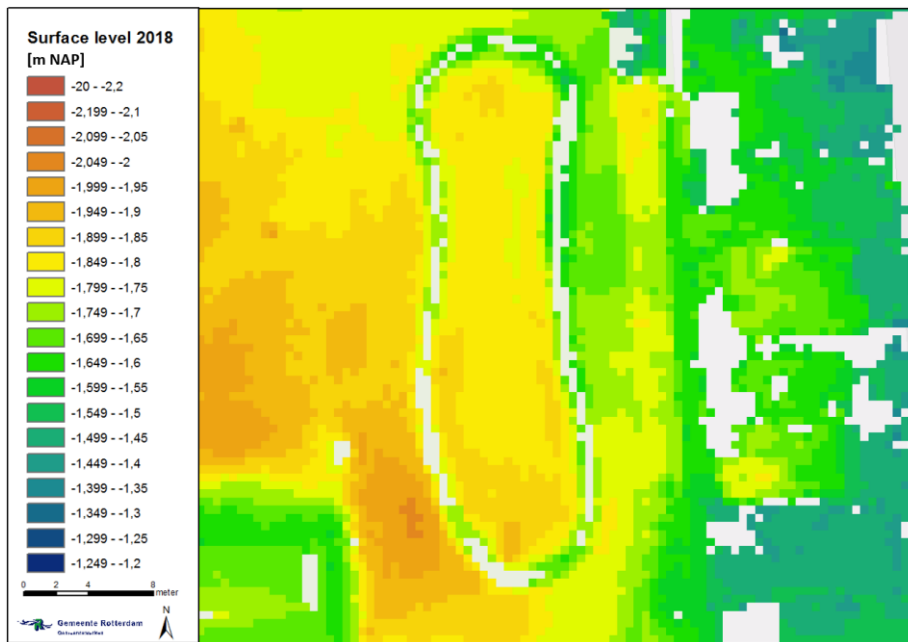


Figure 49: Depth profile bioswale 7, the swale is not the lowest point in the area



Figure 50: Picture bioswale 7, dike separating the swale from the surrounding area

Appendix 2: Discharge measuring device

Need for a new discharge measuring device

In order to measure discharge in different locations, a device was needed which could be transported and installed without high costs. In addition, it should be able to measure in both partially-filled and completely filled drainage pipes. This posed quite a large problem, since there were no current devices in place measuring discharge from drains. Most bioswale discharge research is done with a weir and diver (clear water level-discharge relation), but this is not possible for submerged drains. There are also various flow-meters which can be installed as part of the pipe, but this would bring high costs (on top of the device itself) and only works in completely filled pipes. This goes as well for propeller-methods, and cross-correlation sensors are tailored to completely filled or partially filled pipes. As such, another way of measuring the discharge was needed which fulfilled all requirements.

Designing a new discharge measuring device

A device was constructed based on the pumping stations for polders and sewer systems. Though discharge measuring devices are usually present here, they are checked using the number of times the pumps are started. As the pumps start at a certain water level in the basin, and end at a set lower water level, they pump the same amount every time (minus the difference in inflow during pumping, which is negligible as the pumping capacity is much larger than the inflow). This method is copied using the manhole as basin. To create this basin, all other pipes of the manhole to which the drain connects are closed off. Since the water level in the manhole should fluctuate as little as possible in case of submerged drains (this would influence the discharge from the drain), and the manhole is relatively small, the pump would have to start much more frequent (pumping much smaller amounts at the time). This in itself is desirable, since it enhances the precision drastically. However, this does mean that the inflow to the manhole during pumping cannot be neglected, as the pumping capacity is in the same order as the discharge from the drain.

As such, a time interval for pumping is used instead. Now, when a certain water level is reached, the pump works for a set amount of time (pumping a calibrated amount of water), after which it stops until the set level is reached again. How many times the pump is activated determines the discharge in that time period.

Four issues with this design became clear during field testing. The first issue was that the pump needs to be active a certain time before switching off again, to keep functioning well over time and supply a more constant discharge. This could be quite easily fixed by using low-capacity pumps with longer running times. To ensure the maximum discharge from the drain could still be managed, two pumps were installed instead of one. The second pump had a start-level slightly higher than the first pump, so it will only start when the first pump is at its maximum and can't handle more water. This also introduced more robustness to the system, when one float-sensor or pump failed, the other would take over. The second problem was observed when the pumps were nearing maximum capacity. When this happened, the number of times the pump is activated will decrease (instead of keep increasing). At the moment the pump should have been turned off, it keeps pumping as the float indicates the water level is too high. This is not read as a pump-start, and as such the number of pump-starts decreases (as it shuts-off less, it also starts-up less). The third problem was calibrating the amount of water pumped with the set pumping time.

Even in laboratory conditions (constant power feed, constant temperature, etc.). there were large differences in the amount of pumped water per turn for the same pumping time. However, these were normally distributed and might not necessarily pose a big problem. It did also become clear that the tension of the battery influences the outflow. When using a battery in the field (which has more power at the start and less at the end), this would need to be taken into account.

The fourth and final problem was also the hardest one. It appeared that, due to the screw in the pump still turning slightly after the pump was stopped, it sends a signal back which started the pump again. This was attempted to solve, by extending the wires (more resistance), introducing a waiting-time between pump-starts and adding resistance in the receiver as well. Though this slowed down the process (the device functioned properly for a longer time), it did not resolve the issue. As the accuracy of the outflow was also still far from optimal, a different approach was decided on. Since the restarting problem did not occur without the timer, it was decided to leave this out. Instead, the pumps would work on their respective floaters (with a minimum pumping time to protect against oscillation). As this makes it impossible to determine the amount of water pumped for each pumping turn, an extra part was added to the configuration. The outflow of both pumps is now connected to a tipping bucket, which tips every 3 liters. These tips were recorded against time and used to determine the discharge. Especially low discharges could be measured quite accurately this way, for both submerged and free-flowing drains.

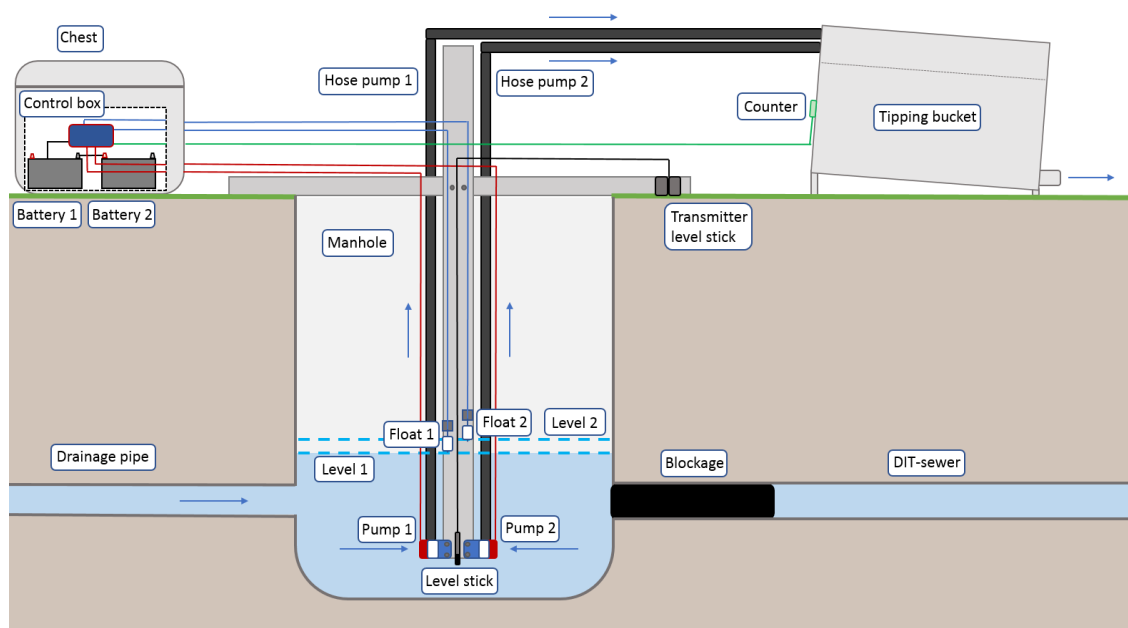


Figure 51: Discharge measurement device schematisation, submerged drain

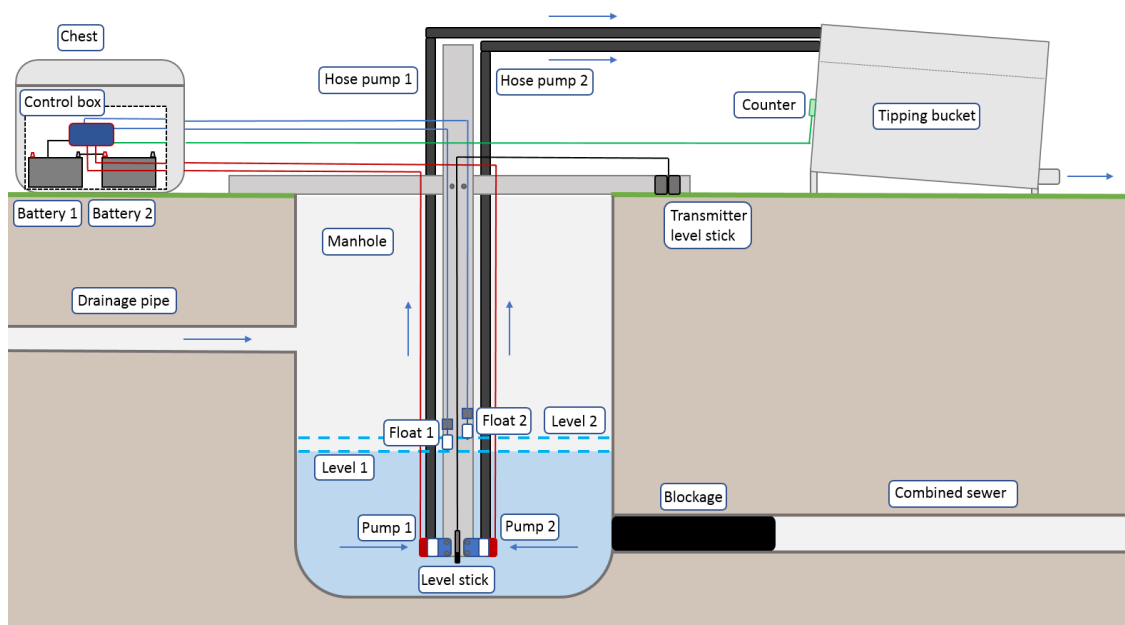


Figure 52: Discharge measurement device schematisation, free-flowing drain

Manholes

In order to measure the discharge, the drain of the bioswale needs to be connected to a manhole. As the drains of bioswale A and E were directly connected to the DIT-sewer, a manhole needed to be placed in between for this study. As the manholes of bioswale B and D are part of the combined sewer system, they were cleaned before the measuring campaign.

Frame

The gantry put inside the manhole consists of two metal beams, which form a cross connected by two bolts. The horizontal beam rests unto the manhole-edge, as far as possible from the outflow of the drain to minimize the disturbance of the water surface due to inflow from the drain for the floaters. The vertical beam can be moved up-and-down with the bolts and secured at the appropriate height, so that float 1 just touches the water surface in the manhole. In case of a free-flowing drain, when no water is present in the manhole, it is first partially filled so the pumps are underwater. This water level should not influence the discharge from the drain and should thus be set deep enough.

Pumps

Onto the bottom of the gantry, two submersible pumps are secured. The pumps work on 12 Volt and 1.9 Ampere. They have a maximum discharge of 31 l/min according to their description, and the maximum head is 2 meters. No head/discharge curve was available. The outflow hoses of the pumps are connected to the tipping bucket. It was estimated that 2 times 31 l/min should be sufficient capacity for the planned tests, considering the permeability of the topsoil-layers.

Floaters

The floaters have a switching voltage of 200 Volt, and a maximal switching current of 0.5 Ampere. The floats have an accuracy of 5 mm, and work with magnetic signals. The floats are connected to their respective pump through the control box, here a minimal pumping time is introduced as well using a timer. When the water level rises due to inflow from the drain, float 1 is activated. This float sends a signal to the control box, which activates pump 1 by connecting the batteries to the pump. The pumping stops when the minimal pumping time has passed and the water level is underneath floater 1 again. When the discharge from the drain is larger than the maximal pumping capacity of pump 1, the water level increases while pump 1 keeps working continuously. When the water level reaches floater 2, pump 2 is activated following the same scheme as pump 1.



Figure 53: Frame in manhole; Pumps, level stick and floaters of the discharge measuring device

Power supply

At the start of the field survey, only 2 batteries were in use. When one battery was used in the measuring setup, the other battery was charging so they could be switched when needed. Later in the measuring campaign, 2 extra batteries were purchased as a single battery had proven not to be sufficient for a storm simulation in the larger bioswales. For the remaining campaign, 2 batteries were linked in parallel to supply the pumps with energy, while the other two were charging in parallel as well. The first set of batteries had a capacity of 95 Amh each, the second pair 105 Amh each.

Tipping counter

The tipping counter receives the water pumped up by the pumps and notes down how many times per minute the bucket inside tips. As every tip marks a 3 liters inflow, this can be used to determine the discharge. This stainless-steel tipping counter is equipped with a detachable roof, to protect it from rainfall and other undesired inflows. To ensure the accuracy of these measurements, the tipping bucket is placed using a spirit level. The data from the tipping counter is sent to the control box.

Control box

The control box is in control of the whole discharge measuring set-up. It relates the signals from the floaters to their respective pumps and gathers data on the number of times each pump is activated. The tipping counter is connected to the control box as well, so it can save the tips per minute registered by the counter. All the data is sent to the ARGUS-network on an hourly bases, so it can be viewed in close to real time. This data can be used to monitor the functioning of the discharge measuring set-up from afar so action can be taken when a problem is detected.

Level stick

In order to determine whether the discharge measuring device is working properly, a level stick was added to the measuring set-up. This level stick measures the water pressure in the manhole, which can be used to determine the water level when corrected for the air pressure. When the water level increases, it shows that the floaters or batteries have failed. Rapid changes in water level indicates malfunction of the floaters or short circuiting in the cables. In addition, this data would make it visible when floater 2 is activated and deactivated again.



Figure 54: Chest with control box and batteries inside; Tipping counter in laboratory set-up

Evaluation discharge device

The device designed is able to measure discharge from drains connected to manholes, for both submerged and free-flowing drains. This method measures low outflow very well and can be installed relatively easy. The selected manhole should not cause problems for the sewer system when temporarily blocked-off. As such, an end-manhole should be selected or different routes should be available to the water. Also bear in mind that the measuring device needs to be protected, so an area around the manhole (at the surface) should be closed-off as well. An outflow needs to be realised, usually to the nearest gully pot is the easiest option. When another manhole is used for the outflow, it should also be closed off for the safety of the residence. Since simple submerged pumps are used, the water should not contain solids which could damage or clog the pumps. The maximal pumping capacity should not be exceeded either (62 l/min), or stronger pumps need to be installed. At last, the batteries also have a limited charge and need to be replaced in time depending on the amount of water pumped and outside temperature (the batteries have shorter lifetime in cold weather). The best option would be to connect the device to the electricity network, especially when the measuring campaign is long and at the same location.

Appendix 3: Placement piezometers in bioswales A, B, D, E and 7

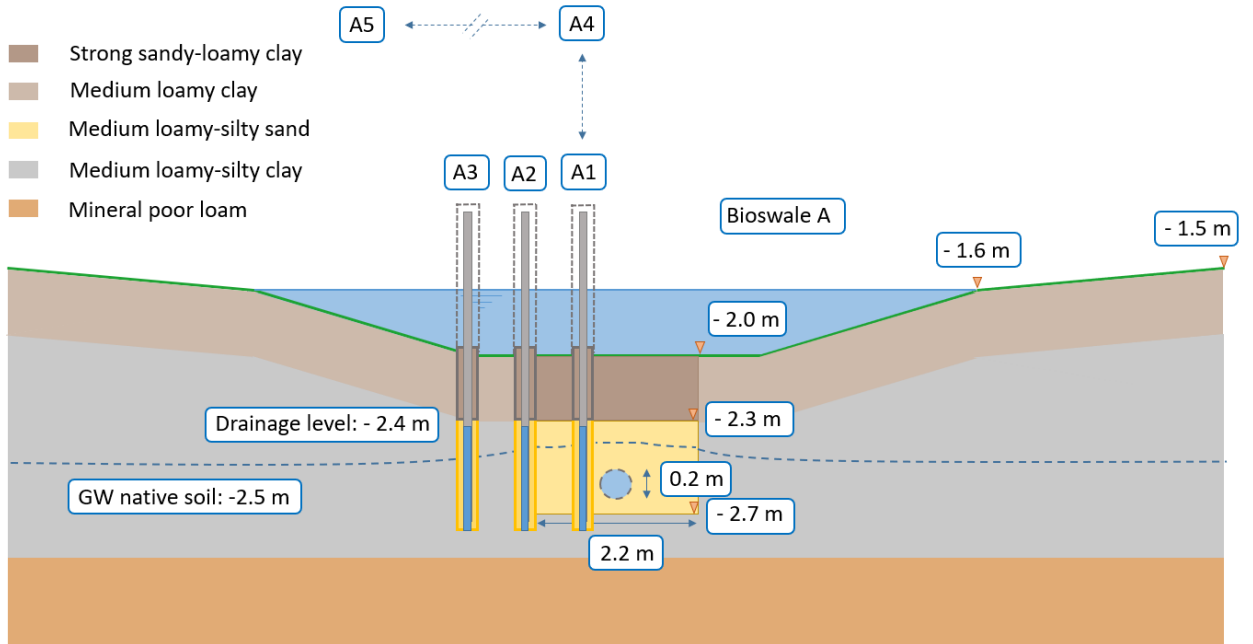


Figure 55: Piezometers bioswale A, cross-section

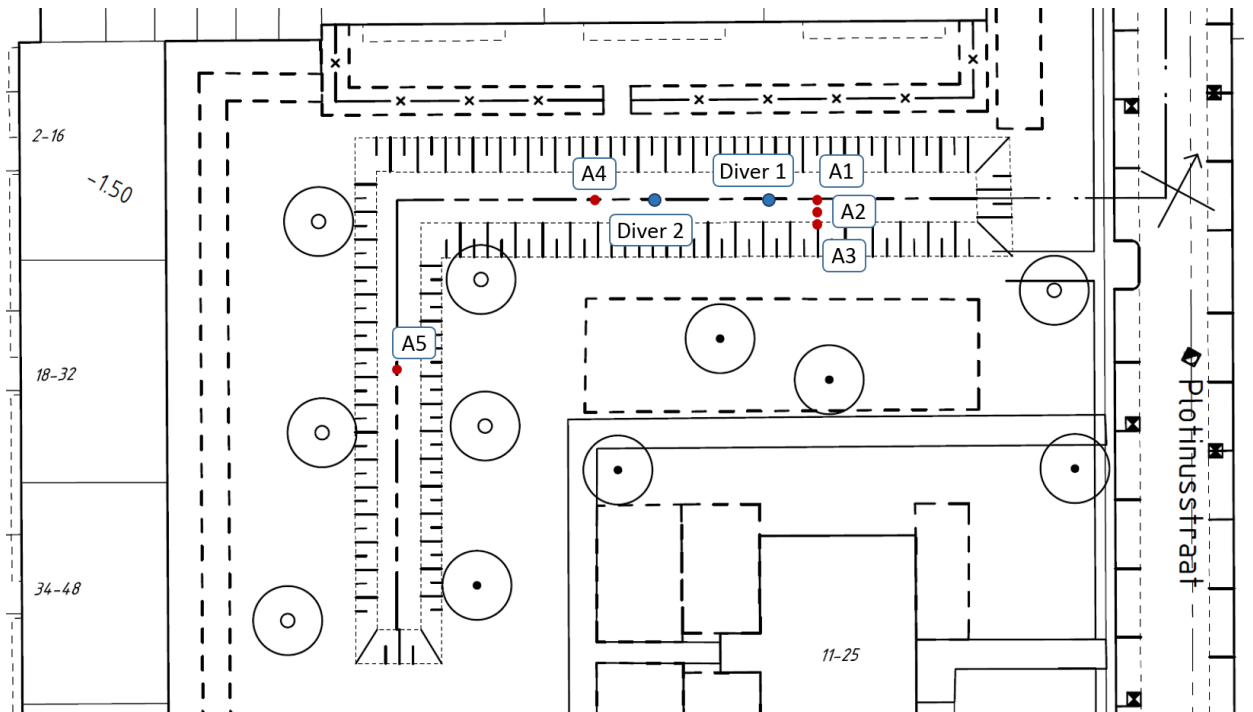


Figure 56: Piezometers and divers bioswale A

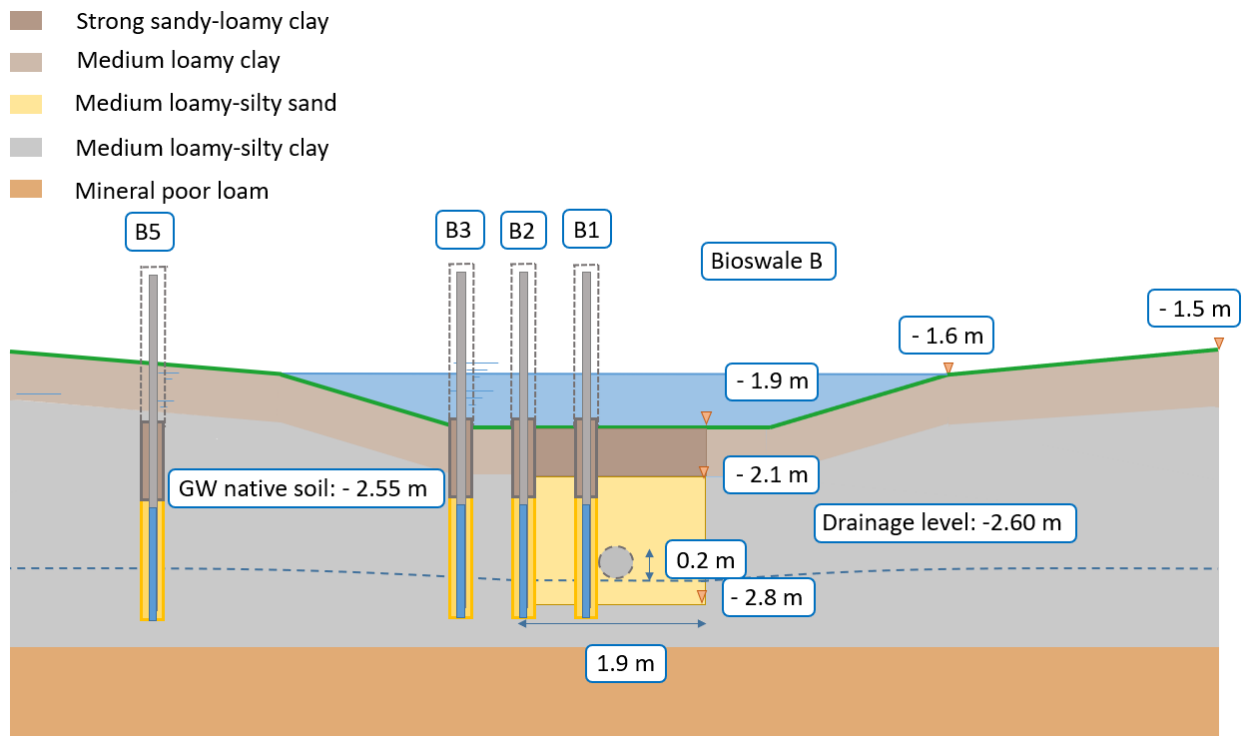


Figure 57: Piezometers bioswale B, cross-section

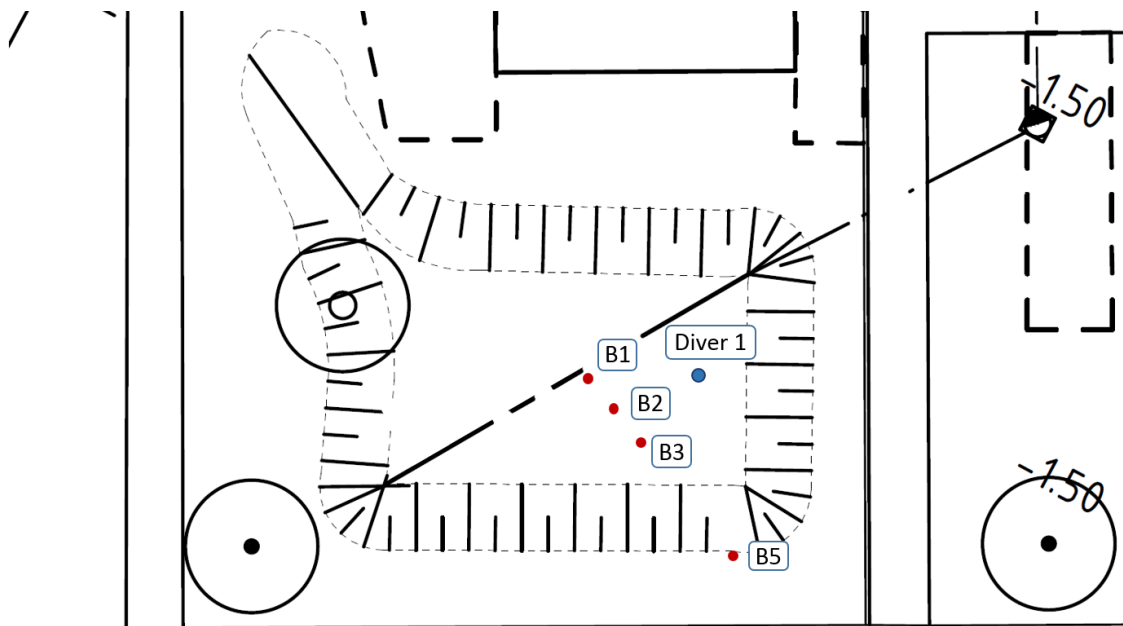


Figure 58: Piezometers and divers bioswale B

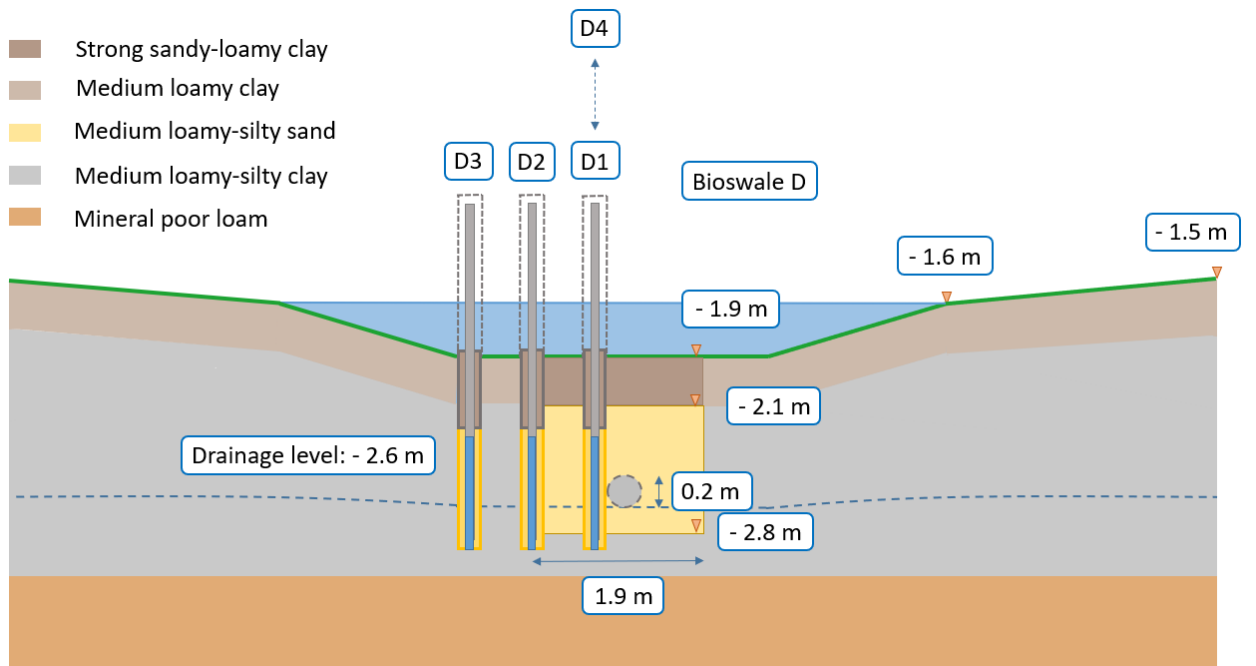


Figure 59: Piezometers bioswale D, cross-section

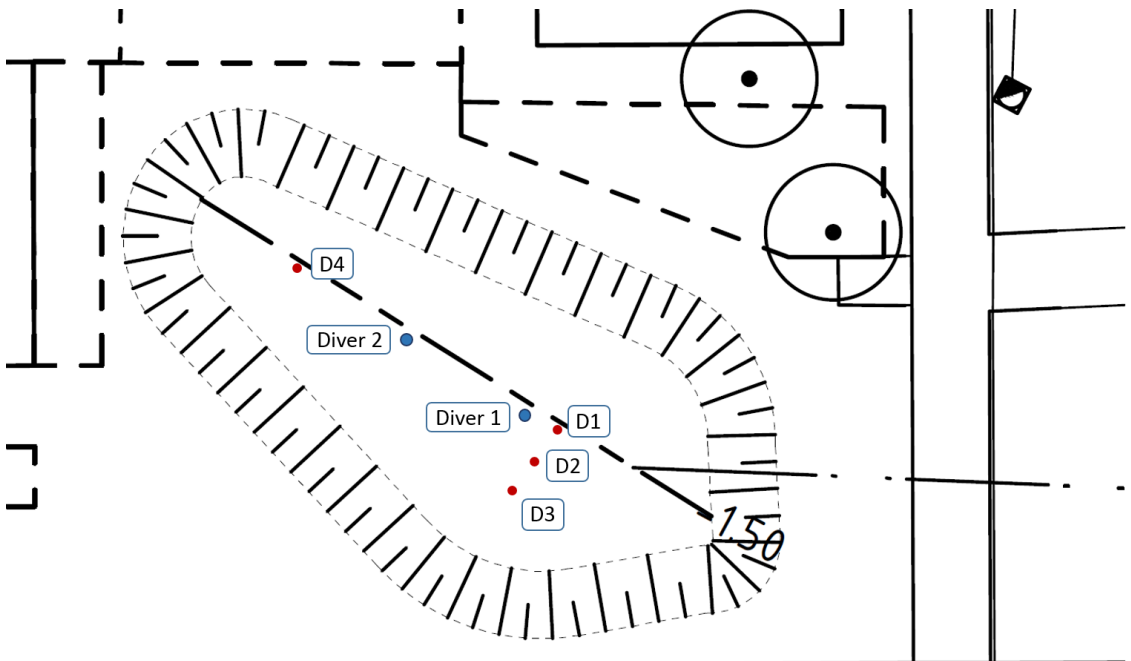


Figure 60: Piezometers and divers bioswale D

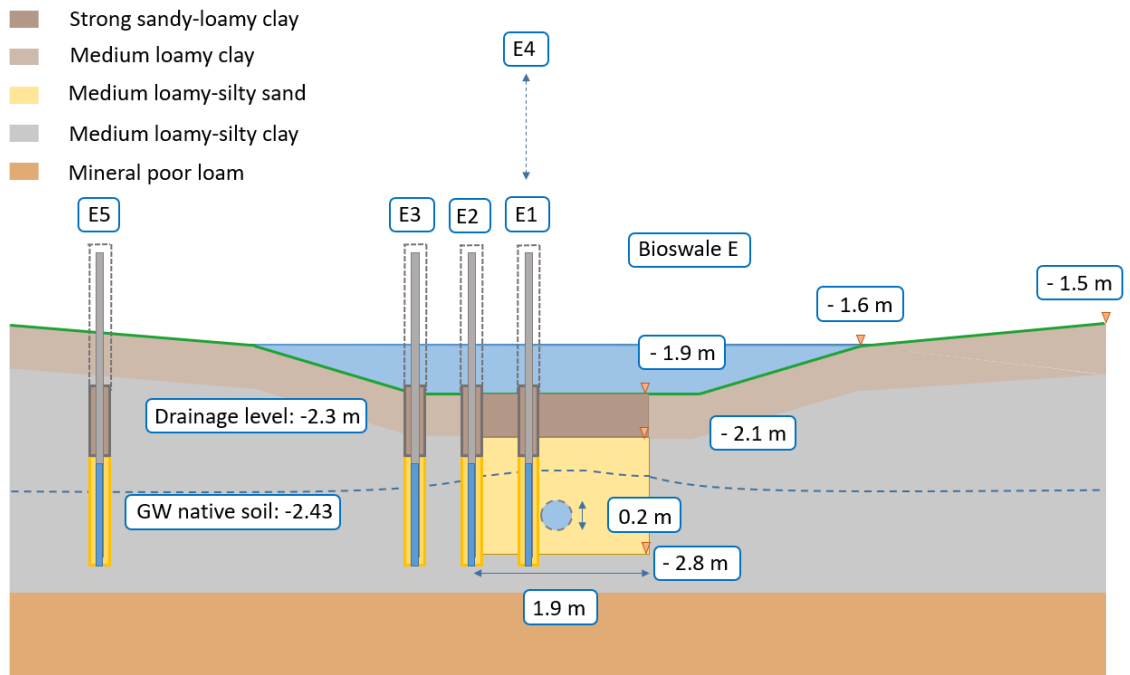


Figure 61: Piezometers bioswale E, cross-section

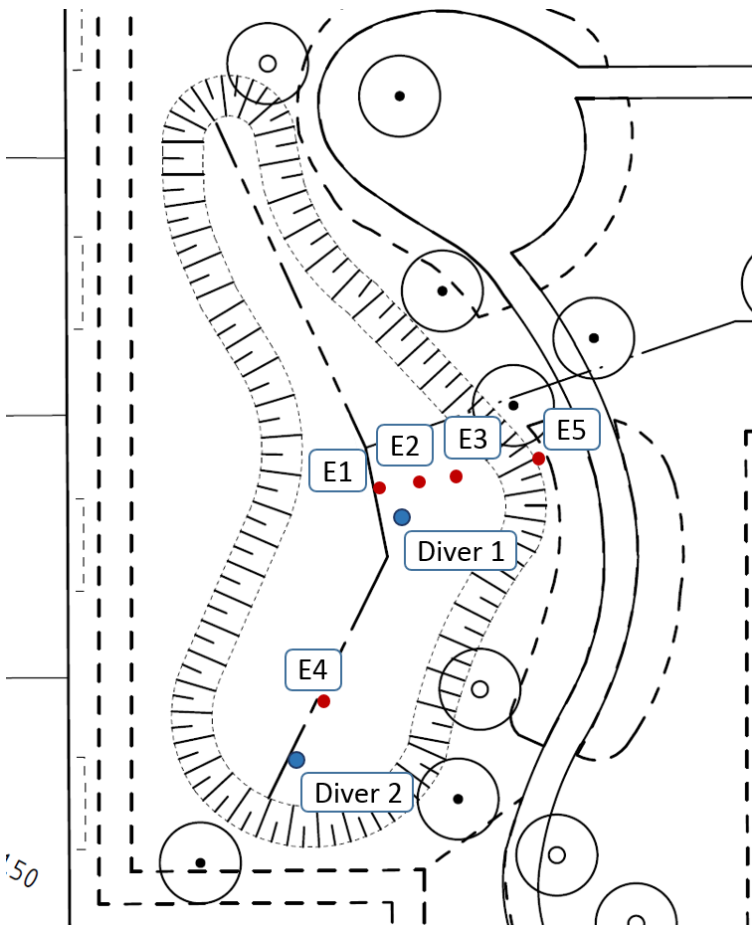


Figure 62: Piezometers and divers bioswale E

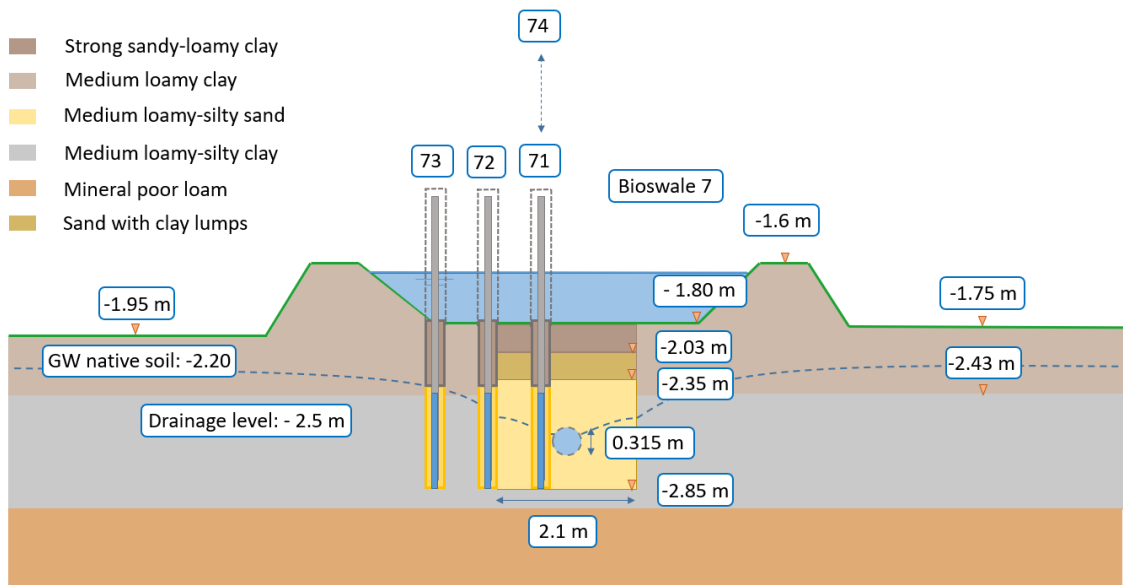


Figure 63: Piezometers bioswale 7, cross-section

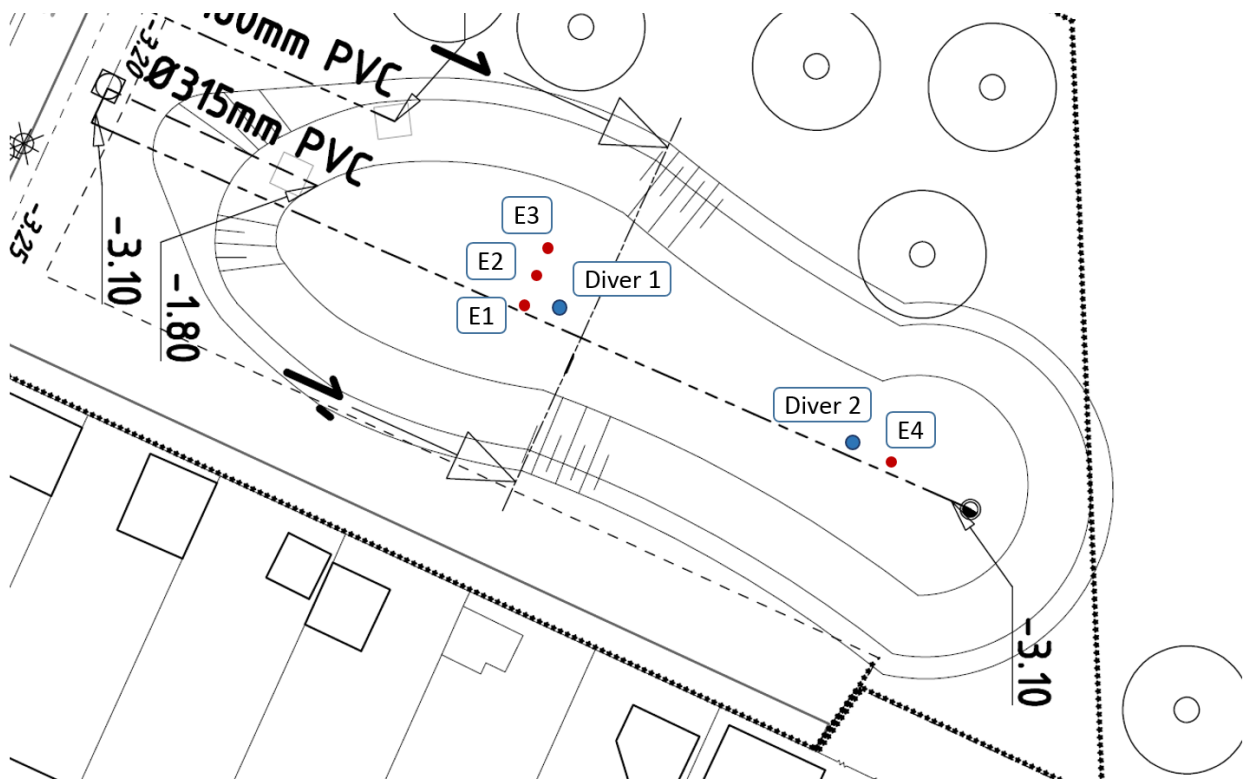


Figure 64: Piezometers and divers bioswale 7

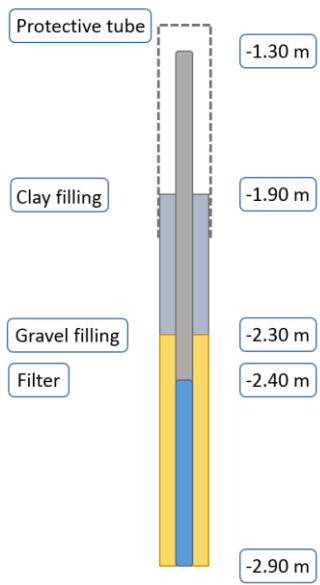


Figure 65: Piezometer placement, sizes indicative

Appendix 4: Complete result tables per storm simulation

Table 21: Heavy dry storm (1) all data

Heavy dry storm (1)	Bioswale A	Bioswale D	Bioswale E
T_{average} [°C]	10.44	6.75	15.92
h_{water} [cm]	20.37	22.58	18.64
$q_{\text{peak-in}}$ [l/min]	500	333	500
$q_{\text{peak1-out}}$ [l/min]	13.95	7.09	23.40
$q_{\text{peak2-out}}$ [l/min]	14.55	7.59	23.90
$t_{q\text{-peak-in}}$ [min]	24	13.50	35
$t_{q\text{-peak1-out}}$ [min]	299	191	118
$t_{q\text{-peak2-out}}$ [min]	539	911	328
V_{in} [l]	30000	20000	30000
V_{out} [l]	22713.75	16477.60	20307.00
$V_{\text{out t-storm}}$ [l]	297.00	80.40	591.00
t_{emptying} [hours]	29.30	38.40	26.43
$R_{p1 \text{ peak}}$ [-]	0.028	0.021	0.047
$R_{p2 \text{ peak}}$ [-]	0.29	0.023	0.048
$R_{p1 \text{ delay}}$ [-]	9.97	6.37	3.93
$R_{p2 \text{ delay}}$ [-]	17.97	30.37	10.93
f_v [-]	0.76	0.82	0.68
T_{delay} [min]	3	12	14
V_{delay} [%]	99.0	99.6	98.0

Table 22: Heavy wet storm all data

Heavy wet storm (2)	Bioswale A	Bioswale D	Bioswale E
T_{average} [°C]	11.20	7.91	18.82
h_{water} [cm]	20.51	21.85	19.07
$q_{\text{peak-in}}$ [l/min]	500.00	333.33	500.00
$q_{\text{peak1-out}}$ [l/min]	13.12	5.78	18.90
$q_{\text{peak2-out}}$ [l/min]	13.86	6.68	19.10
$t_{q\text{-peak-in}}$ [min]	28	13.50	30
$t_{q\text{-peak1-out}}$ [min]	242	367	88
$t_{q\text{-peak2-out}}$ [min]	620	803	118
V_{in} [l]	30000	20000	30000
V_{out} [l]	23226	16206.68	23136
$V_{\text{out t-storm}}$ [l]	387	55	642
t_{emptying} [hours]	38.85	49.18	35.23
$R_{p1 \text{ peak}}$ [-]	0.026	0.017	0.038
$R_{p2 \text{ peak}}$ [-]	0.028	0.020	0.038
$R_{p1 \text{ delay}}$ [-]	8.07	15.29	2.93
$R_{p2 \text{ delay}}$ [-]	20.67	33.46	3.93
f_v [-]	0.77	0.81	0.77
T_{delay} [min]	2	11	7
V_{delay} [%]	98.71	99.72	97.86

Table 23: Two-peak storm all data

Two peak storm (3)	Bioswale A	Bioswale D	Bioswale E
T _{average} [°C]	13.01	7.99	18.47
h _{water1} [cm]	17.37	14.01	15.8
q _{peak1-in} [l/min]	333.33	166.67	333.33
q _{peak1.1-out} [l/min]	10.74	6.7	20.8
q _{peak1.2-out} [l/min]	11.54	7.2	21.3
t _{q-peak1-in} [min]	13.5	5.5	15
t _{q-peak1.1-out} [min]	146	243	148
t _{q-peak1.2-out} [min]	256	430	289
h _{water2} [cm]	12.88	16.11	15.7
q _{peak2-in} [l/min]	166.67	166.67	166.67
q _{peak2.1-out} [l/min]	-	7	-
q _{peak2.2-out} [l/min]	8.24	7.7	21.3
t _{q-peak2-in} [min]	2	4	3
t _{q-peak2.1-out} [min]	-	138	-
t _{q-peak2.2-out} [min]	109	427	38
V _{in} [l]	30000	20000	30000
V _{out} [l]	22455.6	14841	24720
V _{out t-storm1} [l]	317.04	21	471
V _{out t-storm2} [l] total	449.04	378	1245
V _{out t-storm2} [l] own	183	72	201
T _{emptying} [hours]	44.13	43.3	32.48
R _{p1.1 peak} [-]	0.032	0.040	0.062
R _{p1.2 peak} [-]	0.035	0.043	0.064
R _{p1.1 delay} [-]	4.87	8.10	4.93
R _{p1.2 delay} [-]	8.53	14.33	9.63
R _{p2.1 peak} [-]	-	0.042	-
R _{p2.2 peak} [-]	0.049	0.046	0.128
R _{p2.1 delay} [-]	-	4.6	-
R _{p2.2 delay} [-]	3.63	14.23	1.27
f _v [-]	0.75	0.74	0.82
T _{delay 1} [min]	3	49	24
T _{delay 2} [min]	3	14	7
V _{delay} [%]	72.30	72.21	76.68

Table 24: Medium storm all data

Medium storm (4)	Bioswale A	Bioswale D	Bioswale E
T_{average} [°C]	10.08	6.26	16.36
h_{water} [cm]	11.39	7.82	6.22
$q_{\text{peak-in}}$ [l/min]	48.78	23.41	39.52
$q_{\text{peak1-out}}$ [l/min]	-	3.66	-
$q_{\text{peak2-out}}$ [l/min]	6.44	4.06	9.8
$t_{q\text{-peak-in}}$ [min]	58.50	61.00	59
$t_{q\text{-peak1-out}}$ [min]	-	263.00	-
$t_{q\text{-peak2-out}}$ [min]	69.00	503.00	144
V_{in} [l]	5853.74	2996.26	4742
V_{out} [l]	3827.88	2722.64	2604
$V_{\text{out t-storm}}$ [l]	532.80	103.20	150
T_{emptying} [hours]	10.40	12.10	11.42
$R_{p1\text{ peak}}$ [-]	-	0.16	-
$R_{p2\text{ peak}}$ [-]	0.13	0.17	0.25
$R_{p1\text{ delay}}$ [-]	-	4.38	-
$R_{p2\text{ delay}}$ [-]	1.15	8.38	2.4
f_v [-]	0.65	0.91	0.55
T_{delay} [min]	10.00	10.00	29
V_{delay} [%]	90.90	96.56	96.84

Appendix 5: Graphs result field-survey per storm simulation

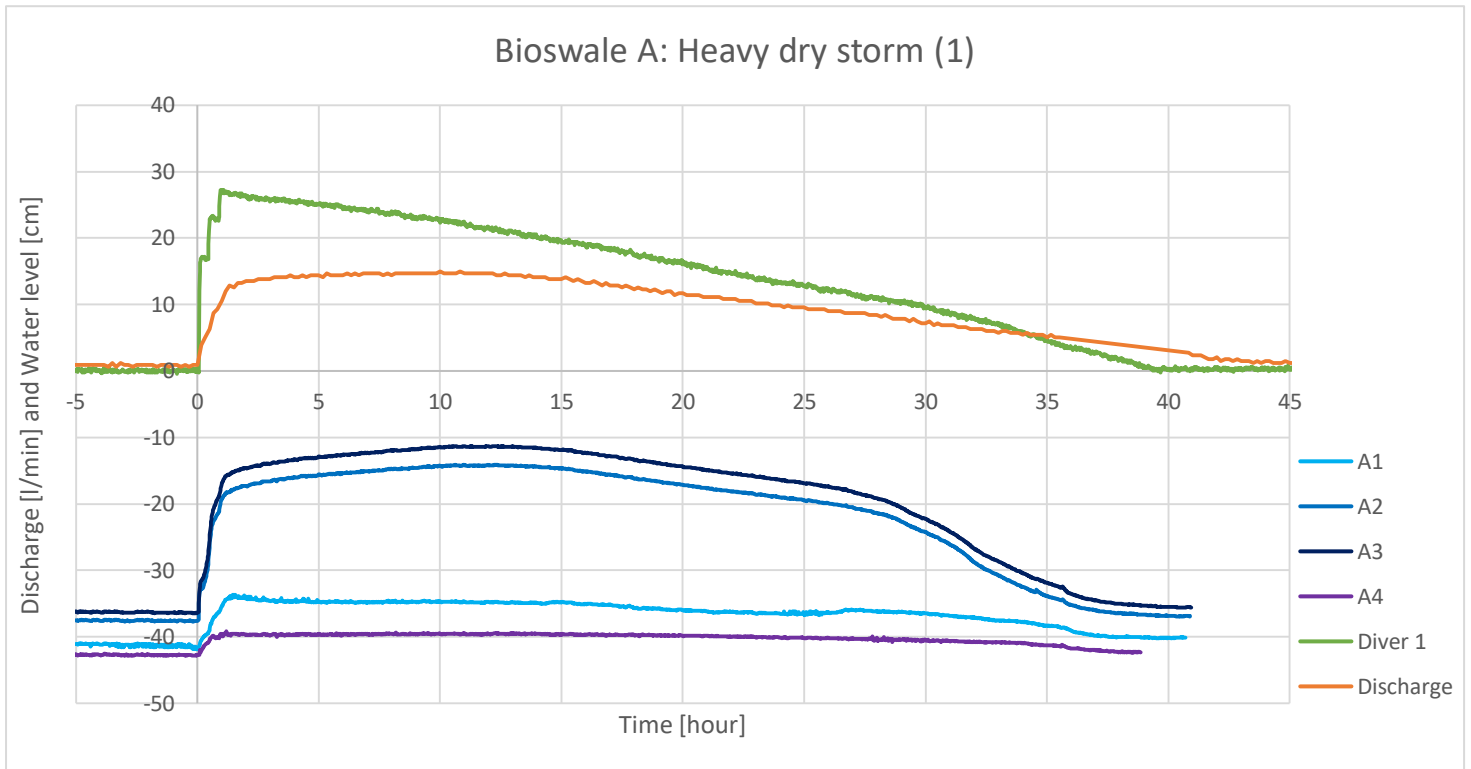


Figure 665: 26/03/2019

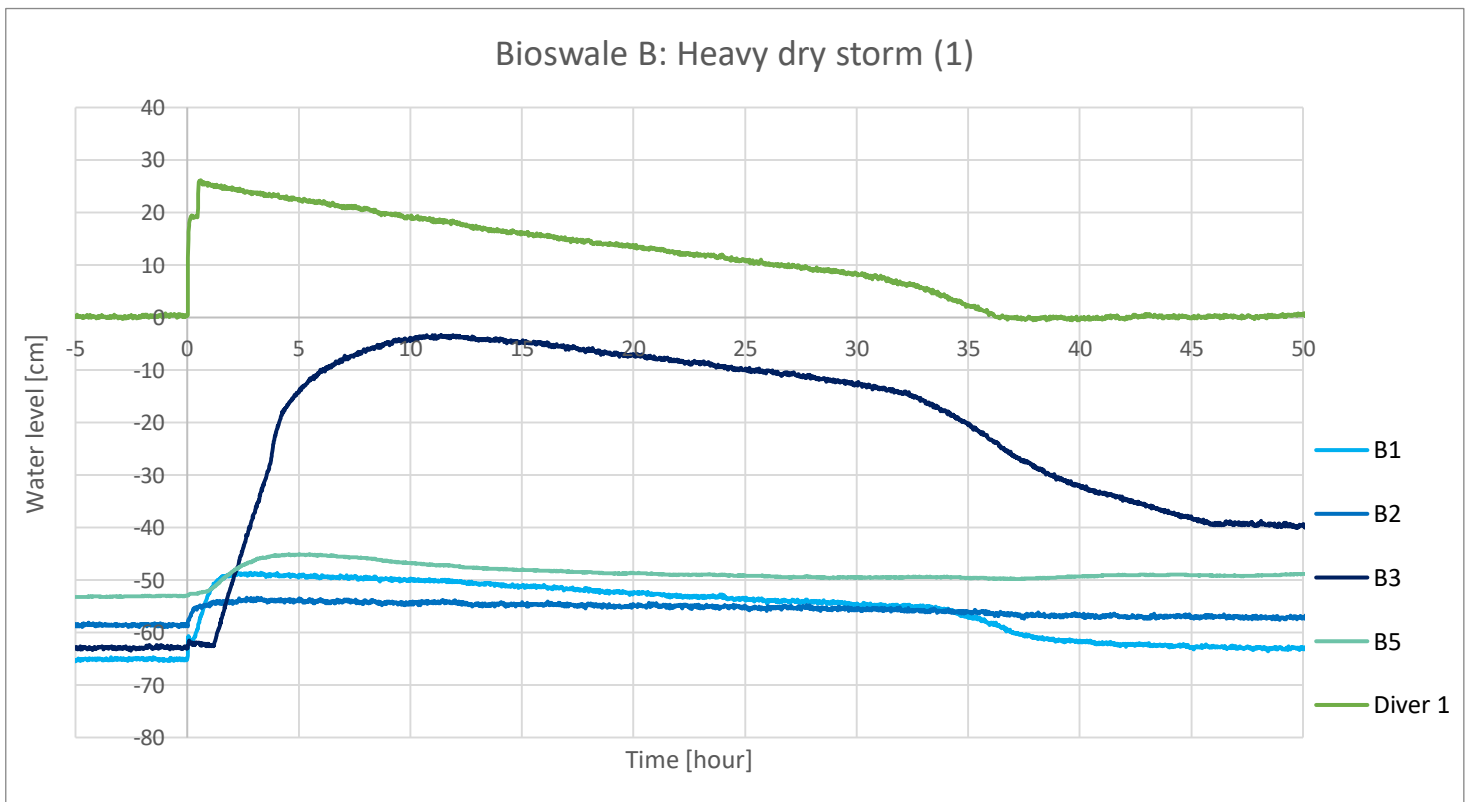


Figure 67: 15/05/2019

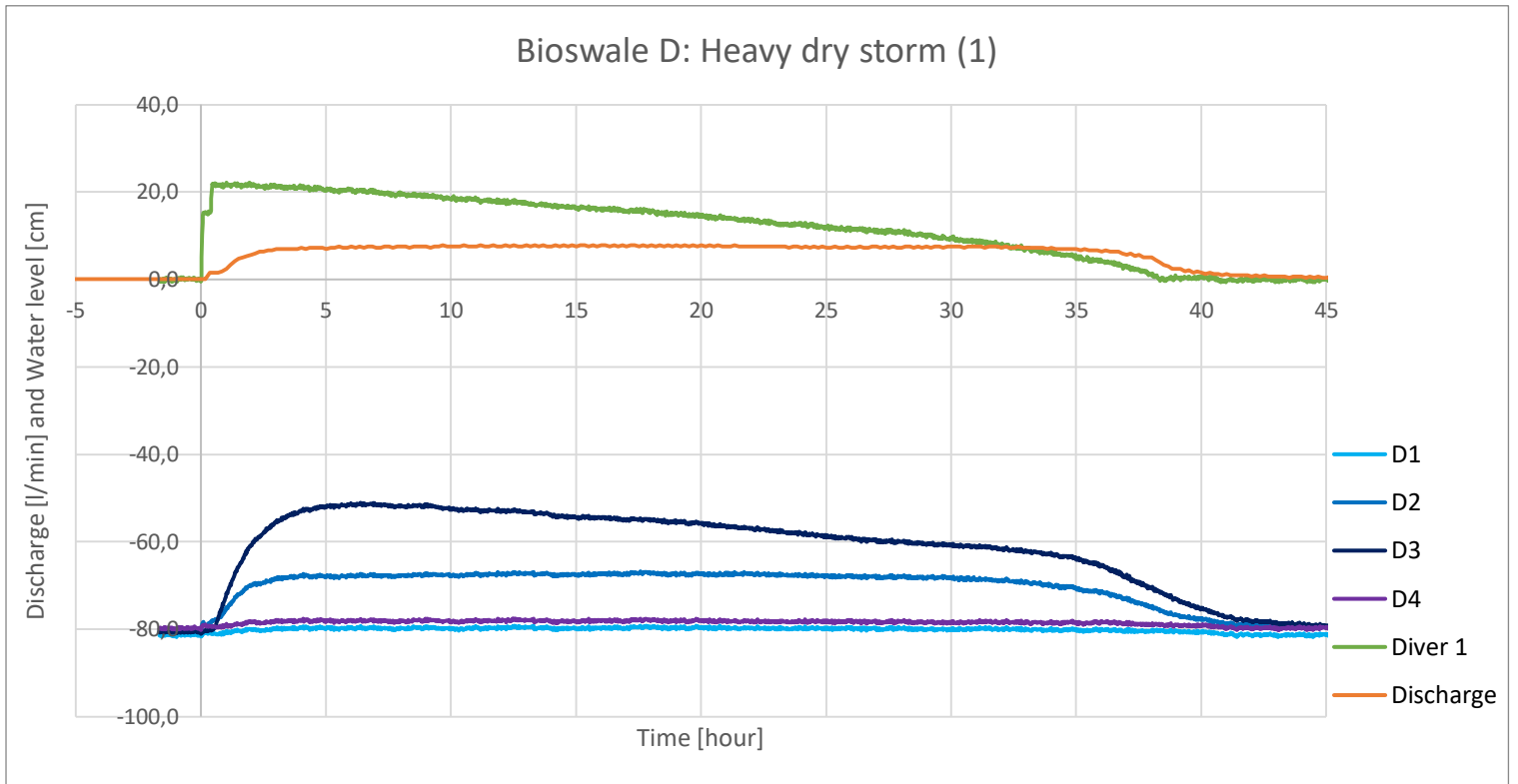


Figure 68: 18/02/2019

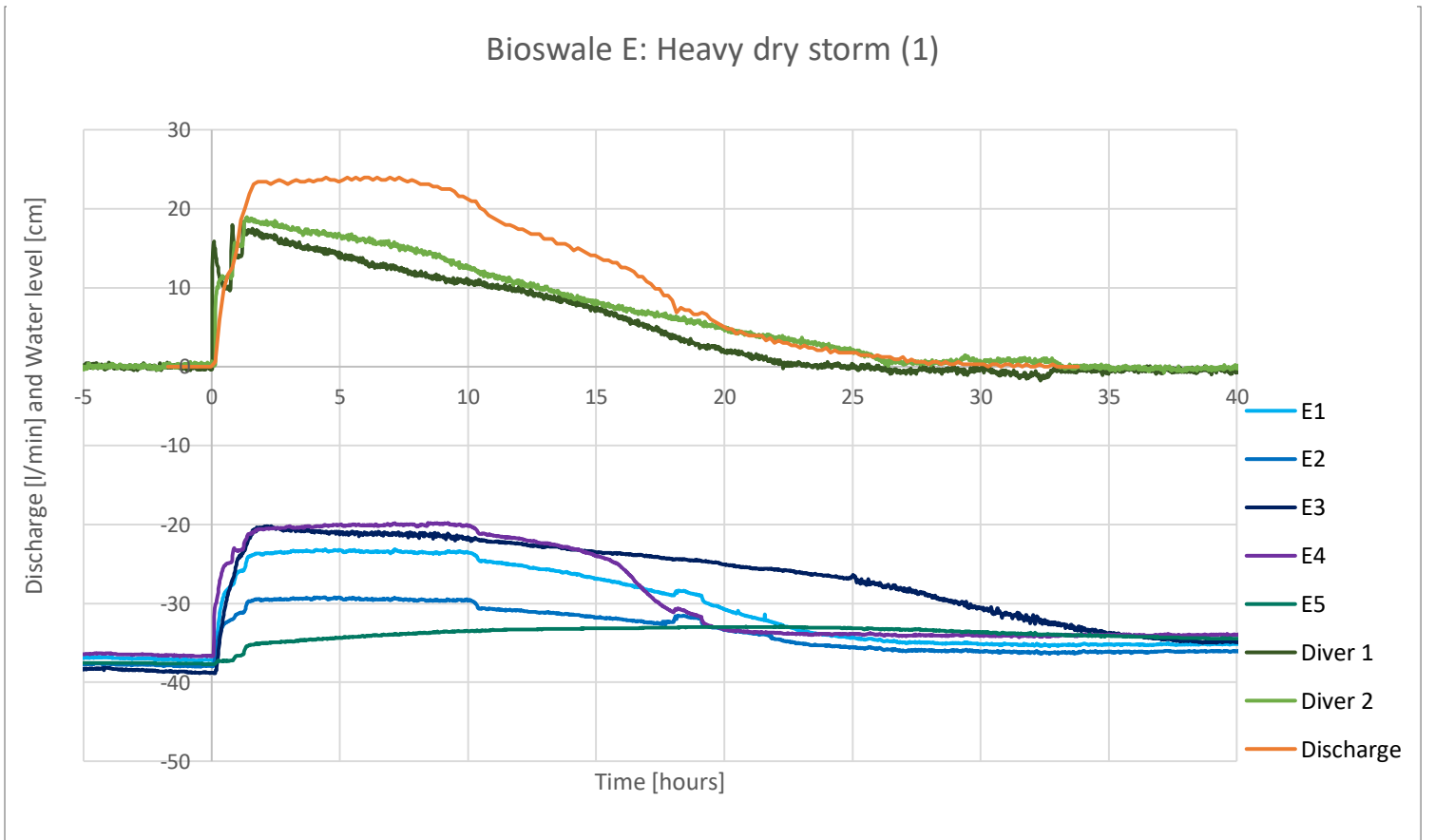


Figure 696: 15/05/2019

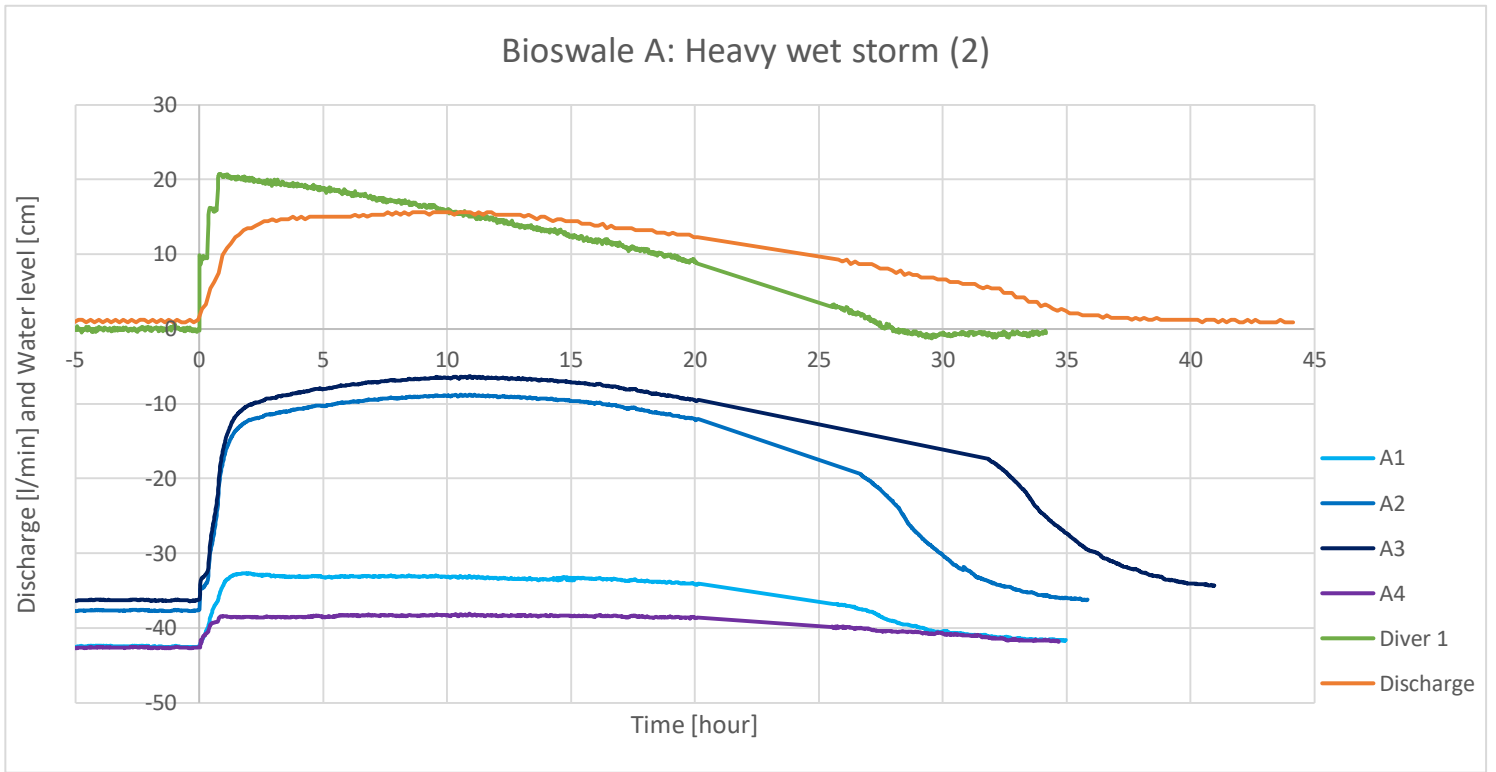


Figure 708: 21/03/2019

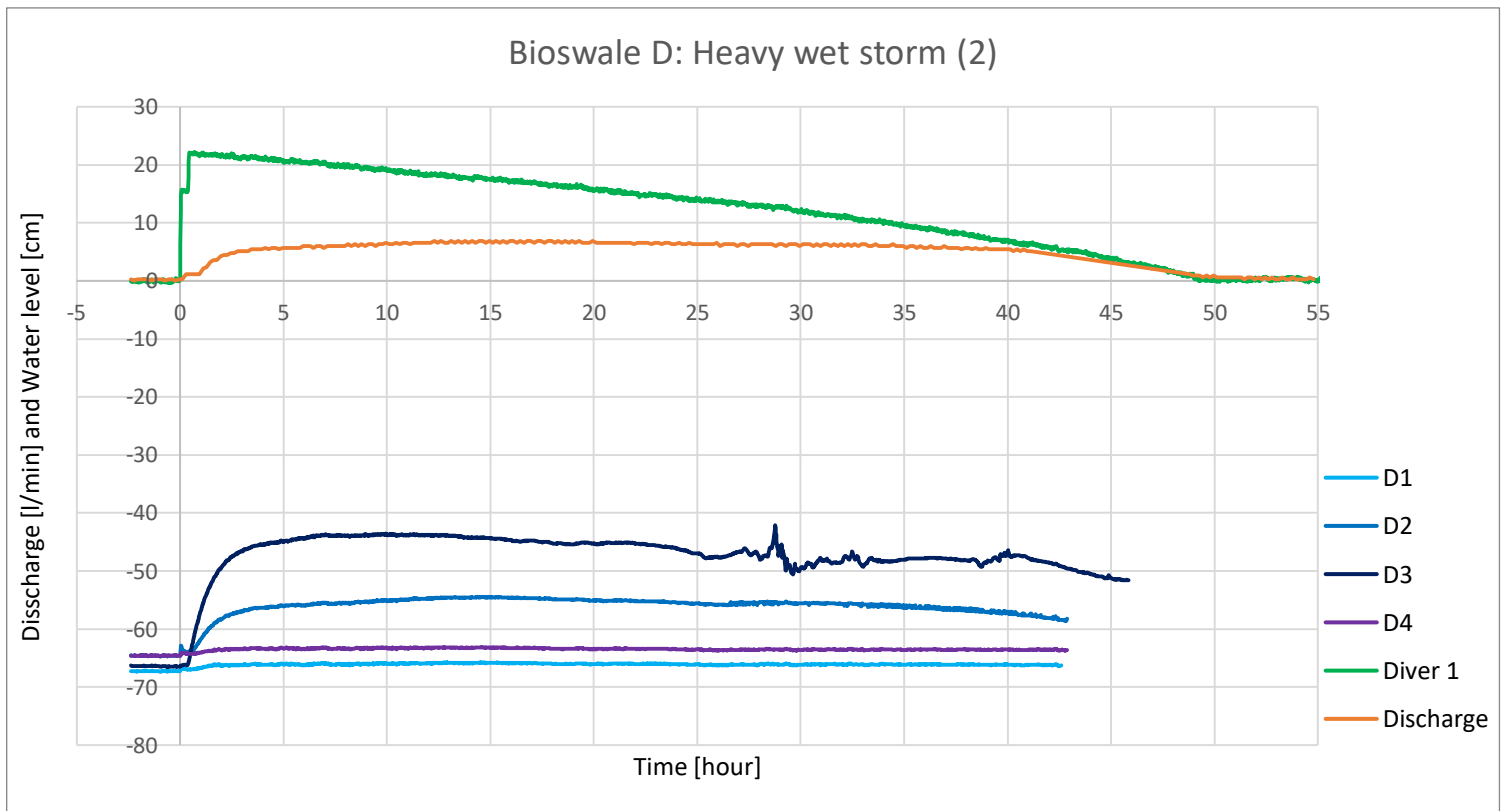


Figure 717: 28/02/2019

Bioswale E: Heavy wet storm (2)

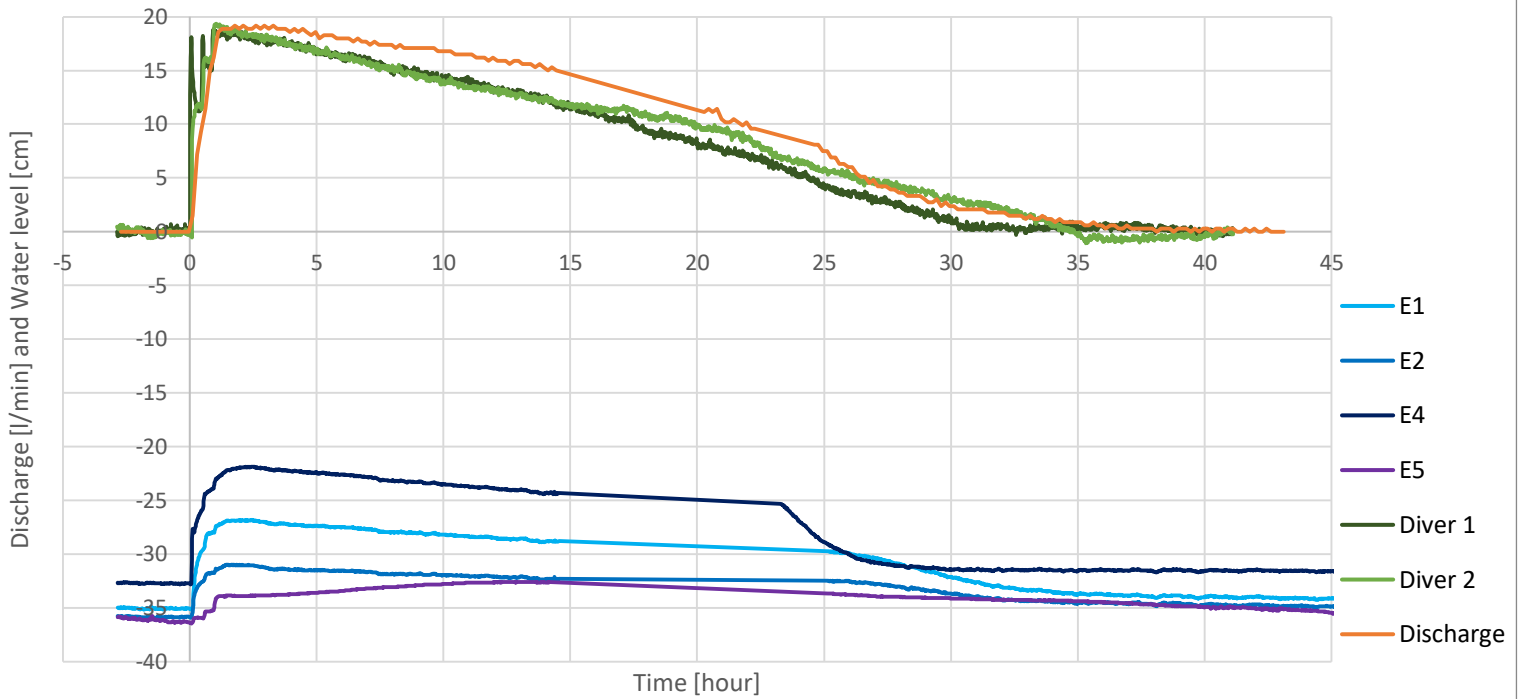


Figure 7210: 23/05/2019

Bioswale A: Two-peak storm (3)

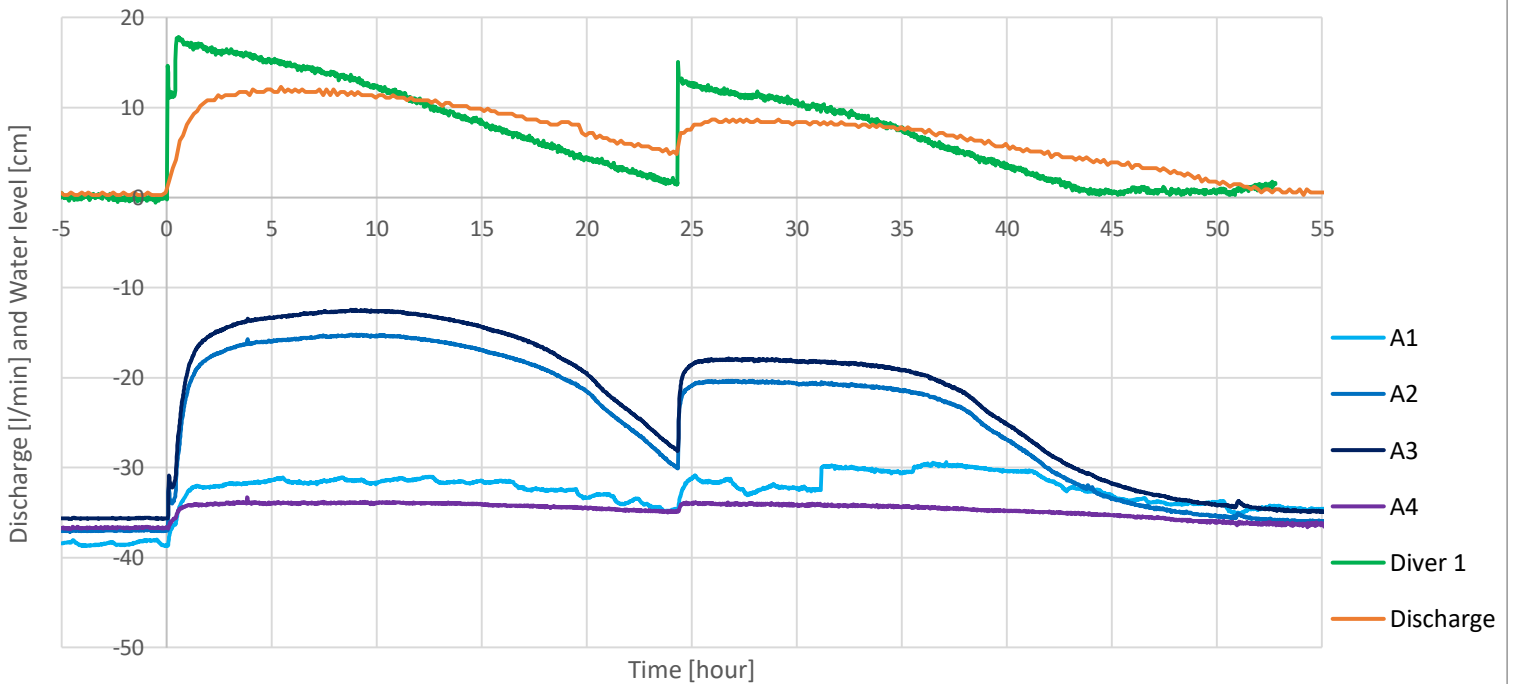


Figure 9: 09/04/2019

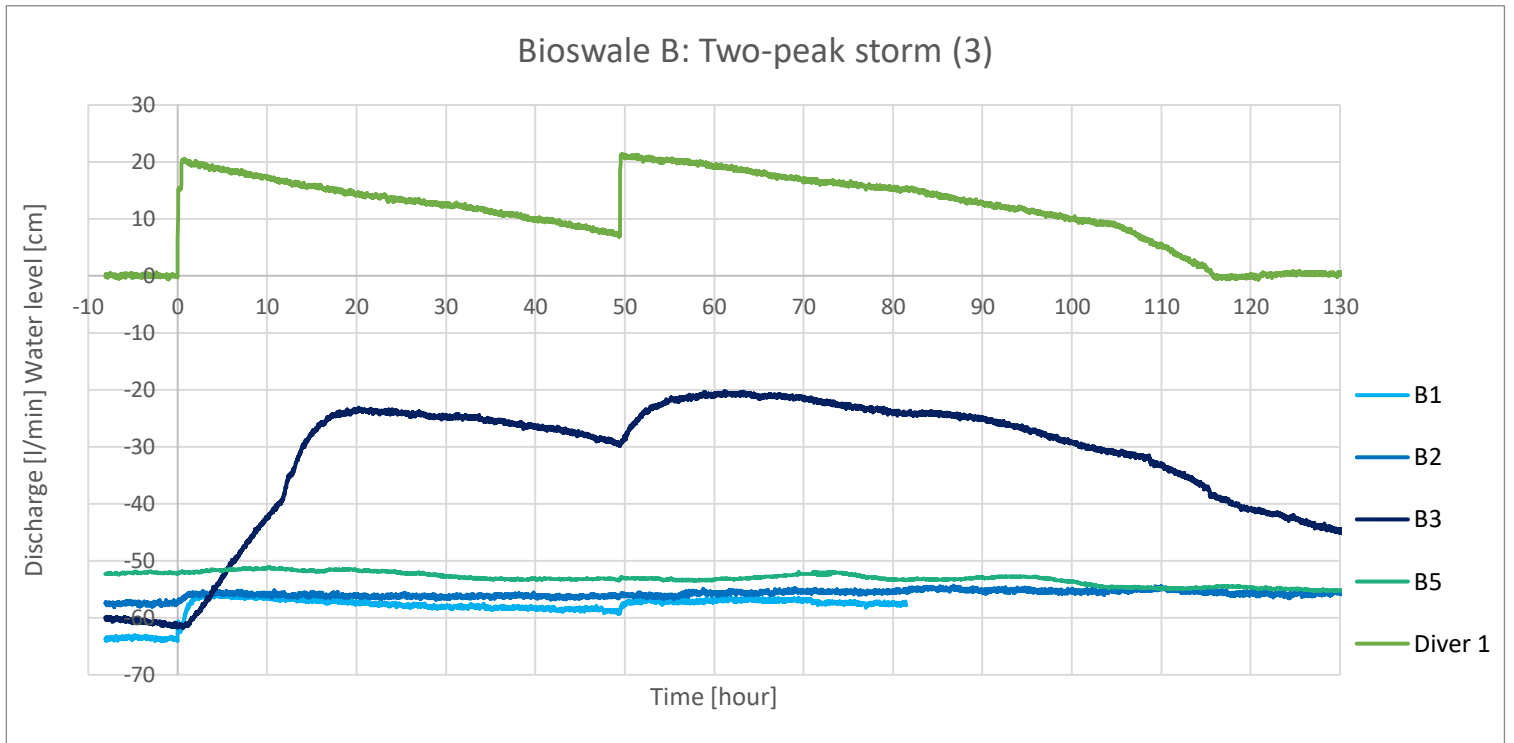


Figure 7412: 20/05/2019

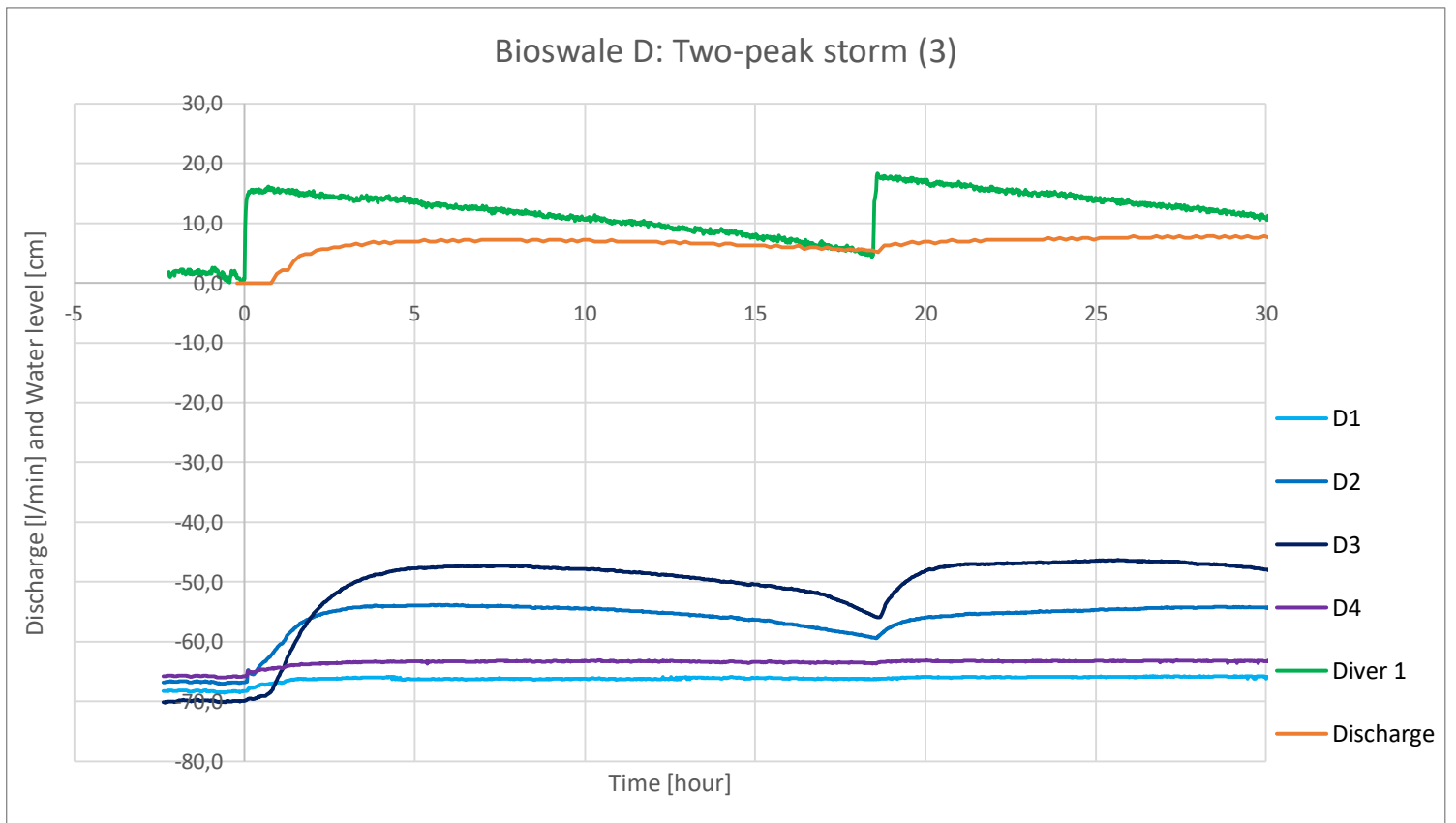


Figure 7511: 05/02/2019

Biowale E: Two-peak storm (3)

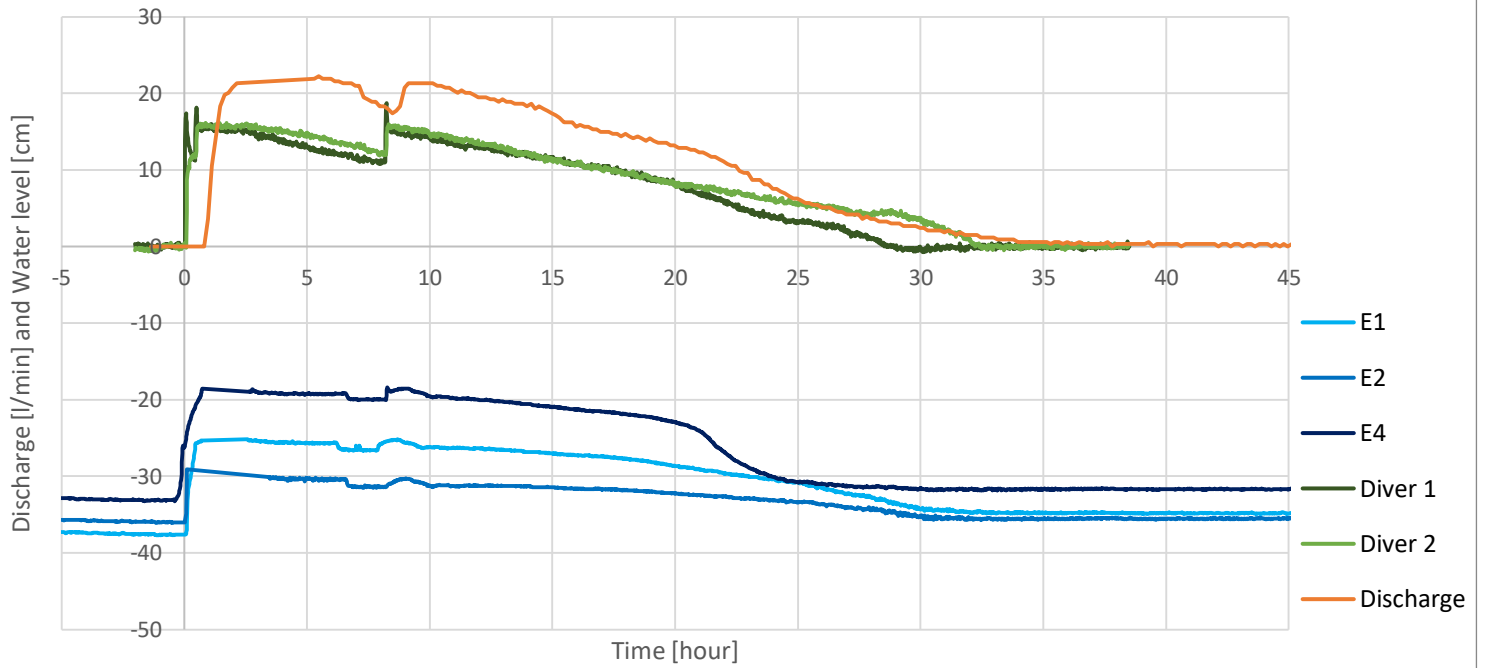


Figure 7614: 29/05/2019

Bioswale A: Medium storm (4)

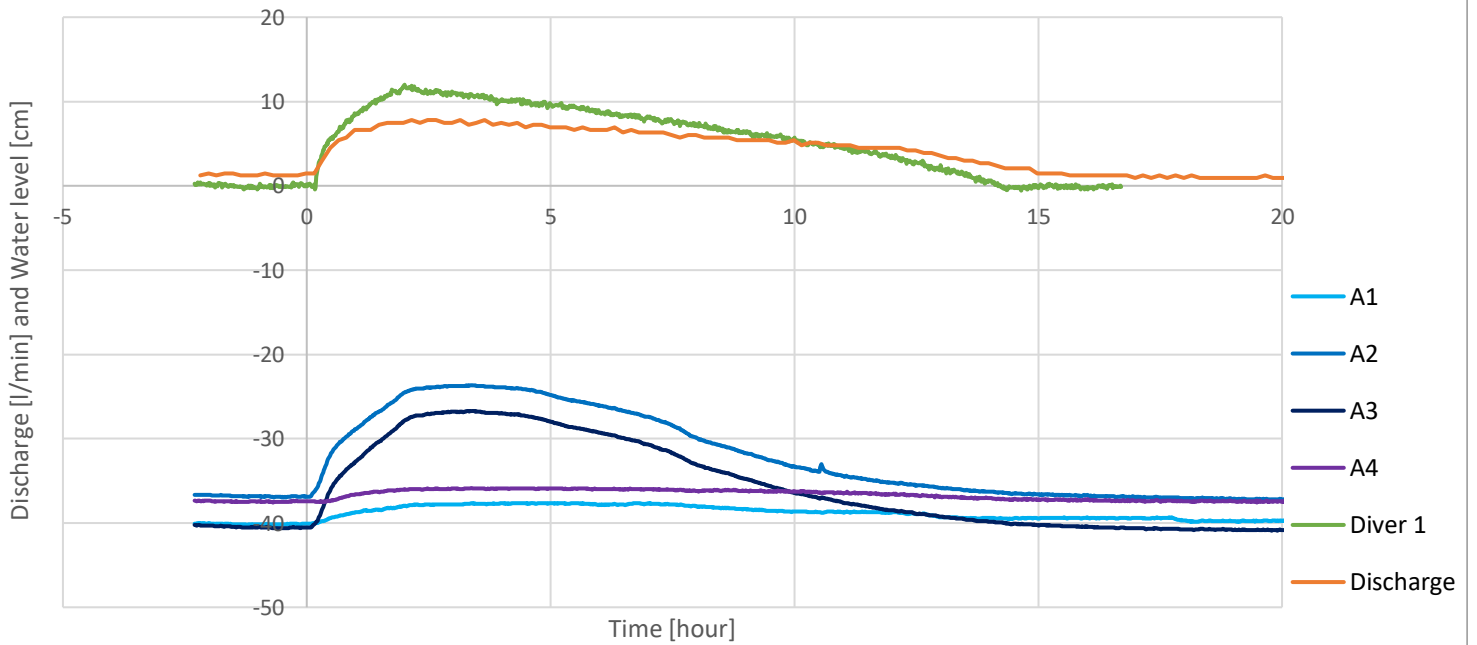


Figure 7713: 28/03/2019

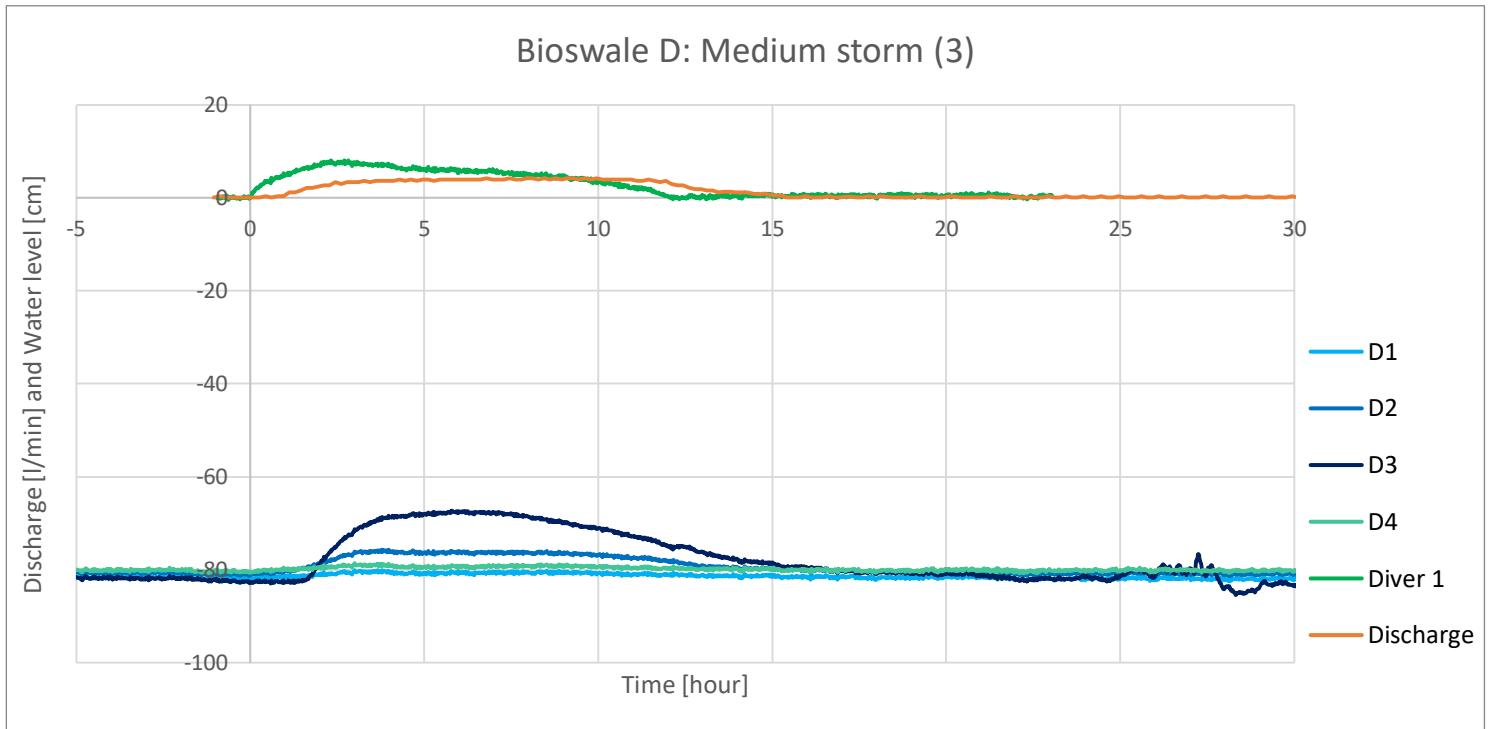


Figure 7816: 21/02/2019

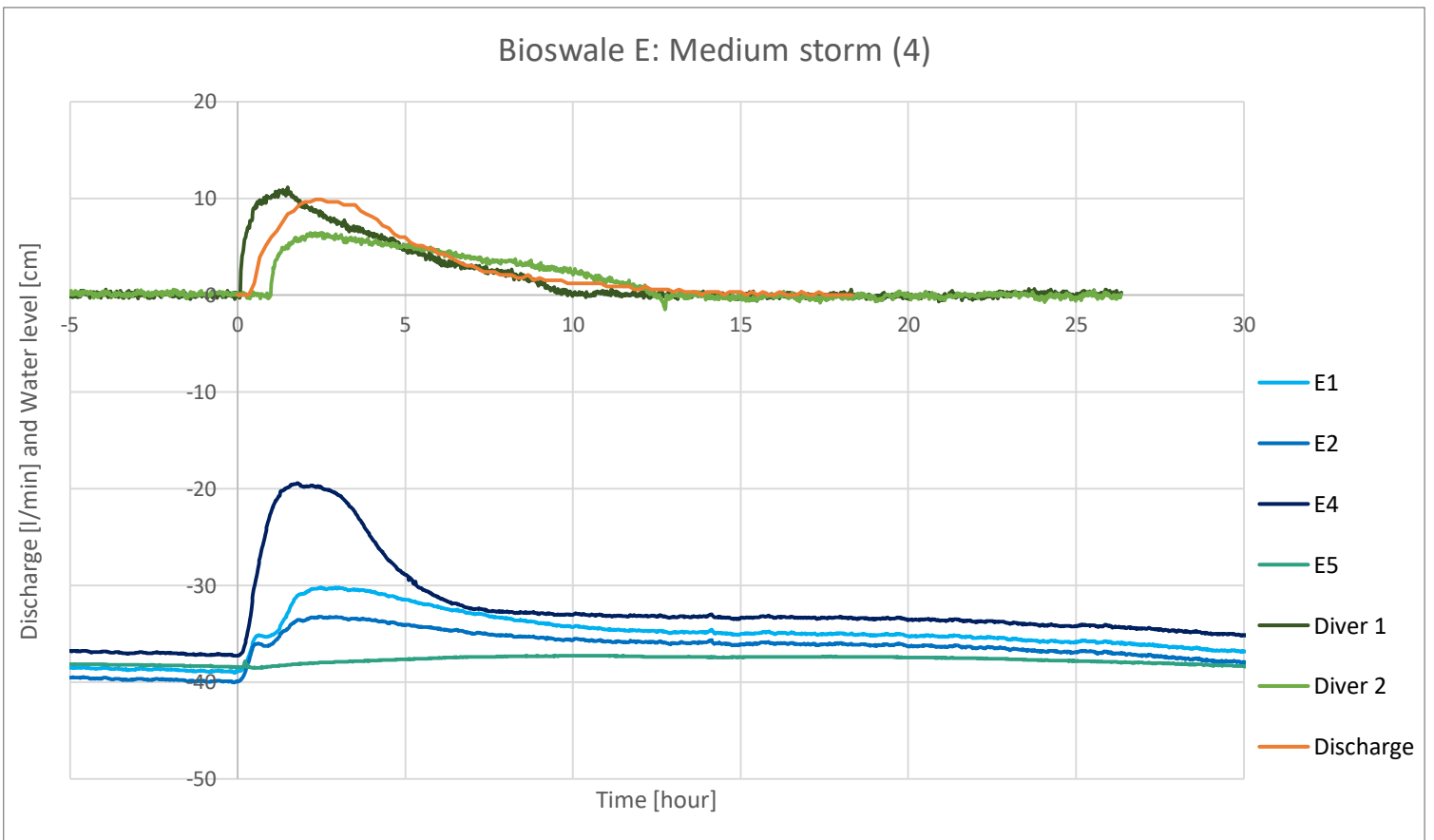


Figure 7915: 20/05/2019

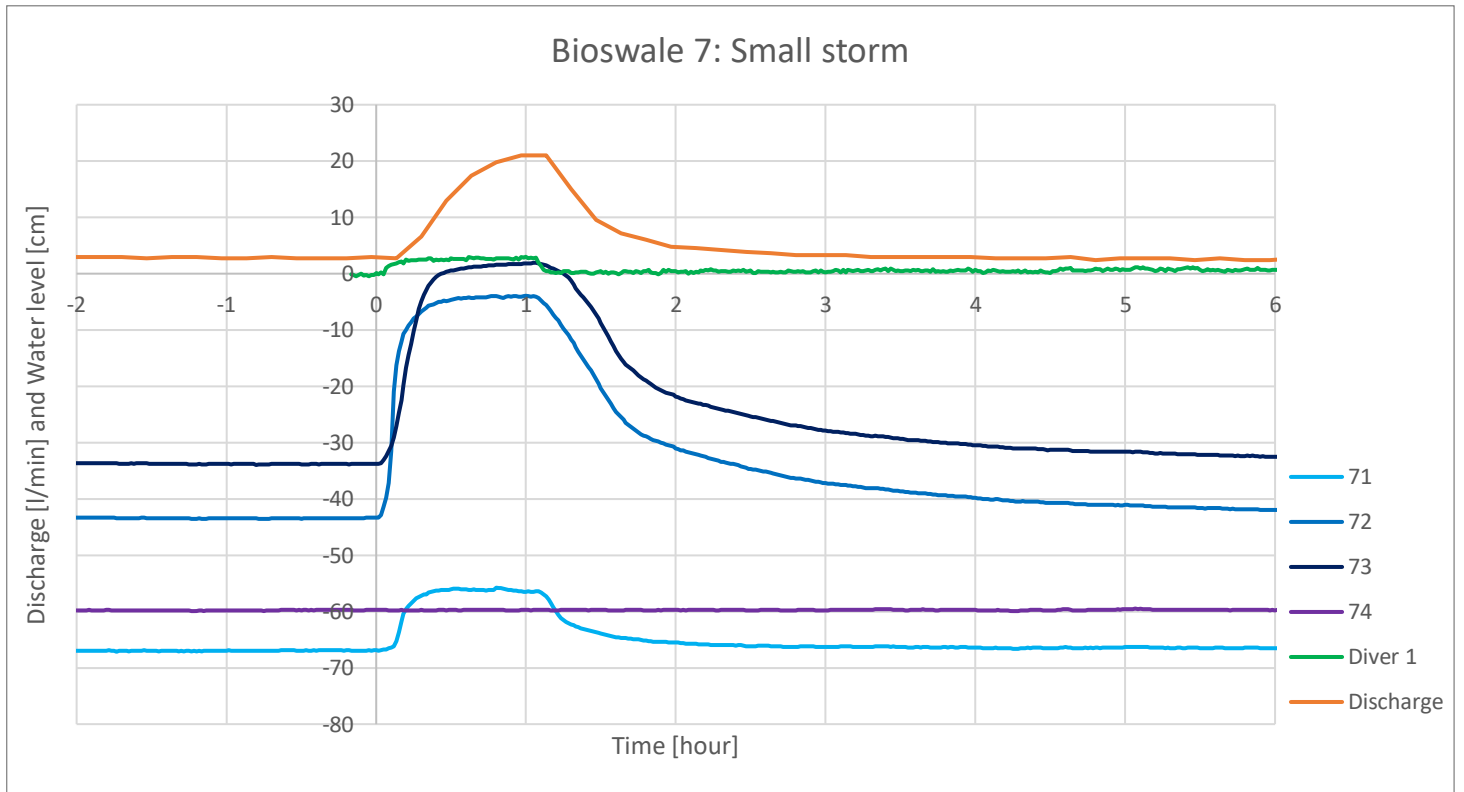


Figure 8018: 19/03/2019

Appendix 6: Graphs storm simulations interrupted by rainfall

Bioswale A: Heavy dry storm (1) interrupted by rainfall

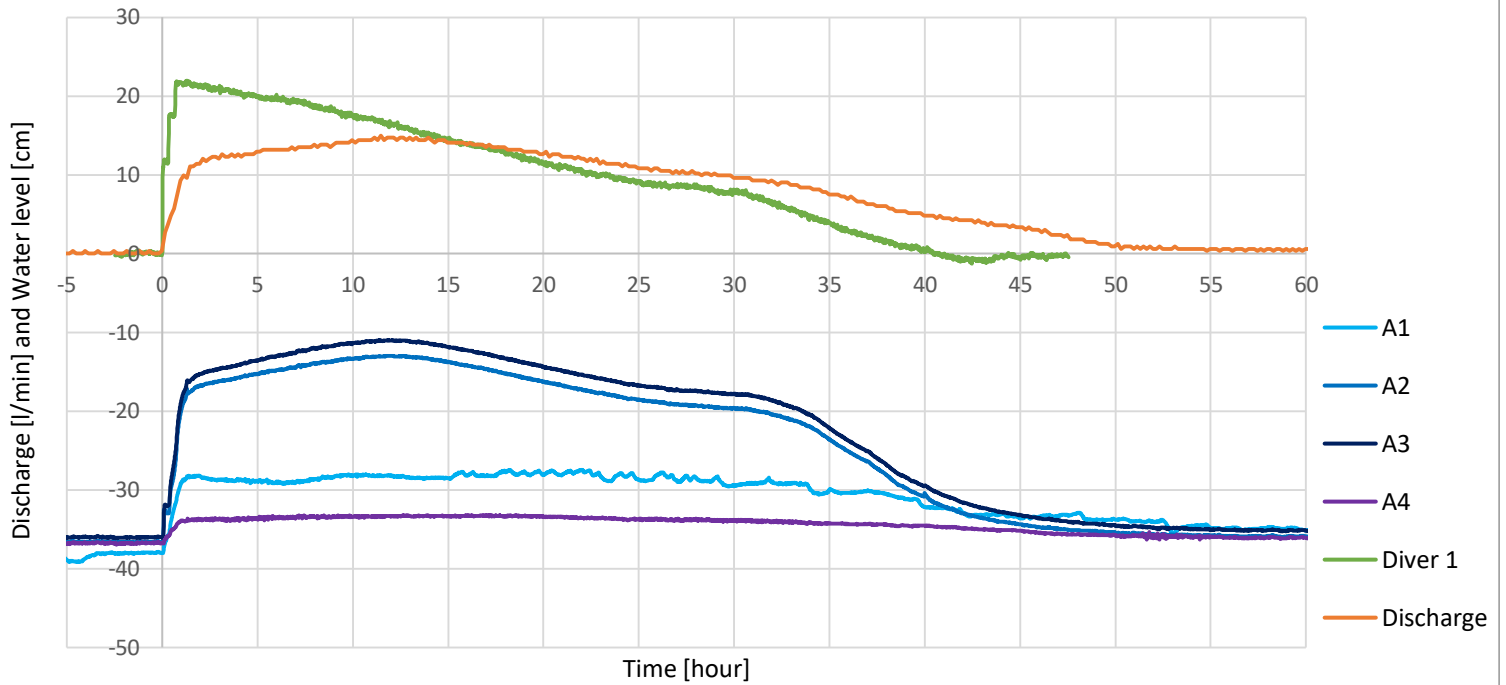


Figure 8119: 15/04/2019

Bioswale A: Heavy wet storm (2) interrupted by rainfall

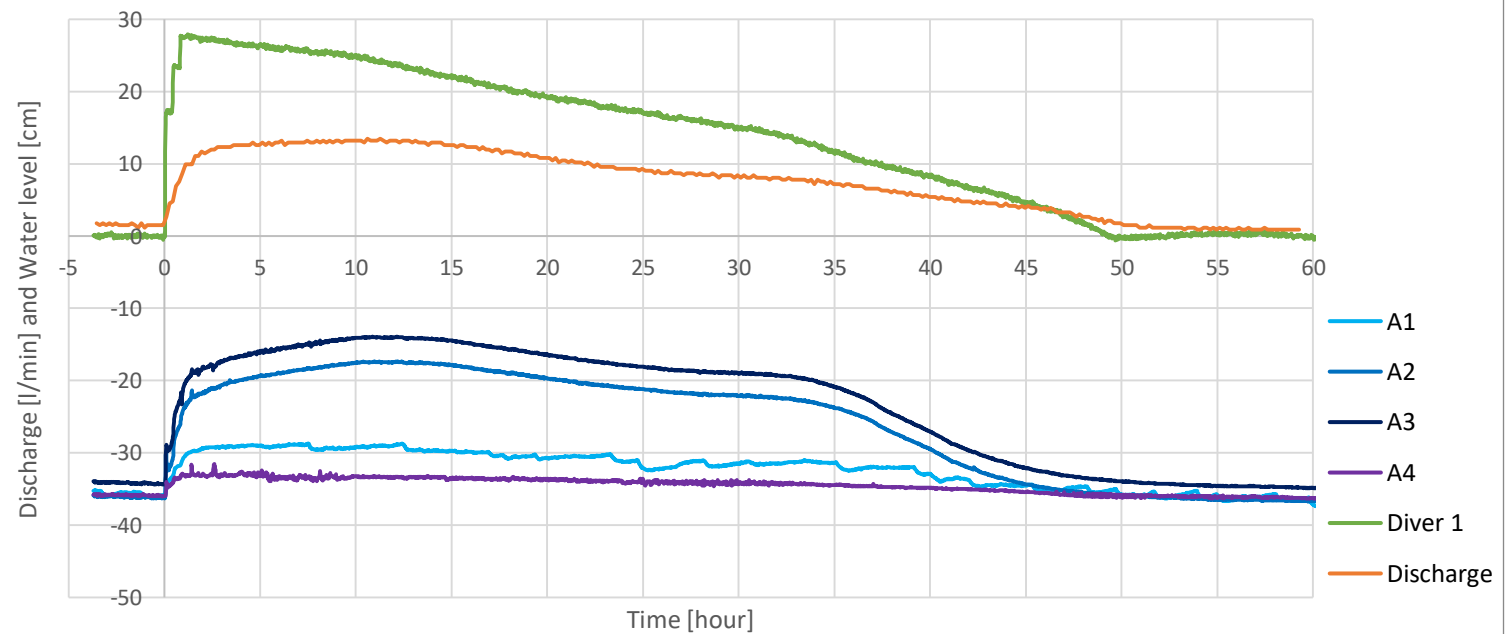


Figure 8220: 04/04/2019

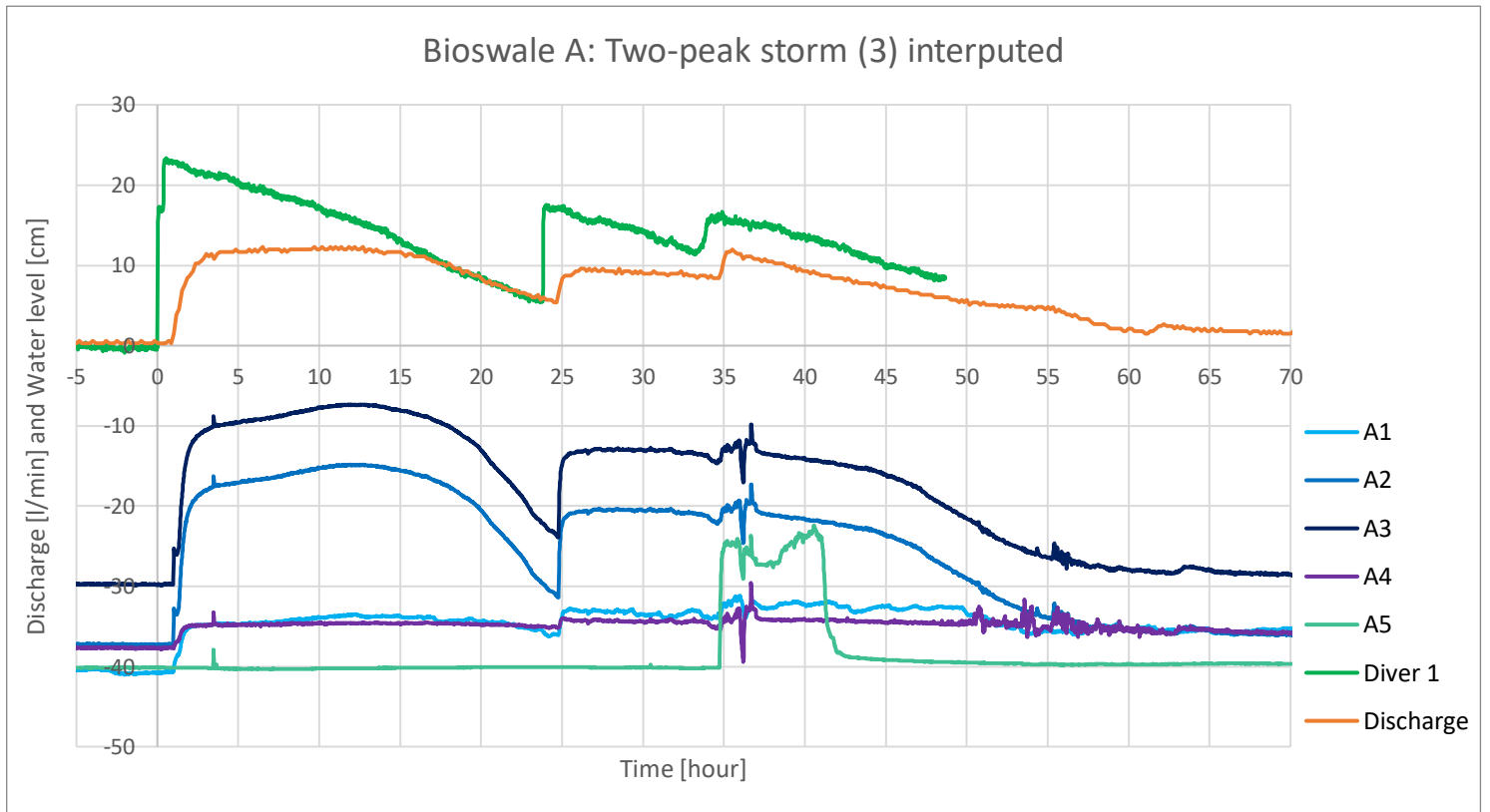


Figure 8322: 01/04/2019

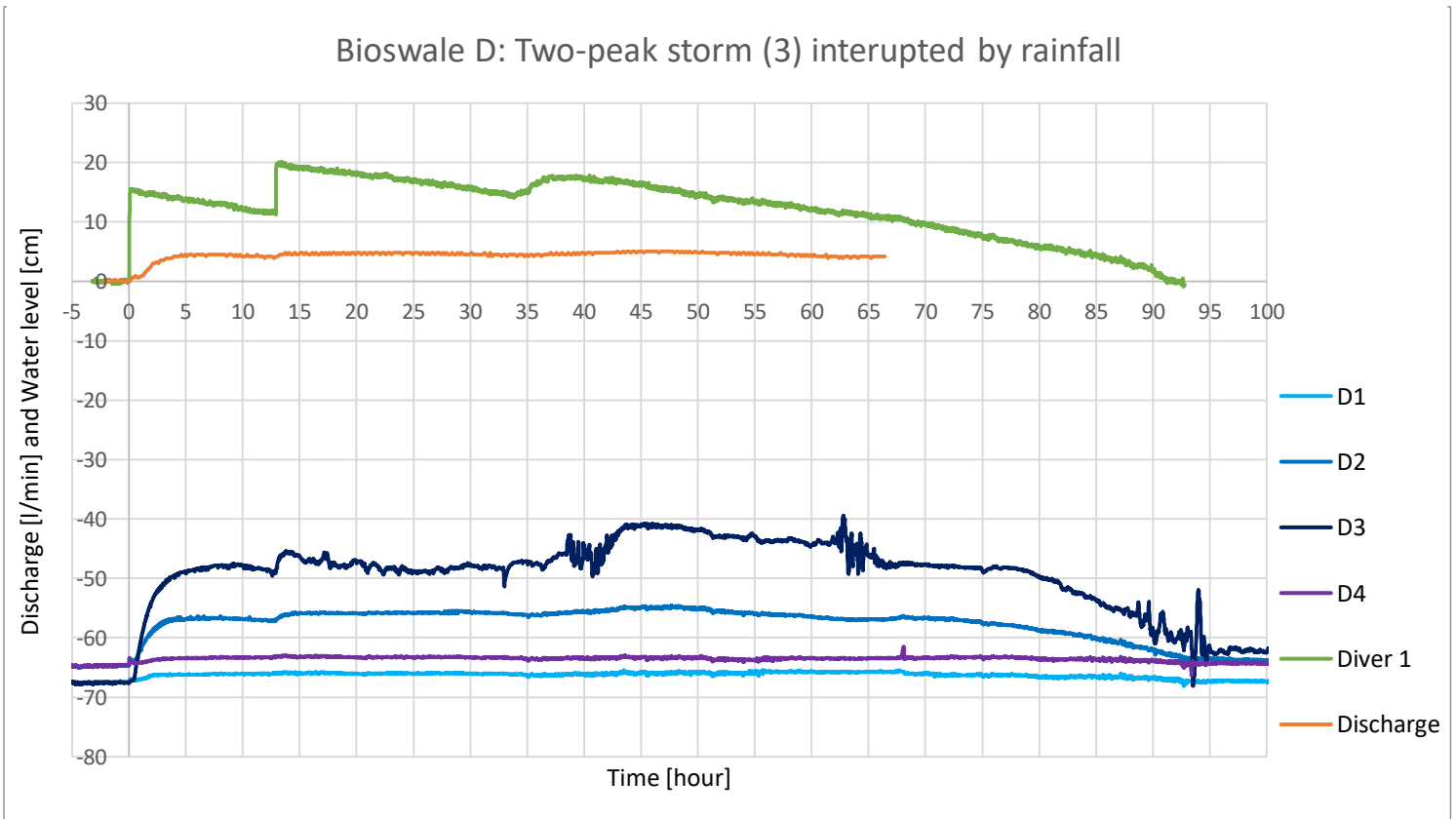


Figure 8421: 05/03/2019

Appendix 7: Hydrus 2D/3D calibration results

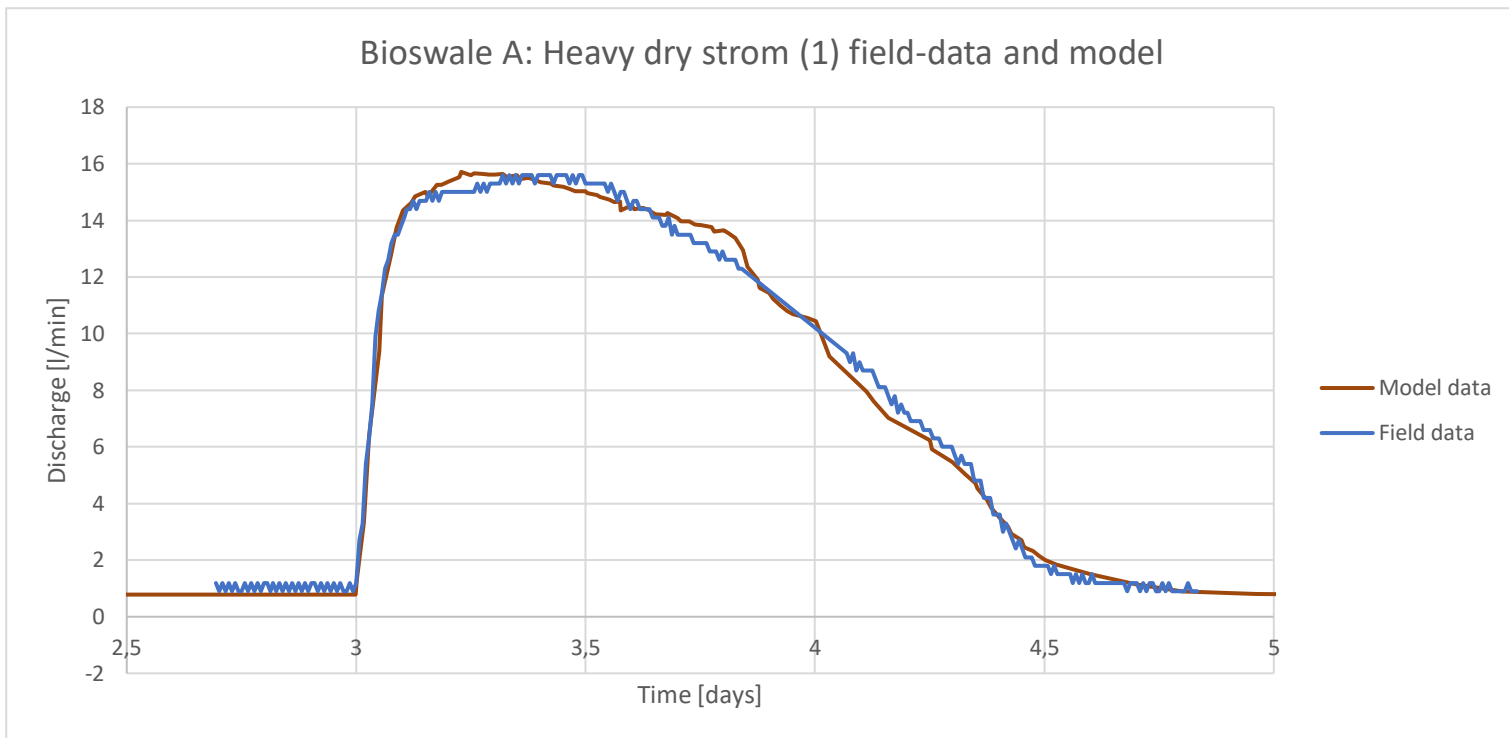


Figure 85: The calibration fits the results quite well, though the exact timing of the second peak proved difficult

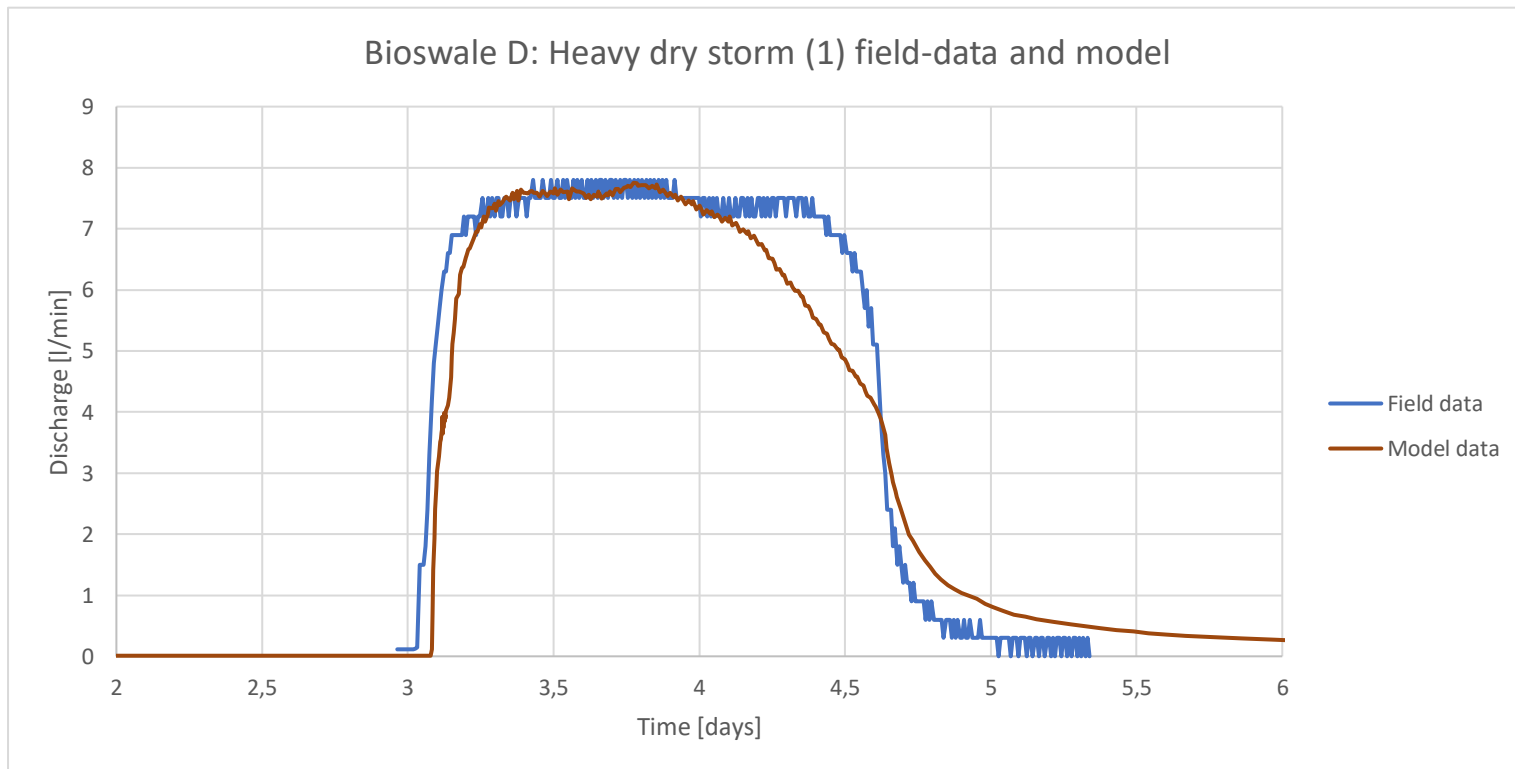


Figure 86: The last part of the curve could not be reproduced, likely due to the un-even cross-section of the bioswale

Bioswale E: Heavy dry storm (1) field data and model

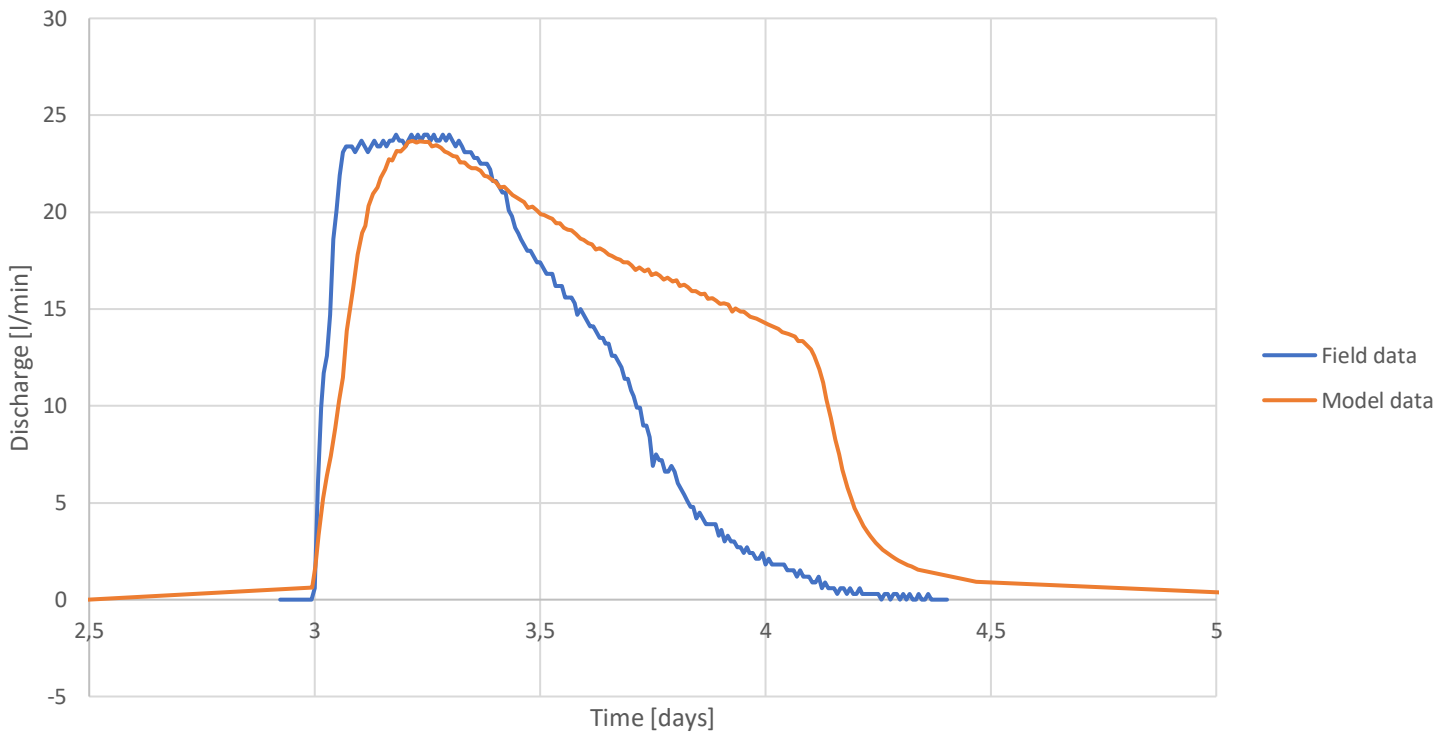


Figure 87: This is the worst fitting bioswale, also likely due to its extremely irregular shape